Dear Aninda Mazumbar,

On behalf of my co-authors, I would like to thank dr. Johan Vellekoop and dr. Andrew Johnson for their insightful constructive comments on our manuscript. Below, I will provide a point-by-point reply (in **bold**) to these comments (in *italics*) and state which changes we will make to the manuscript to take away the reviewers' concerns and prepare the text for publication. I hope that the suggested changes below will be sufficient to allow us to revise our manuscript for publication in Biogeosciences, and I look forward to hearing from you concerning your decision.

Sincerely,

Niels J. de Winter

Interactive comment on "Shell chemistry of the Boreal Campanian bivalve Rastellum diluvianum (Linnaeus, 1767) reveals temperature seasonality, growth rates and life cycle of an extinct Cretaceous oyster" by Niels J. de Winter et al.

Johan Vellekoop (Referee)

johan.vellekoop@kuleuven.be

Received and published: 3 February 2020

The study of de Winter et al. presents interesting trace elemental and stable isotopic data from a set of Rastellum diluvianum specimens from the famous Campanian locality of Ivo Klack. The new datasets highlight both the potential of these kind of studies, and the complexity of interpreting trace elemental data. The authors have generated a wealth of data, providing valuable insights in the age of the Ivo Klack deposits (Sr isotopes), the local temperature seasonality (oxygen isotopes) and in the physiology of the studied oysters (carbon and oxygen istopes and elemental data). At the same time, the complexity of the incorporation of trace elements in mollusk shells limits the usability of large parts of their data. The authors do a good job in highlighting this complexity, and show that, while sometimes elemental records of mollusk show cycling patterns, we are a long way away from successfully developing truly applicable proxies based on this time of data.

While the text is a bit lengthy, and some of the figures are rather complex, overall, this is a well-written manuscript. The authors have generated a substantial dataset, convincingly show that the studied specimens are well-preserved and provide interesting insights in the local climatic conditions at Ivo Klack. Their arguments are solid and their conclusions are sound.

Content wise, my only comments would be on the limited discussion on the possibility of a seasonal variability in d18O of seawater at Ivo Klack. They pass over this issue a bit too hastily, in my opinion. How is the assumption of a constant d18O of seawater justified? Wouldn't such a coastal site be susceptible for seasonal changes in riverine input? Particularly since the fennoscandian shield is usually placed in a wet/temperate climate belt, in Late Cretaceous climate reconstructions. The reference provided by the authors (Thibault et al., 2016) concerns a study on the chalks of the Stevns-1 core, which represents a much more distal site than Ivo Klack. Now, I realize that the authors are limited here, because

constraining d18O of seawater is not easy, and I don't disagree with most of their general conclusions, but it would behoove them to acknowledge their uncertainties in this issue.

We acknowledge that the reconstruction of sea surface temperatures from stable oxygen isotopes suffers from assumptions about water oxygen isotope composition. We realize that we may not have given this fact the proper attention in our manuscript. In the revised version, we will therefore update our discussion of stable oxygen isotopes where these are translated to temperatures and make clear that these conversions are based on assumptions. We will add a paragraph at the beginning of the discussion of our stable oxygen isotope results in which we more clearly explain what assumptions we make about sea water composition. Finally, at the end our discussion of temperature seasonality we will discuss how the type of seasonal changes in sea water isotope composition that may be expected in a rocky shore setting may influence our conclusions.

Apart from this, all my comments and suggestions are relatively minor. Therefore, I recommend this manuscript to be accepted with minor revisions. Please also note the supplement to this comment:

https://www.biogeosciences-discuss.net/bg-2019-74/bg-2019-74-RC1-supplement.pdf

Comments in PDF supplement:

Comments & suggestions:

P2, L54: What does the "it" in this sentence exactly refer to? The Late Cretaceous cooling trend?

Yes, this refers to the cooling trend, we will replace "It" by "The cooling trend" for clarity.

P2, L57-59: In the 90's chalk was still considered to record sea surface conditions faithfully. Over the last decades, this viewpoint has changed. Most chalk consists of recrystallized material. As a result, d18O values usually result in much lower temperatures, e.g. resulting in the (apparent) Cool Tropics Paradox. I advise the authors to read up on this. The values recorded by Jenkyns et al. are in all likelihood a large underestimation of SSTs (with even Cenomanian-Turonian values still below 28 degrees…). In reality, Cretaceous SST's were probably much higher. See for example the review paper of O'Brien et al., 2017.

This is a valid comment, and we will briefly discuss this later insight in our introduction. However, we do note that the introduction of previous work on chalk here mostly serves to introduce the reader into climate reconstructions from successions in the Boreal Chalk Sea. We would therefore rather add some discussion about the validity of SST reconstructions from such successions in the discussion section, where we compare different temperature estimates.

P2 L67-68: With a Tethys ocean still present, a Panama corridor still present and closed-off Tasman and Drake Gateways, I wouldn't state that the continental configuration is "relatively modern". Yes: apart from India, most continents were already close to their present-day position, but from a climatological and paleoceanographical perspective, the Late Cretaceous continental configuration was widely different. Of course, this does not mean that the Campanian could be considered an interesting analogue. I just would not play the continental configuration card.

Valid point, we will rephrase this and nuance our introduction of the Campanian as a reference for future climate, removing the notion of "relatively modern" continental configuration.

P2 L73-75: Does the data represent a fundamental component of the climate system? Or the seasonality? Please rephrase.

We will rephrase this to ", although seasonality constitutes a fundamental component of the climate system"

P3 L93 "The incorporation of these chemical proxies into bivalve shells…": This is a confusing sentence. Are the authors discussing the application of proxies on bivalve shells? Or are they concerned with the incorporation of chemical signals into bivalve shells?

Agreed, we will rephrase this sentence stating that the application of trace element proxies in bivalve shell records is complicated by vital effects.

P3 L109-126 "The Kristianstad Basin….": This paragraph feels a bit misplaced. There is a large jump from the previous paragraph (on the value of mollusks as archives of seasonality) to this one (on the Kristianstad Basin). I think this paragraph would better fit directly after the first paragraph of the Introduction. The first paragraph of the section ends with the notion that Late Cretaceous seasonality records from high latitudes are scares. This could very easily be followed by "The Kristianstad Basin in Sweden provides a great potential for such a high latitude seasonality records. Particularly the Ivo Klack site, located on the southeastern Baltic…. Etcetera).

We thank the reviewer for this suggestion and indeed agree that this paragraph fits better straight after the introduction into the Boreal Chalk Sea reconstructions. We will move the paragraph to this location in the revised version and introduce bivalve shells as climate archives after the site description.

P3 L110-112: suggestion: "The coarsely latest early Campanian shallow marine sediments deposited at Ivö Klack consist of sandy and silty nearshore deposits containing carbonate gravel (Christensen, 1975; 1984; Surlyk and Sørensen, 2010; Sørensen et al., 2015)." (to avoid a confusing "and are.." construction.

We like this suggestion by the reviewer and will implement it with a minor change: "The coarsely uppermost lower Campanian shallow marine sediments deposited at Ivö Klack consist of sandy and silty nearshore deposits containing carbonate gravel (Christensen, 1975; 1984; Surlyk and Sørensen, 2010; Sørensen et al., 2015)."

P3 L114: maybe start a new sentence on the paleolatitude.

Agreed, we will rephrase this to "…Late Cretaceous transgression. The paleolatitude of the site is 50°N."

P3 L115: no glaciotectonic movements in this region?

Post-glacial vertical crustal motion of the Kristianstad Basin is very limited (between -1 and +1 mm/yr), because the area is situated in the neutral uplift zone between compressed crust that is rebounding (most of the Scandinavian peninsula) and the glacial bulge (more to the south; Vestøl et al., 2019). The quiet tectonic history of this area is also documented in a report by Paulamäki & Kuivamäki (2006). Similar observations about the lack of glacio-eustatic rebound and other tectonic activity in the area have been documented by Surlyk and Sørensen (2010) and Christensen (1984).

- **Christensen, W. K.: The Albian to Maastrichtian of southern Sweden and Bornholm, Denmark: a review, Cretaceous Research, 5(4), 313–327, 1984.**
- **Paulamaeki, S. and Kuivamaeki, A.: Depositional history and tectonic regimes within and in the margins of the Fennoscandian shield during the last 1300 million years, Posiva Oy. [online] Available from: http://inis.iaea.org/Search/search.aspx?orig_q=RN:43061185 (Accessed 12 February 2020), 2006.**
- **Surlyk, F. and Sørensen, A. M.: An early Campanian rocky shore at Ivö Klack, southern Sweden, Cretaceous Research, 31(6), 567–576, 2010.**
- **Vestøl, O., Ågren, J., Steffen, H., Kierulf, H. and Tarasov, L.: NKG2016LU: a new land uplift model for Fennoscandia and the Baltic Region, J Geod, 93(9), 1759–1779, doi:10.1007/s00190-019-01280-8, 2019.**

P3 L124: I presume "original shell material " only refers to the calcitic material? Or is aragonite also preserved?

The oyster shells we describe contain very little original aragonitic shell structures (oysters only build thin aragonite structures at the resilium and the adductor muscle scar), so we only investigated calcite preservation in our study. The same holds true for the cited studies into macrofossils at this site. To clarify this, we will specifically refer to "calcite shell preservation" in the revised manuscript text.

P7 L195: TSR and TSA are not specified. What do there abbreviations stand for?

These stand for Time of Stable Accuracy and Time of Stable Reproducibility, terms which are defined in de Winter et al., 2017b. We will revise this section by writing out the full names of these terms and briefly defining what is meant by them in the context of microXRF measurement quality.

P8 L243-244: what percentage of samples were run in duplicate?

Duplicates were measured during every run of ~30 samples. We will mention this in the revised manuscript.

P11 L340-346: There are a lot of 'allows' in this paragraph. Maybe rephrase a sentence or two?

Good point, we rephrase the sentences on lines 341-346 to: "From this extrapolation we could estimate the total shell height from microstructural growth markers (Fig. 3; following Zimmt et al., 2018), linking growth to changes in shell chemistry. This way, chemical changes in the shell can be interpreted in terms of environmental changes by applying calibration curves for trace element proxies that were previously established for modern oyster species (e.g. Surge and Lohmann, 2008; Ullmann et al., 2013; Mouchi et al., 2013; Dellinger et al., 2018)."

P11 L358-360: This sentence is slightly confusing because the "(deeper waters)" directly follows the "bivalves". This reads as if the bivalves live in deeper waters, rather than the belemnites. Please rephrase.

We rephrased this to: "This suggests that $\delta^{13}C$ in belemnite rostra are affected by vital effects while heavier $\delta^{18}O$ values of the belemnites suggest that belemnites lived most of their life away from the coastal environment (in deeper waters),"

P13 L388-389: How is the assumption of a constant d18O of seawater justified? Wouldn't such a coastal site be susceptible for seasonal changes in riverine input? Particularly since the fennoscandian shield is usually placed in a wet/temperate climate belt, in Late Cretaceous climate reconstructions. The reference provided by the authors (Thibault et al., 2016) concerns a study on the chalks of the Stevns-1 core, which represents a much more distal site than Ivo Klack.

This comment reflects the major criticism of the reviewer. We hope that by more thoroughly discussing the stable oxygen isotope composition of sea water we can acknowledge the shortcomings of this assumption of constant seawater $\delta^{18}O$ values.

P13 L394-396 "Superimposed on these changes, a statistically significant ontogenetic trend can be discerned in the d13C records of 10 out of 12 shells. However, the scale and direction of these trends do not seem consistent between shells.":

(1) I understood that only 5 of the 12 specimens were measured for isotopes? How can the authors have d13C data on all 12 shells? In table 1, only the 5 specimens are mentions, of which 3 out of 5 seem to have a statistically significant trend? It looks like something got mixed up here

(2) Please insert a reference to Table 1 here. This was not immediately clear from the text.

(3) I am intrigued by the difference in the direction of supposed ontogenetic trends. On the other hand, the only shell with a negative trend doesn't show a statistically significant trend….

We fully agree with all the reviewer's points of critique here, something must have gotten mixed up here and we apologize for the mistake. We will rephrase this sentence as follows: "Superimposed on these changes, a statistically significant ontogenetic trend can be discerned in the d13C records of 3 out of 5 shells. In specimens that show a statistically significant ontogenetic trend $\delta^{13}C$ increases with age (see Table 1)".

P13 L403: Supplementary file S10 seems to be missing from the supplements

File S10 contains the plots of multiproxy records against age. We regret that these plots did not make it into the supplement and will make sure that they do in the revised version. In response to comments by the second reviewer, we now show $\delta^{18}O$ records of all shells in the main manuscript as well.

P16 L451-453: Is anything known about annual variations in growth rates in modern oysters? Do they respond to food availability? Could this be an early spring phytoplankton bloom? Or some other environmental parameter? Or is there a relationship with something like spawning?

In the revised manuscript, we will add some discussion here about how these findings compare with those in modern oysters. There is some literature on this which suggests indeed that food availability plays a role. We hypothesize the presence of a spring phytoplankton bloom later in the manuscript, but will move this hypothesis forward here, where we can discuss it together with the comparison with modern oyster species.

P20 L568: salinities are usually not indicated in g/kg, but either in psu or in m%

We will convert these values to psu.

P21 L600: "as well as" should be replaced by "including", since bivalves with symbionts are also marine or freshwater bivalves.

Correct, we will rephrase this.

P22 L644 "because not all seasons contributing to the average have long growing seasons": seasons having long growing seasons? This is a confusing sentence. Please rephrase.

We agree that this is a convoluted sentence and will rephrase as follows: "Averaging seasonality (Fig. 8) underestimates the extent of seasonality at Ivö Klack, because not all specimens contributing to the average have long growing seasons, which will reduce the average extent of seasonality."

P23 L696-698: Why would oysters need to compensate for lower ambient Sr concentrations? What is the benefit of building Sr into their shells? How does this help to compensate for lower seawater Sr concentrations?

We agree that "compensate" is not the right term here. We will rephrase as follows: "Therefore, the similarity in absolute calcite Sr/Ca ratios between modern *C. gigas* and Campanian *R. diluvianum* demonstrates that *R. diluvianum* incorporated more Sr into its shell relative to the ambient seawater concentration. This observation may entail that there is a minimum Sr concentration that is favorable for oysters to incorporate, or that there is a fixed physiological limit to oyster's discrimination against building Sr into their shells that is independent of ambient Sr concentrations."

P24 L774-782: Is anything known about the spawning season of modern oysters? Maybe the authors could discuss how similar or dissimilar their results are.

Modern oysters typically spawn at the end of the spring season and spat settles in during summer. This makes our result for *R. diluvianum* different from the modern situation. We will acknowledge this in the revised manuscript and provide references for spawning of modern *C. gigas*.

P25 L819-832: The notion of a spring supply of freshwater, bringing in nutrients, causing a spring phytoplankton bloom, is somewhat conflicting with the assumption of a constant d18O of seawater, discussed in lines 388-389. Note to the authors: at modern day mid- to high latitudes, the spring bloom is often triggered by storm-induced mixing. A spring bloom is not necessarily related to riverine input of nutrients. It could be related to changes in mixed-layer depth as well..

We thank the reviewer for this comment and advice and will add this to the discussion. As mentioned in our reply to his major comment, we will discuss potential changes in seawater composition in more detail in the revised manuscript and specifically revise this paragraph detailing how changes in seawater composition can affect our interpretation in terms of temperature seasonality.

Interactive comment on "Shell chemistry of the Boreal Campanian bivalve Rastellum diluvianum (Linnaeus, 1767) reveals temperature seasonality, growth rates and life cycle of an extinct Cretaceous oyster" by Niels J. de Winter et al.

Andrew Johnson (Referee)

a.l.a.johnson@derby.ac.uk

Received and published: 4 February 2020

See attached PDF

Please also note the supplement to this comment:

https://www.biogeosciences-discuss.net/bg-2019-74/bg-2019-74-RC2-supplement.pdf

Comments in PDF supplement:

Comments on de Winter et al. (submitted to Biogeosciences)

This paper contains a great deal of carefully collected data but I think that it suffers from the sheer volume of information, and the attempt to discuss all issues to which the data may relate. Had the authors started with a question rather than with the data they would have developed a clearer line of argument, making the contribution easier to read, more persuasive and (I think, ultimately) more used. The main 'question' is probably seasonality in the Cretaceous, but we are led in various other directions, and certain important issues relating to the δ18O data go undiscussed in the process. By contrast, there is extensive discussion of the meaning of the trace-element information but these data in the end contribute nothing to the seasonality question – temperature variation is determined entirely from the δ18O data. There is a separate paper to be written on why the trace-element data does not help in determining seasonality. I suggest the authors focus here on doing a good job with the δ18O data (its implications for seasonality, together with those for growth) and deal only with trace-element data in so far as it relates to age and preservation.

This is a valid point, and agree that our trace element data does, in the end, not contribute as much to the seasonality story as we would have hoped initially. We would therefore largely follow the reviewer's suggestion and strongly limit our discussion of the trace element data. However, we do not fully agree that the trace element data by itself would stand alone in a manuscript. Therefore, we would like to keep discussing (albeit more briefly) the patterns in trace element concentrations we find in our specimens. Moreover, we believe that the comment raised here is also partly a result of the (admittedly somewhat chaotic) structure our manuscript inherited in our attempt to tie together several lines of evidence and reasoning about the species' paleobiology and living environment. Besides shortening the discussion of trace element results, we will also make an attempt to streamline the manuscript as a whole to make these lines of reasoning easier to follow.

With respect to the δ18O data my main query is the authors' abandonment of their initial estimate of seasonal temperature range (5.2°C) in favour of a much higher figure (13.4°C), representing the difference between the maximum and minimum temperatures from all the shells sampled. They then go on to compare this with figures for seasonal temperature range in the North Sea now and at lower latitudes in the Cretaceous, but it is not clear whether these figures are derived from equivalent (extreme) summer and winter values. If they are not the comparisons are worthless, and the conclusions about latitudinal seasonality variation in the Cretaceous compared to now will need to be reformulated. It looks like the figure for the North Sea now is based on extreme values (the stated range of 16–20°C is much higher than the mean range of about 11°C in the southern North Sea) but the authors need to explain this.

This is a valid comment, and we will reevaluate this part of the manuscript where we compare our seasonality results with modern and reconstructed seasonality data. Data such as SST profiles of the present-day North Sea will invariably show differences depending on where these data were sampled from (e.g. from which water depth or locality). We will therefore be more careful in stating how exactly the data were sourced, whether these are extreme seasonal ranges or (more conventionally) differences between extreme monthly temperatures and how they compare to reconstructed seasonal amplitudes.

Another obscure use of the δ18O data is in Fig. 10. I looked at this, the caption, and the accompanying text for a long time but could not understand how the time of spawning was being inferred. The statement (LL 493–494) 'The onset of the first growth year in each shell at its precise position relative to the seasonal temperature cycle showed in which season spawning occurred (Fig. 10c)' does not mean anything to me – what is 'the first growth year'? The caption of part b added to my confusion since it does not describe what is illustrated—a bivariate plot of minimum growth temperature against mean annual temperature.

We acknowledge that Fig. 10 may not be very clear, and we will attempt to revise this figure to clarify what we would like to show here. We take out Figure 10b as it distracts from the main point: that spawning occurs in the cold season, just before or after the growth cessation. The time of spawning could be placed relative to the seasonal stable oxygen isotope cycle by noting during which part of the annual cycle shell growth started. Assuming the regular variations in stable oxygen isotope composition reflect temperature seasonality, the season in which the bivalve started growing can be inferred from phase of the oxygen isotope sinusoid during onset of growth. We will clarify how this is achieved in more detail in the revised version of the manuscript.

These two instances where further explanation is required of the use of δ18O data only emphasise the need to exclude discursive trace-element data and discussion, especially if (as recommended below) all the δ18O profiles are included in the main text.

Some other points:

LL54–55. How is the cooling trend 'recorded in the white chalk successions…'?

The cited references are of studies in which (mostly) oxygen isotope records from these chalks have been used to document this cooling trend. For clarity, we will rephrase this sentence as: "The cooling trend is well documented in stable oxygen isotope records from the white chalk successions of the Chalk Sea, which covered large portions of northwestern Europe during the Late Cretaceous Period…"

L99. The 'vital effects' largely relate to trace element content. A small effect on isotopic composition has been noted in Pecten maximus but little or no effect in other scallop species.

Agreed, we will clarify this in the revised version. "Vital effects" on oxygen isotope composition in bivalves are rare, and most of them are thought to precipitate at or close to isotopic equilibrium.

Fig. 3a. The use of the false yellow colour needs to be explained in the caption. What is the (non-sediment) yellow-coloured area – maybe altered pallial myostracum? If so, the early ontogenetic samples would be from the inner shell layer – not ideal material (deposited far from the shell edge) and maybe an explanation for some aberrant data.

We will add a description of the yellow color in the figure caption. This is indeed the color we use to highlight highly altered shell material and sediment infilling, as seen in the XRF maps below.

L 258. Some brief justification is required for the choice of value for water δ18O, even if it repeats Thibault et al. (2016) – this is an important issue in the present context.

This comment touches on the major comment posed by our other reviewer (dr. Johan Vellekoop). We hope that the changes we will make in reply to his comment will satisfy this comment as well.

L288. The parallelograms are not in 'different shades of blue'.

Correct, this is a remnant of an earlier version of this figure. We will correct this by stating that the specimens are represented by parallelograms of different colors matching the probability distributions below.

L348. Exclude 'multi-proxy' (redundant).

Agreed, this will be removed.

L368. Exclude 'vast' – there are quite a lot of δ18O values associated with a Mn content of more than 100 µg/g.

Agreed, we will remove "vast"

L373. The results for C. gigas are not in 'grey/black'.

Correct, this again refers to a previous version of the figure. We have overlooked this error and will correct it in the revised version, stating that the results of *C. gigas* are in yellow/brown.

Fig. 6. Explain the vertical dashed lines (corresponding to the maxima in the δ18O plot); change 1.0 to -1.0 for the water value on the y-axis. I think it would be worth having the d18O profiles from all the shells (not just this one) in the main text, so that the reader can get a picture of all the important data (see also comment on L457).

We will add a sentence to the caption stating that the vertical dashed lines separate growth years. In addition, we will correct the typographic error in our assumed $\delta^{18}O_{sw}$ value. We will add a composite figure displaying all $\delta^{18}O$ data used in this study.

L425. 'virginica' in italics.

Certainly, we will change this in the revised text.

L437. 'follows' rather than 'shows'

Correct, this will be rephrased.

LL450–451. You don't mean 'seasonal temperature range … was between 16°C and 21°C'. I suggest you say 'temperature varied between 16°C in winter and 21°C in summer'.

Agreed, we will rephrase this accordingly.

L457. This is where you need to be able to refer to all the δ18O profiles.

Agreed, we will refer to the composite figure we will add showing all $\delta^{18}O$ records here.

Fig. 9. It is not clear to me how ages were derived for the start of the growth curves. Were growth increments used?

For most specimens, $\delta^{18}O$ measurements were possible until very close to the onset of mineralization. For the specimens were this was not the case, we used a combination of annual growth increments and extrapolation of the $\delta^{18}O$-based age model to infer the age of the ontogenetically oldest $\delta^{18}O$ measurements. We will clarify this in the revised version.

L583. 'placed' rather than 'replaced'.

Agreed, we will rephrase this.

LL664–665, 703–704. Repetitions of earlier statements.

Agreed, we will significantly shorten these sections about trace element concentrations and remove these repetitions. This is also in response to the major comments by the reviewer stating (rightfully) that the discussion of trace element patters distracts from the main seasonality discussion in the manuscript which is mostly based on $\delta^{18}O$ records.

LL752–3. 'cemented together in groups' suggests there would have been space competition and a 'high-energy environment' is not obviously something that would reduce space competition – needs explanation.

Here we wanted to refer specifically to the competition with other taxa, which would not thrive in this high-energy environment. In addition, the *in situ* distribution of oysters on the fossil rocky shored of Ivö Klack as documented in Surlyk and Christensen (1974) and Sørensen et al. (2012) shows that there is limited competition for space. We will rephrase "cemented together in groups" into "cemented next to each other in groups" to clarify that the oysters are not cemented on top of each other (as modern *C. gigas* often is) and have less space limitations that modern oysters.

L760. 'deep shelf' for 'deep marine' – Placopecten magellanicus does not occur in anything other than shelf environments.

Correct, we will change this throughout the text.

General point: please refer in the text to relevant parts of figures (where identified by letter) rather than the whole figure, to facilitate rapid appreciation of data.

In the revised manuscript, we will go through all the figure references and specify the parts of figures wherever relevant.

Shell chemistry of the Boreal Campanian bivalve *Rastellum diluvianum* (Linnaeus, 1767) reveals temperature seasonality, growth rates and life cycle of an extinct Cretaceous oyster.

Niels J. de Winter[1], Clemens V. Ullmann[2], Anne M. Sørensen[3], Nicolas ~~R.~~ Thibault[4], Steven Goderis[1], Stijn J.M. Van Malderen[5], Christophe Snoeck[1,6], Stijn Goolaerts[7], Frank Vanhaecke[5], Philippe Claeys[1]

[1]AMGC research group, Vrije Universiteit Brussel, Pleinlaan 2, B-1050 Brussels, Belgium.

[2]Camborne School of Mines, University of Exeter, Penryn, Cornwall, TR10 9FE, UK.

[3]Trap Danmark, Agem All 13, DK-2970, Hørsholm, Denmark.

[4] Department of Geoscience and Natural Resource Management, University of Copenhagen, Øster ~~voldgade~~ Voldgade 10, DK-1350 Copenhagen C., Denmark.

[5]A&MS research unit, Ghent University Campus Sterre, Krijgslaan 281, Building S12, B-9000 Ghent, Belgium.

[6]G-Time laboratory, Université Libre de Bruxelles, 50 Avenue F.D. Roosevelt, B-1050, Brussels, Belgium.

[7]Directorate of Earth and History of Life, Royal Belgian Institute of Natural Sciences, Vautierstraat 29, B-1000 Brussels, Belgium.

Correspondence to: Niels J. de Winter (niels.de.winter@vub.be)

Abstract

The Campanian age (Late Cretaceous) is characterized by a warm greenhouse climate with limited land ice volume. This makes ~~the Campanian~~this period an ideal target for ~~the study of~~studying climate dynamics during greenhouse periods, which are essential for predictions of future climate change due to anthropogenic greenhouse gas emissions. Well-preserved fossil shells from the Campanian ~~age~~ (±78 Ma) high ~~paleolatitude~~ mid-latitude (50°N) coastal faunas of the Kristianstad Basin (southern Sweden) offer a unique snapshot of short-term climate and environmental variability ~~during the Campanian~~, which complement ~~traditional~~ existing long-term climate reconstructions. In this study, we apply a combination of high-resolution spatially resolved trace element analyses (µXRF and LA-ICP-MS), stable isotope analyses (IRMS) and growth modelling to study short-term (seasonal) variations recorded in the oyster species *Rastellum diluvianum* from the Ivö Klack locality. ~~A combination of trace element and stable isotope~~Geochemical records ~~of~~ through 12 specimens shed~~s~~ light on the influence of specimen-specific and ~~age-specific~~ontogenetic effects on the expression of seasonal variations in shell chemistry and allows disentangling vital effects from environmental influences in an effort to refine palaeoseasonality reconstructions of Late Cretaceous greenhouse climates. Growth ~~modelling~~ models based on stable oxygen isotope records ~~from *R. diluvianum* further allows to discuss~~yield information on the mode of life, circadian rhythm and reproductive cycle of these extinct oysters ~~and sheds light on their ecology~~. This multi-proxy study reveals that mean annual temperatures in the Campanian high~~er mid~~-latitudes were 17 to 19°C with winter minima of ~~-~~13°C and summer maxima of 26°C, assuming a Late Cretaceous seawater oxygen isotope composition of -1‰VSMOW~~a maximum extent of seasonality of 14°C~~. These results yield Campanian ~~show that the~~ latitudinal temperature gradient~~s~~ ~~in mean annual temperatures during the Late Cretaceous was~~similar to the present, but with smaller latitudinal differences in temperature seasonality ~~steeper than expected based on climate models and that the difference in seasonal temperature variability between latitudes was much smaller in the Campanian compared to today.~~, contrasting with previous notions of "equable climate" during the Late Cretaceous. Our results also demonstrate that species-specific differences and uncertainties in the composition of Late Cretaceous seawater prevent trace element proxies (Mg/Ca, Sr/Ca, Mg/Li and Sr/Li) to be used as reliable temperature proxies for fossil oyster shells. However,

trace element profiles can serve as a quick tool. for diagenesis screening and investigating seasonal growth patterns in ancient shells.

1. Introduction

The Late Cretaceous was marked by a long cooling trend that brought global mean annual temperatures (MAT) down from the mid-Cretaceous climate maximum (±28°C surface ocean temperatures) in the Cenomanian and Turonian (±95 Ma) to slightly cooler temperatures (±22°C surface ocean temperatures) around the Campanian-Maastrichtian boundary (±72.1 Ma; Clarke and Jenkyns, 1999; Pearson et al., 2001; Huber et al., 2002; Friedrich et al., 2012; Scotese, 2016). This cooling trend was likely caused by a change in ocean circulation, initiated by the opening of the Equatorial Atlantic Gateway that separated the proto-North and -South Atlantic Ocean basins (Friedrich et al., 2009). It The cooling trend is well documented in stable oxygen isotope records from the white chalk successions of the Chalk Sea, which covered large portions of northwestern Europe during the Late Cretaceous Periodis well recorded in the white chalk successions of the Chalk Sea, which covered large portions of northwestern Europe during the Late Cretaceous Period (Reid, 1973; Jenkyns et al., 1994; Jarvis et al., 2002; Voigt et al., 2010). The connection of the Chalk Sea to the (proto-)North Atlantic Ocean makes it an interesting area of study to constrain Late Cretaceous paleogeography and climate. These chalk successions featured in various paleoclimate studies, because they are accessible in good outcrops and consist predominantly of calcareous nannofossils which were thought to faithfully record sea surface conditions (e.g. Jenkyns et al., 1994). However, recent studies (e.g. O'Brien et al., 2017; Tagliavento et al., 2019) have shown that diagenetic overprinting likely biases these records towards cooler temperatures, resulting in the apparent Cool Tropics Paradox (Pearson et al., 2001). Furthermore, the connection of the Chalk Sea to the (proto-)North Atlantic Ocean makes it an interesting area of study to constrain Late Cretaceous paleogeography and climate. Even with this prolonged cooling trend in the Late Cretaceous, proxy data and climate models show that the Campanian was still characterized by a relatively warm global climate with a shallow equatorial temperature gradient compared to today (Huber et al., 1995; Brady et al., 1998; Huber et al., 2002). Even though sea level changes seem to indicate possible small changes in land ice volume during the Late

Cretaceous, warm high-latitude paleotemperatures ~~seem to~~likely rule out the possibility of extensive polar ice sheets comparable in volume to modern ice caps (Barrera and Johnson, 1999; Huber et al., 2002; Jenkyns et al., 2004; Miller et al., 2005; Thibault et al., 2016).

~~-~~Given ~~these~~ its warm, land ice free ~~climatic~~ conditions ~~and a relatively modern continental configuration~~, the Campanian serves as an interesting analogue for Earth's climate in the ~~near~~ future, should anthropogenic and natural emissions continue to contribute to the rise in global temperatures and decrease global ice volume on Earth (IPCC, 2013; Donnadieu et al., 2016). However, ~~M~~most Late Cretaceous climate reconstructions focus on reconstructing and modelling long-term evolutions of humid/arid conditions on land ~~and/~~or past atmospheric and oceanic temperatures (DeConto et al., 1999; Thibault et al., 2016; Yang et al., 2018). Data on the extent of seasonal variability from this time period, especially ~~from high-latitudes~~outside the tropics, are scarce, although ~~such data~~seasonality constitutes a fundamental component of the climate system (Steuber, 1999; Steuber et al., 2005; Burgener et al., 2018). Furthermore, many proxies used for paleoclimate reconstruction risk being seasonally biased, and thus independent seasonality reconstructions serve as important tools to verify other climate reconstructions.

2. Background

2.1 Geological setting

The Kristianstad Basin, our study site, is located on the southeastern Baltic Sea coast of the southern Swedish province of Skåne, which is presently located at ~~(~~56°2' N, 14° 9' E~~;~~ (see **Fig. 1**), somewhat higher than its Campanian paleolatitude, which is estimated at 50°N (van Hinsbergen et al., 2015).~~)~~. The uppermost lower Campanian shallow marine sediments deposited at Ivö Klack consist of sandy and silty nearshore deposits containing carbonate gravel~~Shallow marine sediments deposited at Ivö Klack consist of sandy and silty nearshore deposits containing carbonate gravel and are coarsely dated in the latest early Campanian~~ (Christensen, 1975; 1984; Surlyk and Sørensen, 2010; Sørensen et al., 2015). The ~~sediments were deposited in a near-shore setting~~depositional setting is described as a rocky coastline that was inundated during the maximum extent of the Late Cretaceous transgression~~,~~ (Kominz et al., 2008; Csiki-Sava et al., 2015). ~~the paleolatitude is 50°N (Kominz et al., 2008; Csiki-Sava et al., 2015).~~ Since the region

has remained tectonically quiet since the Campanian, the deposits of Kristianstad Basin localities remain at roughly the same altitude as when they were deposited and have been subject to limited burial (Christensen, 1984; Surlyk and Sørensen, 2010).

-The rocky shore deposits of Ivö Klack are characterized by a diverse shelly fauna, consisting of well-preserved fossils and fragments of brachiopods, belemnites, echinoids and asteroids, polychaete worms, gastropods, corals, ammonites and thick-shelled oysters, with a total of almost 200 different recognized species (Surlyk and Sørensen, 2010). In this diverse rocky shore ecosystem, various habitat zones can be distinguished, each with their distinct suite of organisms adapted to local conditions of varying amounts of sunlight, sedimentation and turbulence (Surlyk and Christensen, 1974; Sørensen et al., 2012). This unique combination of marine biodiversity and preservation of original calcite shell material makes the localities in the Kristianstad Basin ideal for studying sub-annual variability in shell chemistry and reconstructing paleoseasonality and environmental change in the Campanian (Sørensen et al., 2015).

2.2 Bivalve shells

Fossil bivalve shells offer a valuable ~~record~~ archive for studying past climates on a seasonal scale. ~~The chemistry of their shells records information on the environment in which bivalves grew, and i~~Incremental measurements of ~~chemical changes~~shell chemistry ~~along the~~in growth direction (~~sclerochronological~~ sclerochronology studies) potentially yield records of seasonal ~~environmental~~ changes in the environment (Mook, 1971; Jones, 1983; Klein et al., 1996~~a~~; Schöne and Gillikin, 2013). Their distribution allows paleoseasonality reconstructions from bivalves across a wide range of latitudes (Roy et al., 2000; Jablonski et al., 2017), and the preservation potential of calcitic shell structures (especially in oyster shells) makes them ideal, if not ~~one of the only~~unique, recorders of pre-Quarternary seasonality and sub-annual environmental change (Brand and Veizer, 1980; 1981; Al-Aasm and Veizer, 1986a; b; Immenhauser et al., 2005; Alberti et al., 2017). The incremental ~~growth of bivalve shells~~deposition of shell carbonate ~~in practice~~ means, in theory, that the limits in terms of time resolution of ~~reconstructions from~~the bivalve shell archive~~s~~ are governed by sampling resolution rather than the resolution of the record itself. ~~While~~ While periods of growth cessation can occur (especially in high latitudes, Ullmann et al., 2010)~~,~~ and the true mechanisms of

shell deposition on a very high (e.g. daily) temporal resolution are poorly constrained (see de Winter et al., 2020a and references therein), in practice ~~this~~ incremental shell deposition allows reconstructions of changes down to sub-daily timescales given the right sampling techniques (Schöne et al., 2005; Sano et al., 2012; Warter et al., 2018; de Winter et al., ~~in review~~2020a). Examples of chemical proxies used ~~for these~~in ~~paleoseasonality~~ such sclerochronology studies~~reconstructions~~ include stable carbon and oxygen isotope ratios and trace element ratios (e.g. Steuber et al., 2005; Gillikin et al., 2006; McConnaughey and Gillikin, 2008; Schöne et al., 2011; de Winter et al., 2017a; 2018).

2.3 Trace element proxies

The incorporation of ~~these chemical proxies~~trace elements and carbon isotopes into bivalve shells is ~~challenged by the~~ influenced ~~of~~ by so-called vital effects: biological controls on the incorporation of elements in the shell independent of the environment (Weiner and Dove, 2003; Gillikin et al., 2005). These vital effects have been shown to mask the characteristic relationships between shell trace element chemistry and the ~~environment, and~~environment and appear to be distinct not only between different bivalve species but also between specimens of different ontogenetic age (Freitas et al., 2008). Differences between bivalve families mean that the trace element chemistry of some taxa (like scallops: Family Pectinidae) are especially affected by vital effects (Lorrain et al., 2005; Freitas et al., 2008), while other families like oysters (Family Ostreidae) seem to be more robust recorders of environmental conditions (Surge et al., 2001; Surge and Lohmann, 2008; Ullmann et al., 2010; 2013). ~~Nevertheless, t~~The effect on shell composition and preservation of changes in microstructure and the amount of organic matrix present in different ~~parts of (oyster) shells~~shell layers ~~on shell chemistry and preservation~~ introduces uncertainty as to which parts of the shells are well-suited for reconstruction purposes (Carriker et al., 1991; Kawaguchi et al., 1993; Dalbeck et al., 2006; Schöne et al., 2010; 2013). The key to disentangling these vital effects from recorded environmental changes lies in the application of multiple proxies and techniques on the same bivalve shells (the “multi-proxy approach”; e.g. Ullmann et al., 2013; de Winter et al., 2017a; 2018) and to base reconstructions on more than one shell (Ivany, 2012).

2.4 Stable isotope ratios

Because nearly all bivalves precipitate their shells at or near oxygen isotope equilibrium, the stable oxygen isotope ratio of bivalve shell carbonate is less susceptible to vital effects, such as growth kinetics (Uchikawa and Zeebe, 2012). Therefore, stable oxygen isotope ratios in bivalve shell carbonate ($\delta^{18}O_c$) are solely dependent on calcification temperature and sea water oxygen isotope composition ($\delta^{18}O_{sw}$), and this proxy is frequently used in sclerochronology studies as a paleothermometer (Kim and O'Neil, 1997; Schöne et al., 2005; Butler et al., 2013; Ullmann et al., 2013; Huyghe et al., 2015; de Winter et al., 2020b). Oxygen isotope records can function as a reference in the above-mentioned multi-proxy studies aimed at resolving vital effects, environmental and climatic changes. However, the weakness of this proxy lies in the fact that $\delta^{18}O_{sw}$ is not always known, especially in deep time settings (Veizer and Prokoph, 2015). As a result, a constant $\delta^{18}O_{sw}$ of 0‰VSMOW for modern icehouse climate conditions, or -1‰VSMOW for an ice-free world (such as the Eocene or the Late Cretaceous; after Shackleton, 1986) is often assumed (e.g. Andreasson and Schmitz, 1996; Ivany and Runnegar, 2010; Huyghe et al., 2015). An offset of 1‰ between assumed $\delta^{18}O_{sw}$ and actual $\delta^{18}O_{sw}$ can result in a ~4.6°C temperature offset in temperature reconstructions (Kim and O'Neil, 1997) This assumption may therefore introduce inaccuracies in absolute temperature reconstructions, but relative variations in $\delta^{18}O_c$ can still yield important insights into high-resolution climate dynamics.

In marine mollusks, dissolved inorganic carbon (DIC) in the ambient sea water contributes the largest fraction of carbon (90%) used for shell mineralization (McConnaughey, 2003; Gillikin et al., 2007) and therefore heavily influences $\delta^{13}C$ values of shell carbonate. However, changes in respiration rates can alter the carbon budget of shell carbonate by adding or removing isotopically light respired carbon in the form of CO_2 (Lorrain et al., 2004). Environmental changes in DIC can also have a strong influence on this carbon budget, especially when bivalves grow in nearshore or estuarine conditions with large (seasonal) variations in environmental $\delta^{13}C$ of DIC and organic carbon (Gillikin et al., 2006). Conceptual models exist that attempt to correlate shell $\delta^{13}C$ in modern mollusks to environmental and physiological variations, but these require knowledge of ambient CO_2 pressures and $\delta^{13}C$ values of DIC, gas ventilation rates in the animal and CO_2 and O_2 permeabilities of calcifying membranes (McConnaughey et al., 1997), which are not available in fossil bivalve studies.

2.5 Aim

~~The Kristianstad Basin is located on the southeastern Baltic Sea coast of the southern Swedish province of Skåne (56°2' N, 14° 9' E; see **Fig. 1**). Shallow marine sediments deposited at Ivö Klack consist of sandy and silty nearshore deposits containing carbonate gravel and are coarsely dated in the latest early Campanian (Christensen, 1975; 1984; Surlyk and Sørensen, 2010; Sørensen et al., 2015). The sediments were deposited in a near shore setting described as a rocky coastline that was inundated during the maximum extent of the Late Cretaceous transgression, the paleolatitude is 50°N (Kominz et al., 2008; Csiki-Sava et al., 2015). Since the region has remained tectonically quiet since the Campanian, the deposits of Kristianstad Basin localities remain at roughly the same altitude as when they were deposited and have been subject to limited burial (Surlyk and Sørensen, 2010). The rocky shore deposits of Ivö Klack are characterized by a diverse shelly fauna, consisting of well-preserved fossils and fragments of brachiopods, belemnites, echinoids and asteroids, polychaete worms, gastropods, corals, ammonites and thick-shelled oysters, with a total of almost 200 different recognized species (Surlyk and Sørensen, 2010). In this diverse rocky shore ecosystem, various habitat zones can be distinguished, each with their distinct suite of organisms adapted to local conditions of varying amounts of sunlight, sedimentation and turbulence (Surlyk and Christensen, 1974; Sørensen et al., 2012). This unique combination of marine biodiversity and preservation of original shell material makes the localities in Kristianstad Basin ideal for studying sub-annual variability in shell chemistry and reconstructing paleoseasonality and environmental change in the Campanian (Sørensen et al., 2015).~~

In this study, we present a detailed, multi-proxy comparison of the growth and chemistry of well-preserved fossil shells of the thick-shelled oyster *Rastellum diluvianum* (Linnaeus, 1767) recovered from the Ivö Klack locality on the northern edge of the Kristianstad Basin. We combine stable isotope proxies conventional in sclerochronological studies ($\delta^{13}C$ and $\delta^{18}O$; e.g. Goodwin et al., 2001; Steuber et al., 2005) with less well-established trace element proxies (Mg/Ca, Sr/Ca, Mg/Li and Sr/Li; e.g. Bryan and Marchitto, 2008; Schöne et al., 2011; Füllenbach et al., 2015; Dellinger et al., 2018) and growth modelling based on $\delta^{18}O$ seasonality (Judd et al., 2018) in an attempt to disentangle the effects of growth rate, reproductive cycle and environmental change on shell chemistry. The data gathered in this study allow a detailed discussion on seasonal changes in temperature and water chemistry in the coastal waters of the Kristianstad Basin in the

575 late early Campanian, as well as on the life cycle of *R. diluvianum* and its response to seasonal changes in
576 its environment.
577

578

579

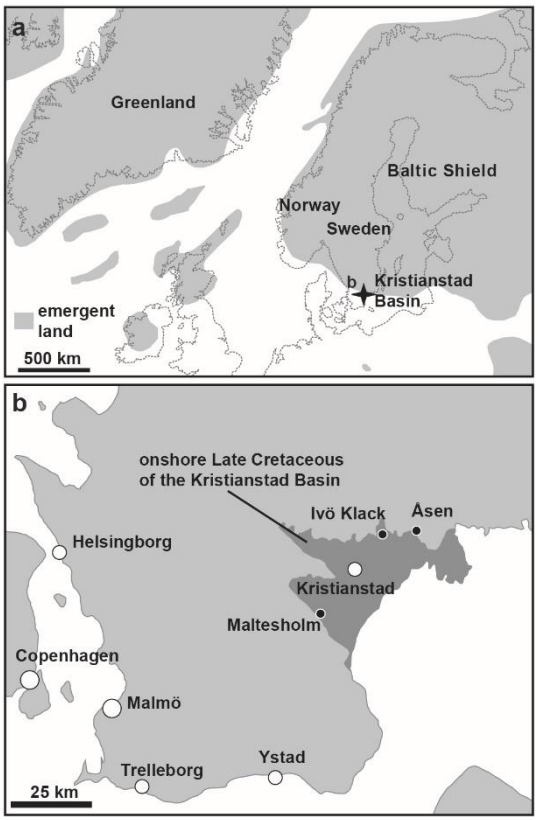

Figure 1: Paleogeographic map of the Boreal Chalk Sea (**a**) and the area of present-day southern Sweden (**b**) showing the location of Ivö klack (modified after Sørensen et al., 2015)

580

~~2~~3. Materials and Methods

~~2~~3.1 Sample acquisition and preparation

Complete valves of twelve individual *R. diluvianum* oysters were obtained from the Ivö Klack locality (see **Fig. 2**). Specimens of *R. diluvianum* were found *in situ* attached to the vertical sides of large boulders that characterized the rocky shore of Ivö Klack (Surlyk and Christensen, 1974) and are biostratigraphically assigned to the latest early Campanian *B. mammillatus* belemnite zone. The valves were cleaned and fully embedded in Araldite® 2020 epoxy resin (Bodo Möller Chemie Benelux, Antwerp, Belgium). Dorsoventral slabs (±10 mm thick) were cut perpendicular to the hinge line using a water-cooled slow rotating saw with a diamond-coated blade (thickness ± 1 mm; **Fig. 2**). The surfaces cut on the central growth axis were progressively polished using silicon-carbide polishing disks (up to P2500, or 8.4 µm grain size). Polished surfaces were scanned at high (6400 dpi) resolution using an Epson Perfection 1650 flatbed color scanner (Seiko Epson Corp., Suwa, Japan). Resulting color scans of all polished *R. diluvianum* shell cross sections are provided in **Fig. 2** and **S1**. Shell microstructures in *R. diluvianum* shells were studied in detail on high-resolution scans and by using reflected light optical microscopy. Microstructural features were used to reconstruct the relative timing of shell growth (see **Fig. 3**). Fragments of visually well-preserved material from different microstructures in the shells were coated with gold and studied under a Scanning Electron Microscope (Quanta 200 ESEM) and imaged at 1000x – 2000x magnification (**Fig. 3b-e**). Chemical analyses were carried ~~-~~out sequentially on polished cross sections in order of ~~sample size and~~ destructive character of sampling (starting with the least destructive measurements: µXRF, LA-ICP-MS, microdrilling for IRMS and finally MC-ICP-MS analysis on ~26 mg samples).

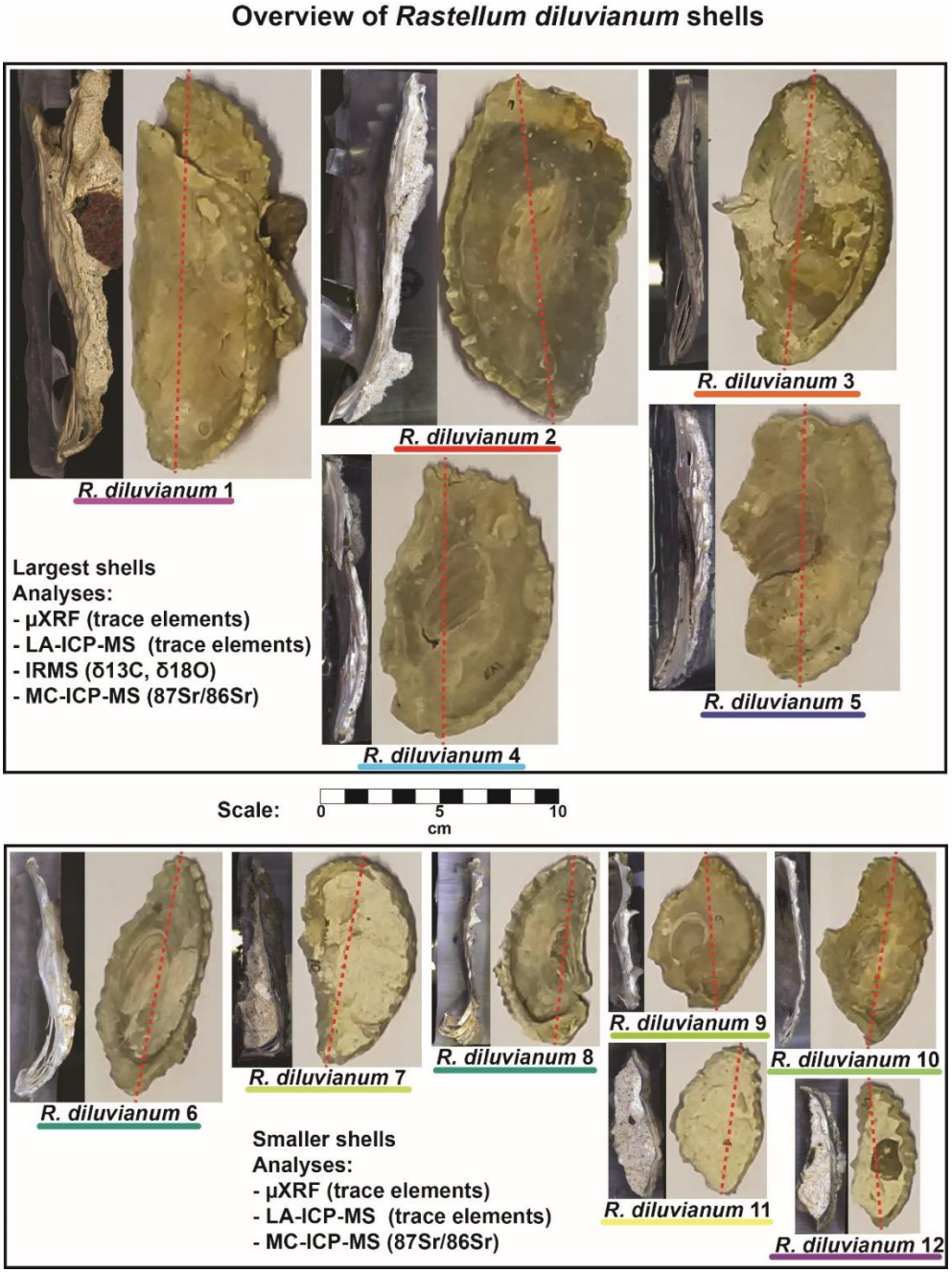

Figure 2: Overview of the 12 *Rastellum diluvianum* shells used in this study. All shells are depicted on the same scale (see scalebar in center of image). Colors of the lines under sample names correspond to the colors of the lines in Fig. 4, **Fig.** ~~7~~6, Fig. 8 and **Fig.** ~~9~~10. Every shell is represented by an image of the inside of the valve analyzed, as well as a color scan of the cross section through the shell on which high-resolution analyses were carried out. ~~The d~~Dashed red lines ~~s~~shows the location of these cross sections. The largest 5 shells (1-5, on top half) were sampled for IRMS analyses ($\delta^{13}C$ and $\delta^{18}O$). All shells were subjected to micro X-ray fluorescence (µXRF), laser ablation inductively coupled plasma mass spectrometry (LA-ICP-MS) and multi-cup inductively coupled

plasma mass spectrometry (MC-ICP-MS) analyses. Full-size versions of the high-resolution color scans of shell cross sections are provided in **S1**.

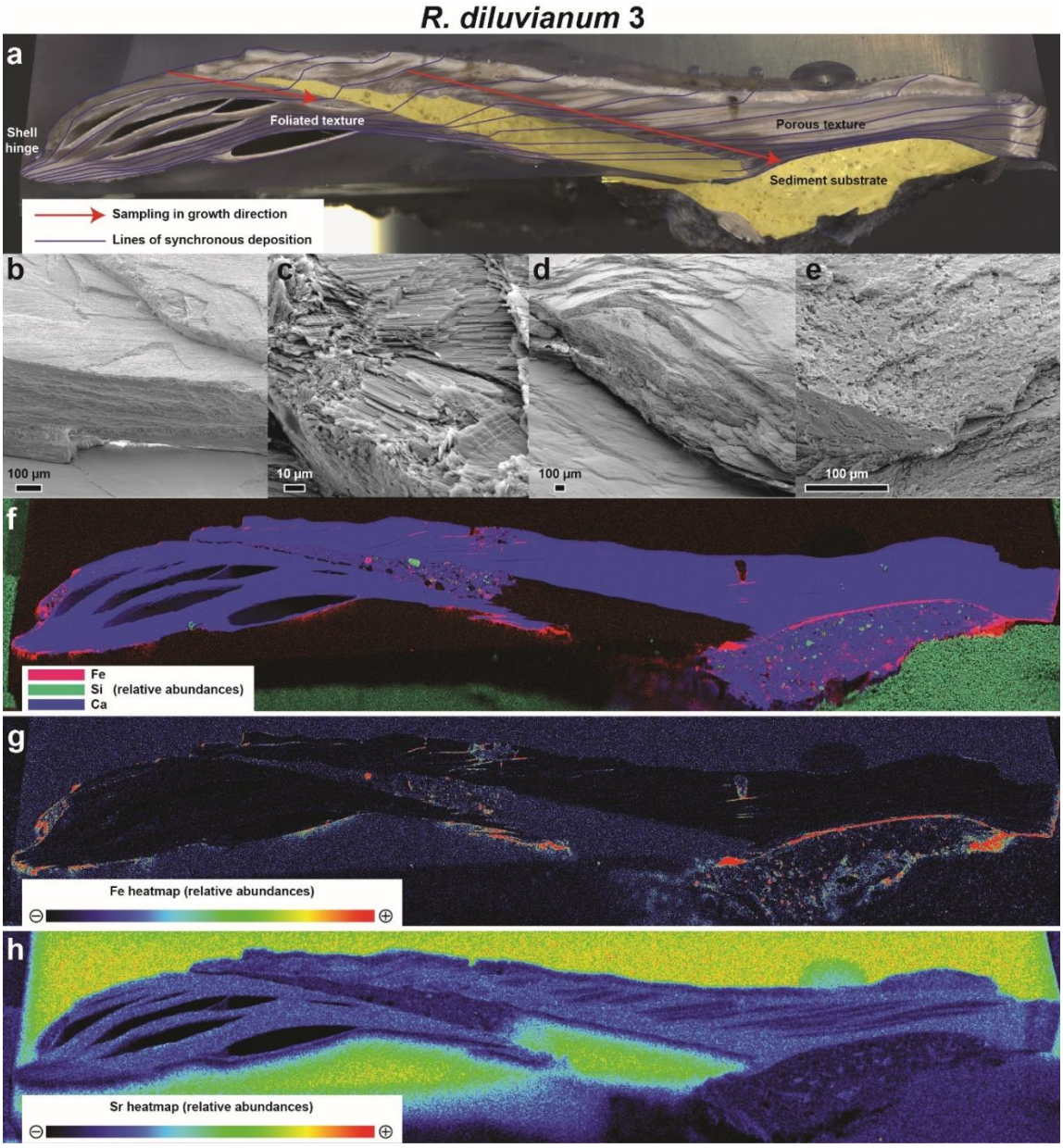

Figure 3: Overview image showing a high-resolution color scan of the cross section through *R. diluvianum* 3 (**a**) on which the different shell textures as well as the directions of high-resolution analyses (in growth direction) are indicated. Thin blue lines denote parts of the shell that were deposited at the same time (growth increments). Areas marked in yellow represent sediment infilling below and between the valves. (**b**) and (**c**) show SEM images of the well-preserved foliated calcite in the shell. More porous structures in the shell (vesicular calcite) are depicted in SEM images shown in (**d**) and (**e**). Below are shown three XRF elemental maps of the same cross section: ~~A~~An RGB-colored map displaying the relative abundances of Fe, Si and Ca (**f**), A heatmap of Fe concentrations (**g**; see scalebar below map) and a heatmap of Sr concentrations (**h**; see scalebar below map). XRF mapping only yields relative (semi-quantitative) abundance of elements.

622

~~2~~3.2 Micro-XRF mapping

Elemental abundance maps of all *R. diluvianum* shell cross sections were obtained using a Bruker Tornado M4 energy-dispersive micro-X-Ray Fluorescence scanner (µXRF; Bruker nano GmbH, Berlin, Germany) All µXRF analyses carried out with the Bruker M4 Tornado are non-destructive. The µXRF is equipped with a Rh filament metal-ceramic tube X-Ray source operated at 50 kV and 600 µA (30 W; maximum energy settings). The circular spot projected on the same surface is estimated to have a diameter of 25 µm (Mo-Kα). A µm-precision XYZ translation stage allows for quick and precise sample movement such that a grid of 25 µm XRF spots can be measured on the sample surface by continuous scanning to construct elemental maps ($3 * 10^6$ - $5 * 10^6$ pixels per map). Exposure times of the X-ray beam per sampling position in mapping mode (1 ms/pixel) are too short to gain adequate signal-to-noise ratio for pixel-by-pixel quantification of elemental concentrations. Instead, processing of entire map surfaces using the Bruker Esprit™ software allows semi-quantitative elemental abundance maps to be created of the sample surface based on a mapping of the count rate in Regions of Interest of elements (see de Winter and Claeys, 2016; de Winter et al., 2017b; **Fig. 3**). XRF maps allow for a rapid assessment of the preservation state of original shell calcite based on variations in Si, Mn, Fe and Sr concentrations and guide the selection of sampling protocols for further analyses (de Winter and Claeys, 2016; **Fig. 3**). Results of XRF mapping on all 12 *R. diluvianum* shell cross sections are provided in **S2**.

~~2~~3.3 Micro-XRF line scans

After XRF mapping, quantitative line scans were measured in growth direction on shell cross sections. Dwell times of 60 seconds per measurement yielded sufficiently high signal-to-noise ratios ~~sufficient to allow~~ for individual points in line scans to be quantified. This acquisition time was chosen as to provide the optimal compromise between increasing run time (improved signal/noise ratio; enhanced reproducibility) and increasing the number of sampling positions (improving sampling density and allowing duplicate measurements) for the elements Mg, Al, Si, P, S, Ca, Ti, Mn, Fe, Cu, Zn and Sr (~~TSR and TSA;~~ see discussion in de Winter et al., 2017b). The sampling ~~density~~ interval of line scans was 50 µm, adding up to a total of 11056 individual quantitative XRF spectra measured for this study. Spectra were quantified using

the Bruker Esprit software calibrated using the matrix-matched BAS-CRM393 limestone standard (Bureau of Analyzed samples, Middlesbrough, UK), after which individual measurements were calibrated offline using 7 matrix-matched certified reference materials (CCH1, COQ1, CRM393, CRM512, CRM513, ECRM782 and SRM1d), which were treated as samples (see Vansteenberge et al., ~~in review~~2020). R^2 values of calibration curves exceeded 0.99 and reproducibility standard deviations were better than 10% relative to the mean. Even though line scans were positioned on well-preserved shell calcite based on the XRF map results, a second check was carried out in which individual points were rejected based on conservative thresholds for diagenetic recrystallization or detrital contamination ([Ca] < 38 wt%, [Si] > 1 wt%, [Mn] > 200 µg/g or [Fe] > 250 µg/g; [Sr]/[Mn] < 100 mol/mol; see Al-Aasm and Veizer, 1986a; Sørensen et al., 2015). Concentrations of Ca, Mg and Sr in well-preserved shell sections were used to explore the potential of Mg/Ca and Sr/Ca molar ratios as paleoenvironmental proxies. Unprocessed results of XRF line scanning are provided in **S3**.

~~2~~3.4 LA-ICP-MS line scans

Spatially resolved elemental concentrations for Li, B, Mg, Si, P, Ca, Ti, V, Cr, Mn, Fe, Ni, Zn, Rb, Sr, Ba, Pb and U were calculated from a calibrated transient MS signal recorded during Laser Ablation-Inductively Coupled Plasma-Mass Spectrometry (LA-ICP-MS) line scanning in the growth direction (parallel to the XRF line scans) on ~~the~~ shell cross sections~~ using Laser Ablation-Inductively Coupled Plasma-Mass Spectrometry (LA-ICP-MS)~~. LA-ICP-MS measurements were carried out at the Atomic and Mass Spectrometry – A&MS research unit of Ghent University (Ghent, Belgium) using a 193 nm ArF*excimer-based Analyte G2 laser ablation system (Teledyne Photon Machines, Bozeman, USA), equipped with a HelEx 2 double-volume ablation cell, coupled to an Agilent 7900 quadrupole-based ICP-MS unit (Agilent, Tokyo, Japan). Continuous scanning along shell transects using a laser spot with a diameter of 25 µm, scan speed of 50 µm/s and detector mass sweep time of 0.5 s yielded profiles with a lateral sampling interval of 25 µm, amounting to a total of 9505 LA-ICP-MS data points gathered. The aerosol was transported using He carrier gas into the ICP-MS unit via the aerosol rapid introduction system (ARIS; Teledyne Photon Machines, Bozeman, USA). Elemental concentrations were calibrated using bracketed analysis runs on US Geological Survey (USGS) BCR-2G, BHVO-2G, BIR-1G, GSD-1G and GSE-1G and National Institute of Standards and Technology (NIST) SRM612 and SRM610 certified reference materials.

Calcium concentrations (measured via ^{43}Ca) were used as internal standard for data normalization and drift correction during the measurement campaign, and Ca concentrations of 38.5 wt% were assumed for pristine shell carbonate. Coefficients of determination (R^2) of a linear model fitted to the calibration curves were better than 0.99 and the standard deviation of reproducibility for elemental concentrations was better than 5% relative to the mean value. Individual LA-ICP-MS measurements were inspected for diagenetic alteration or contamination by detrital material using the same thresholds as used for XRF data (see above). LA-ICP-MS and µXRF measurements were combined to cover a wider range of elements, since some elements (e.g. S and Sr) were measured more reliably using µXRF, while others (e.g. Li or Ba) could only be ~~determined~~ quantified using LA-ICP-MS. Concentrations of Li, Mg, and Sr were used to explore the potential of Mg/Li and Sr/Li molar ratios as proxies for paleoenvironmental change. Unprocessed results of LA-ICP-MS line scans are provided in **S4**.

~~2~~3.5 Isotope Ratio Mass Spectrometry

A transect of powdered samples (±200 µg) was sampled for Isotope Ratio Mass Spectrometry (IRMS) analysis in growth direction along well-preserved foliated calcite (**Fig. 3**) in the five largest of the twelve *R. diluvianum* shells (*R. diluvianum* 1-5; see **Fig. 2**) using a microdrill (Merchantek/Electro Scientific Industries Inc., Portland (OR), USA) equipped with a 300 µm diameter tungsten carbide drill bit, coupled to a microscope (Leica GZ6, Leica Microsystems GmbH, Wetzlar, Germany). A total of 531 IRMS samples were taken at an interspacing of 250 µm. Stable carbon and oxygen isotope ratios ($\delta^{13}C$ and $\delta^{18}O$) were measured in a NuPerspective IRMS equipped with a NuCarb carbonate preparation device (Nu Instruments, UK). The sample size (50-100 µg) allowed duplicate measurements to be carried out regularly (roughly once every 30 samples) to assess reproducibility. Samples were digested in 104% phosphoric acid at a constant temperature of 70°C and the resulting CO_2 gas was cryogenically purified before being led into the IRMS through a dual inlet system. Isotope ratios were corrected for instrumental drift and fractionation due to variations in sample size and the resulting values are reported ~~in per mille ratios calibrated~~relative to the Vienna Pee Dee Belemnite standard (‰VPDB) using repeated measurements of the IA-603 stable isotope standard (International Atomic Energy Agency, Vienna, Austria). Reproducibility of $\delta^{18}O$ and $\delta^{13}C$ measurements on this standard were better than 0.1‰ and 0.05‰ (1σ; N=125)

respectively. All stable isotope analysis results are provided in **S5** and plots of stable isotope and trace element records from all shells are ~~shown~~ given in **S6**.

~~2~~3.6 Growth and age modelling

Stable oxygen isotope curves measured in *R. diluvianum* were used to produce age models for the growth of the shell using a bivalve growth model written in MatLab (Mathworks, Natick, MA, USA) which simulates $\delta^{18}O$ curves using a combination of ~~a~~ growth and ~~sinusoid and a~~ temperature sinusoids ~~to fit the $\delta^{18}O$ data~~ (Judd et al., 2018). This simulation model was modified to calculate its temperatures based on calcite $\delta^{18}O$ (following Kim and O'Neil, 1997) rather than from the aragonite $\delta^{18}O$-temperature relationship used in the original approach (after Grossman and Ku, 1986; see Judd et al., 2018). A value of -1.0‰ VSMOW was assumed for $\delta^{18}O$ of Campanian ocean water (Shackleton, 1986; Thibault et al., 2016). Additional minor modifications in the source code allowed results of intermediate calculation steps in the model to be exported. The modified Matlab source code is provided in **S7**. Note that this model assumes that the shape and absolute value of $\delta^{18}O$ curves depend solely on water temperature and growth rate (ignoring changes in ~~sea water~~ $\delta^{18}O_{sw}$), and that a modelled year contains 365 days by construction (while this number should be slightly larger in the Late Cretaceous; ~~e.g. Meyers and Malinverno, 2018;~~ de Winter et al., ~~in review~~2020a). ~~Nevertheless~~Despite these caveats, shell chronologies reconstructed from seasonal patterns in $\delta^{18}O$ should still be reliable as they are only based on the shape of the $\delta^{18}O$ curves ~~regardless of their origin~~. Uncertainties on modelled temperature curves were derived by propagating the measurement uncertainty on $\delta^{18}O$. Age models thus obtained for shells *R. diluvianum* 1-5 were used to align all proxy records on a common time axis. Age models for *R.diluvianum* 6-12 were constructed by extrapolating relationships between modelled seasonality and microstructures and trace element concentrations observed in *R. diluvianum* 1-5. Simultaneously deposited microstructural features in shell cross sections (see **Fig. 3**) were used to determine the actual dorsoventral height of the shells at different ages, linking shell height to the age and allowing the construction of growth curves for all twelve *R. diluvianum* shells. The total age and the season of spawning (or: the start of shell growth) were determined by extrapolating the $\delta^{18}O$-based age models and by using the relationship between $\delta^{18}O$ profiles and trace element records and growth increments observed in the shell.

~~2~~3.7 Strontium ~~isotopic~~ isotope analysis

Samples (on average 26 mg) for strontium isotop~~ic~~e analysis were obtained by drilling the well-preserved foliated calcite in all shells using a Dremel 3000 dental drill with a 0.5 mm tungsten carbide drill bit. Calcite samples placed in Teflon beakers (Savillex LLC, Eden Prairie, MN, USA), ~~were~~ dissolved in subboiled concentrated (14 M) nitric acid (HNO_3) at 120°C and left to dry out at 90°C overnight, after which the residue was redissolved in ~~1~~ 2 M HNO_3. ~~Strontium~~ Carbonate-bound strontium in the samples was purified following the ion-exchange resin chromatography method detailed in Snoeck et al. (2015). The $^{87}Sr/^{86}Sr$ of purified Sr samples were determined using a Nu Plasma (Nu Instruments Ltd, Wrexham, UK) multi-collector (MC) ICP-MS unit in operation at the Université Libre de Bruxelles (ULB). During the measurement run, repeated analyses of NIST SRM987 standard solution yielded a ratio of 0.710250 ± 0.000040 (2 SD; N = 14), statistically consistent with the literature value of 0.710248 ± ~~5.8~~0.000058 (2 s.e.; McArthur et al., 2001; Weis et al., 2006). All results were corrected for instrumental mass discrimination by internal normalization and normalized to the literature value of NIST SRM987 (0.710248) through a standard-sample bracketing method. For each sample, $^{87}Sr/^{86}Sr$ are reported with ~~a~~ 2σ ~~standard deviations~~ uncertainty (**S8**).

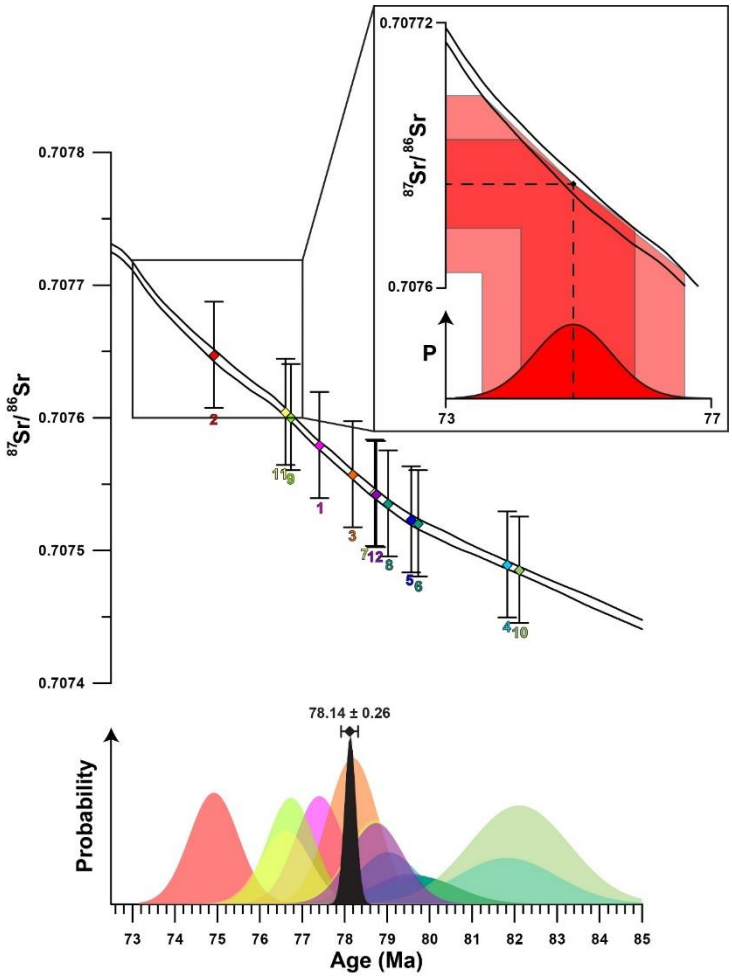

Figure 4: Plot showing the results of Sr-isotopic analyses with error bars (2σ ~~SD~~) plotted on the Sr-isotope curve of McArthur et al. (2016; top of image). Numbers below the error bars indicate ~~sample~~ specimen number. Measurements from the 12 specimens of *R. diluvianum* are represented by parallelograms in different ~~shades of blue~~colors which ~~correspond to the graph~~match the probability distributions plotted below. The probability distribution curves in the lower pane show the distribution of uncertainty on each Sr-isotope measurement as well as the uncertainty on the Sr-isotope curve propagated to the age domain (colors of individual shells are the same as in **Fig. 2**). Insert shows schematically how uncertainties of the isotope measurements as well as the isotope curve are propagated into the age domain. The black curve shows the total uncertainty distribution function compiled from the 12 individual measurements following Barlow (2004), with the combined age estimate including uncertainty (2σ ~~SD~~) shown above.

~~2~~3.8 Strontium isotope dating

R. diluvianum specimens were independently dated by comparing $^{87}Sr/^{86}Sr$ values measured in the samples with the Sr-isotope curve in the 2016 Geological Timescale (McArthur et al., 2016). Uncertainties in $^{87}Sr/^{86}Sr$ measurements were propagated into dates by finding the closest date of the mean $^{87}Sr/^{86}Sr$ value as well as the dates of the minimum (-2σ) and maximum (+2σ) $^{87}Sr/^{86}Sr$ values by linearly interpolating ages in the $^{87}Sr/^{86}Sr$ curve matching the measured $^{87}Sr/^{86}Sr$ value, including the uncertainty estimated on the Sr-isotope curve itself. A composite age for the Ivö Klack deposits was obtained by combining the age uncertainty distributions of the individually dated $^{87}Sr/^{86}Sr$ samples into a single age. Due to the non-linear shape of the $^{87}Sr/^{86}Sr$ curve, uncertainties on the $^{87}Sr/^{86}Sr$ ages were asymmetrical. Since no mathematical solution exists for the combination of asymmetric uncertainties, the asymmetric uncertainty on the total age ~~has~~ had to be approximated through maximum likelihood estimation using the combined log likelihood function (Barlow, 2003). The approximation of the total uncertainty of combined $^{87}Sr/^{86}Sr$ dating results in this study was carried out using the mathematical approach of Barlow (2004) in R (R Core Team, 2013; Roger Barlow, personal communication; code available on https://zenodo.org/record/1494909). The uncertainty interval of the composite age is represented by 2 times the standard error (~95.5% confidence level). A plot of the uncertainty distributions of the individual specimens and the total uncertainty distribution is shown in **Fig. 4**. Raw $^{87}Sr/^{86}Sr$ data ~~is~~ are provided in **S8**.

~~3~~4. Results

~~3~~4.1 Strontium isotope ~~D~~dating

Results of strontium isotope analyses are given in **S8**. The mean strontium isotope ratio of all *R. diluvianum* specimens is 0.707552 (±0.000112; 95% confidence level). The compilation of $^{87}Sr/^{86}Sr$ results from 12 specimens of *R. diluvianum* (**Fig. 4**) shows how age estimates from individual specimens have considerable uncertainties (standard deviations around 1 Myr, see **S8**), yet the uncertainty on the composite age is significantly smaller. The composite age for the Ivö Klack deposits is 78.14 Ma (±0.26; ~~2 standard errors~~95%

Formatte
Formatte
Formatte

confidence level). This result places the age of the Ivö Klack deposits close to the early/late Campanian boundary when applying a twofold division of the Campanian and in the middle Campanian when applying a threefold division scheme (Ogg et al., 2016). This age estimate is similar to the age obtained when plotting the *B. mammilatus* zone on the recent integration schemes of the Campanian (Wendler, 2013). Earlier estimates (Christensen, 1997; Surlyk and Sørensen, 2010; Sørensen et al., 2015) yielded ages about 2-4 Myr older (80-82 Ma), but those relied on presently outdated and partly incorrect age models.

~~3~~4.2 Shell structure and preservation

A combination of high-resolution color scans, SEM images and µXRF mapping of shell cross sections reveals that *R. diluvianum* shells consist of thin layers of dark, foliated calcite, interwoven with lighter, more porous carbonate layers (**Fig. 3a-e**). The latter are characterized by higher concentrations of Mn, Fe and Si and lower Sr concentrations (**Fig. 3f-h**). Foliated calcite layers are more densely packed on the inside of the shell, especially in the region of the adductor muscle scar, and at the shell hinge (**Fig. 3a**). They are characterized by high Sr concentrations and low concentrations of Mn, Fe and Si (**Fig. 3f-h**; **S2**). ~~Foliated layers are also densely packed at the shell hinge.~~ Further away from the shell hinge and the inside of the valve, porous carbonate layers become more dominant. In these regions, µXRF mapping also clearly shows that detrital material (high in Si and Fe) is often found between the shell layers (**Fig. 3f**). SEM images show that the shell structure of *R. diluvianum* strongly resembles ~~to~~ that of modern oyster species, as described in previous studies (**Fig. 3b-e**; Carriker et al., 1979; Surge et al., 2001; Ullmann et al., 2010; 2013; Zimmt et al., 2018). The major part of the shell consists of ~~(foliated and porous)~~ calcite ~~structures~~, of which the foliated structures were sampled for chemical analyses in this study. As in modern oyster species, aragonite may originally have been deposited on the resilium of the shell, but this region is not considered for analyses (see outer tip of shell hinge in **Fig. 3a**; Stenzel, 1963; Carriker et al., 1979; Sørensen et al., 2012). Close similarities with modern oysters allow to infer that shell growth in *R. diluvianum* occurred in a similar way as it does in modern oyster species like *Ostrea edulis*, *Crassostrea virginica* and *C. gigas*. From this extrapolation we could estimate the total shell height from microstructural growth markers (dashed lines in **Fig. 3a**; following Zimmt et al., 2018), linking growth to changes in shell chemistry. ~~This extrapolation allows to estimate the total shell height from microstructural growth markers (**Fig. 3**; following Zimmt et al., 2018), linking growth to changes in shell chemistry. It also allows chemical changes in the shell to be interpreted~~

~~in terms of environmental changes by applying calibration curves for trace element proxies that were previously established for modern oyster species (e.g. Surge and Lohmann, 2008; Ullmann et al., 2013; Mouchi et al., 2013; Dellinger et al., 2018).~~

~~3~~4.3 Trace element analyses results

The similarity in growth between *R. diluvianum* and modern oyster species is used to assess whether trace element variability in *R. diluvianum* can be interpreted in terms of environmental changes in a similar way as in modern oyster shells (e.g. Surge and Lohmann, 2008; Ullmann et al., 2013; Mouchi et al., 2013; Dellinger et al., 2018). The combination of µXRF~~,~~ and LA-ICP-MS ~~and IRMS~~ analyses on *R. diluvianum* shells resulted in ~~multi-proxy~~ records of changes in Mg/Ca, Sr/Ca (µXRF), Mg/Li~~,~~ and Sr/Li (LA-ICP-MS) as well as individual concentrations of trace elements such as Mg, Mn, Fe and Sr (**Figure 5**)~~, δ^{13}C and δ^{18}O (IRMS, only for shells 1-5, see **Fig. 2**)~~. All chemical analyses were carried out on the dense foliated calcite exposed in cross sections close to the inner edge of the shell valve (**Fig. 3a**). High-resolution color scans and detailed recording of sampling positions allowed these records to be plotted on a common axis (see **S6**, **S10**). In **Fig. 5**, results of chemical analyses of *R. diluvianum* specimens (including diagenetic parts) are compared with data from three other mollusk taxa (the belemnite *Belemnellocamax mammillatus*, the oyster *Acutostrea incurva* and the radiolithid rudist ~~*radiolithid rudists*~~*Biradiolites suecicus*) from Ivö Klack (Sørensen et al., 2015), as well as data from extant oysters (Rucker and Valentine, 1961; Surge et al., 2001; Ullmann et al., 2013). ~~**Figure 5** shows that stable isotope ratios of the rudist and oyster shells overlap, while belemnites are characterized by much lower δ^{13}C and heavier δ^{18}O values. This suggests that δ^{13}C in belemnite rostra are affected by vital effects while heavier δ^{18}O values of the belemnites suggest that these animals lived most of their life span in a different environment than the bivalves (deeper waters), as previously suggested by Sørensen et al. (2015). By contrast, stable isotope ratios recorded in the bivalve shells overlap and match the isotope ratios measured in Campanian chalk deposited in the neighboring Danish Basin (Thibault et al., 2016).~~ Multi-proxy analysis revealed periodic variations in stable isotope and trace element ratios (see **Fig. 6**). The amplitudes of these variations plotted in **Fig. 5** show that Mg and Sr concentrations measured in all three fossil bivalve taxa are similar, while concentrations in the belemnite rostra are much higher. Finally, plots ~~of Sr and δ^{18}O against Mn concentrations~~in **Fig. 5b** and **Fig. 5d**

demonstrate that diagenetic alteration (evident from elevated Mn concentrations) reduces the Sr concentration in carbonate of all four taxa. Stable oxygen isotope ratios of the shells are affected to a lesser degree (see below). The ~~vast~~ majority of measurements in all four taxa show very little signs of diagenetic alteration, with most measurements characterized by low (< 100 µg/g) Mn concentrations (**Fig. 5**).

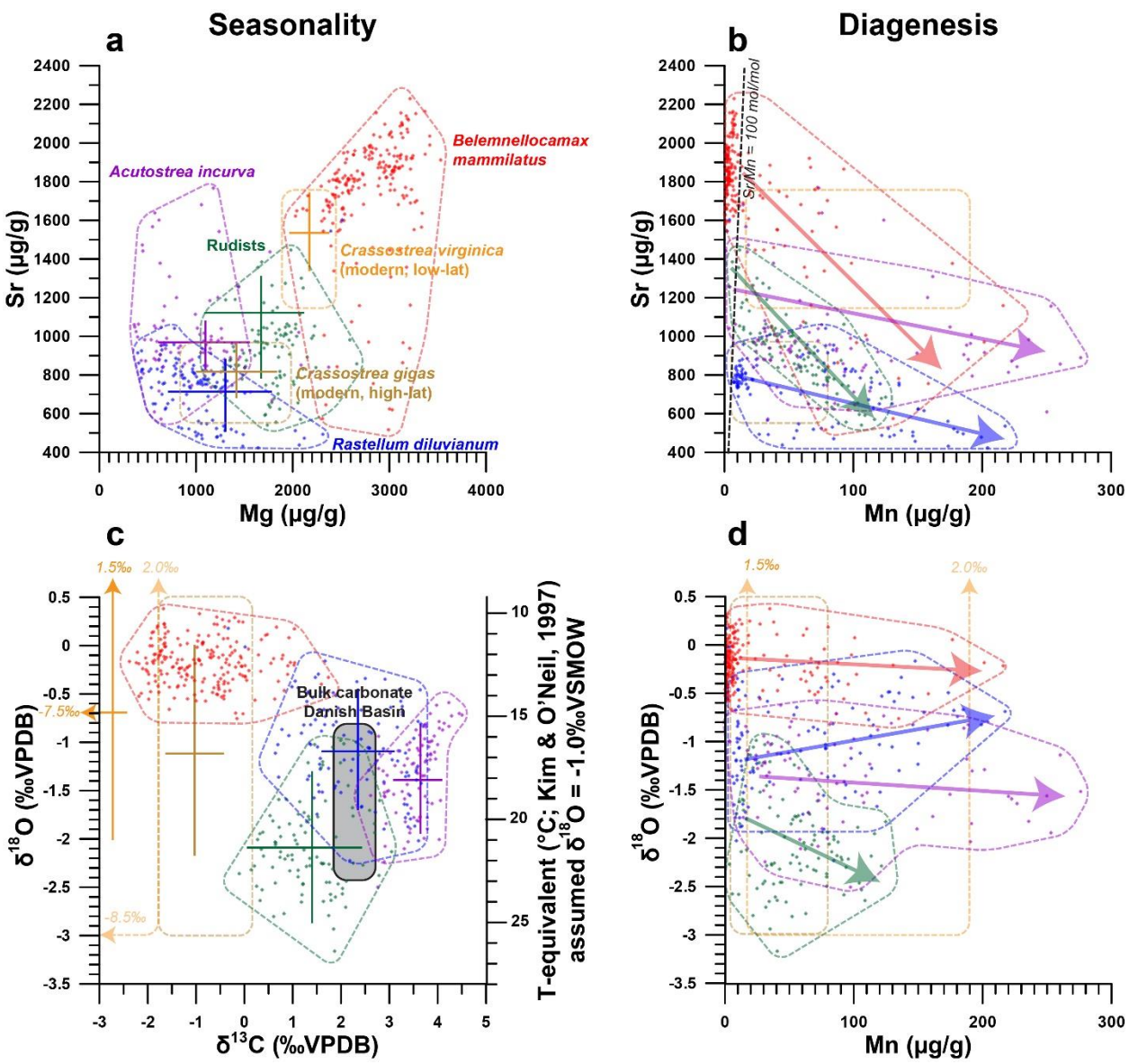

871

872 ***Figure 5:*** Cross plots summarizing the results of trace element and stable isotope analyses of the oysters *R. diluvianum* (blue), *A.*
873 ~~*incurve*~~ *incurva* (purple), ~~associated~~ the rudist ~~*rudist bivalves*~~*Biradiolites suecicus* (green) and the belemnite *B. mammilatus* (red, after
874 Sørensen et al., 2015) from the Kristianstad basin. Results ~~in~~ from modern *C. gigas* (~~grey/black~~brown; Ullmann et al., 2013) and *C.*
875 *virginica* (~~orange/~~yellow; Rucker and Valentine, 1961; Surge et al., 2001) oysters are plotted for comparison. Points indicate individual
876 data points, drawn polygons illustrate the range of the data and crosses indicate the extent of seasonality (if present). (**a**) Strontium
877 concentrations plotted against magnesium concentrations. (**b**) Strontium concentrations plotted against manganese concentrations.
878 Arrows indicate the interpreted direction of diagenetic alteration and the black dashed line shows the Sr/Mn diagenesis threshold
879 proposed for belemnite rostra by Sørensen et al. (2015; 100 mol/mol). (**c**) $\delta^{18}O$ plotted against $\delta^{13}C$. Grey area indicates the range of

880 stable isotope ratios measured in Campanian chalk deposits from the nearby Danish Basin by Thibault et al. (2016) (**d**) $\delta^{18}O$ plotted

881 against manganese concentrations, with arrows indicating proposed direction of diagenetic alteration.

882

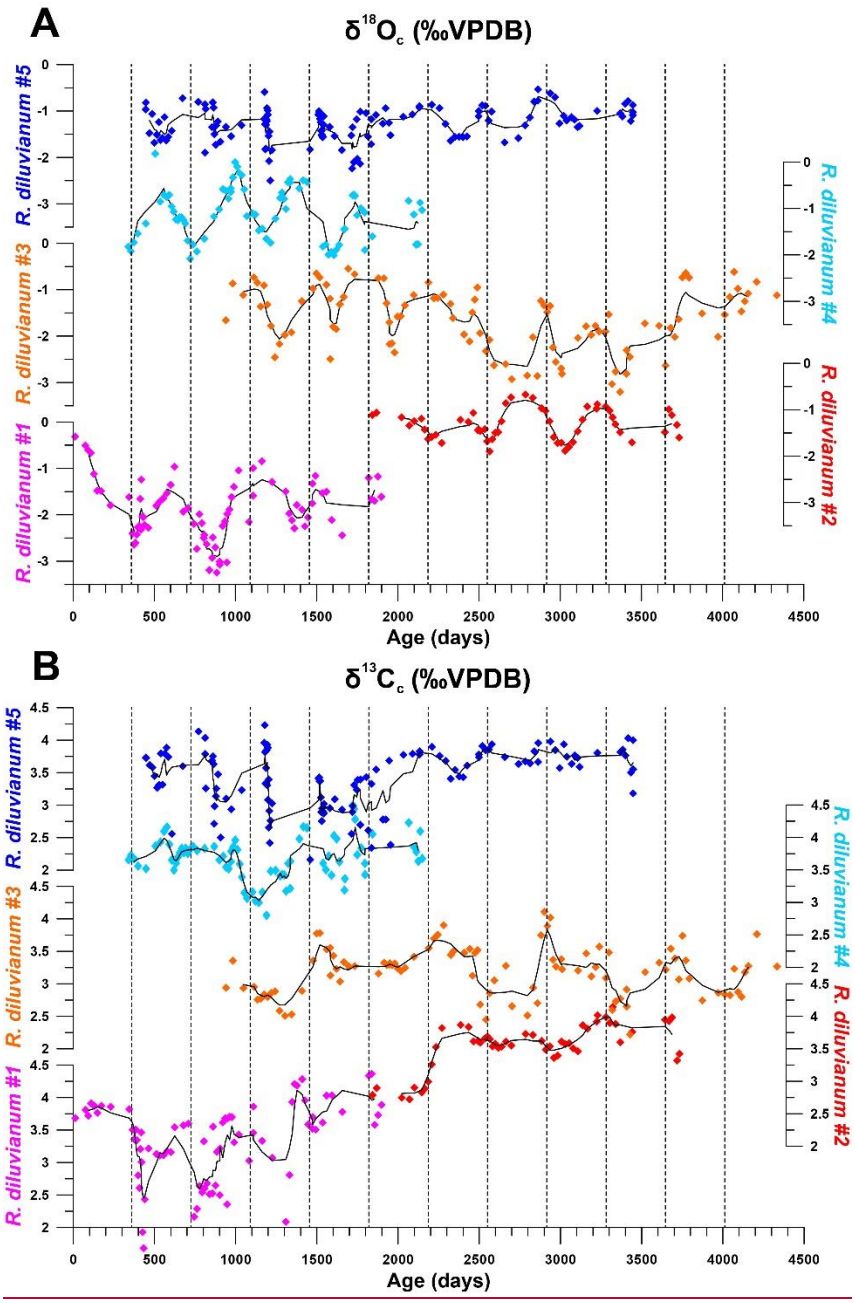

Figure 6: Overview of stable oxygen (**A**) and carbon (**B**) profiles from all five shells in which stable isotope profiles are measured plotted against ontogenetic ages. Black lines indicate 5point running averages through the time series. Vertical dashed lines separate years of growth. All vertical axes of $\delta^{18}O$ and $\delta^{13}C$ have the same scale. Colors coding is the same as in **Figure 7**.

~~3~~4.4 Stable isotope records

An overview of stable isotope results of *R. diluvianum* (IRMS, only for shells 1-5, see **Fig. 2**) compared with the different taxa in Kristianstad Basin and modern oyster data is given in **Figure 5**. Stable isotope ratios of the rudist and oyster shells overlap, while belemnite rostra of the species *B. mammillatus* are characterized by much lower $\delta^{13}C$ and heavier $\delta^{18}O$ values. This suggests that $\delta^{13}C$ in belemnite rostra from this species are affected by vital effects while heavier $\delta^{18}O$ values of the belemnites suggest that belemnites lived most of their life away from the coastal environment (in deeper waters), as previously suggested by Sørensen et al. (2015). In contrast, stable isotope ratios recorded in the bivalve shells overlap and match the isotope ratios measured in Campanian chalk deposited in the neighboring Danish Basin (Thibault et al., 2016).

Records of $\delta^{13}C$ and $\delta^{18}O$ in the growth direction through *R. diluvianum* shells exhibit periodic variations (**Figure 6**). These variations are much more regular in $\delta^{18}O$ records, which show extreme values ~~of~~ below -3‰ and up to 0‰ VPDB (**Fig. 6a**). Some shells, such as *R. diluvianum* 3 (**Fig. ~~6~~7**), exhibit longer term trends on which these periodic variations are superimposed. These trends suggest the presence of multi-annual cyclicity with a period in the order of 10-20 years, but the length of *R. diluvianum* records (max. 10 years) is smaller than the estimated period of these changes and is therefore i~~not~~ nsufficient to statistically validate the presence of this cyclicity.

~~-~~The extreme values in $\delta^{18}O$ records translate to tentative temperatures in the range of extremes of 12°C to 26°C when assuming a constant $\delta^{~~18~~}O_{~~seawater~~}$ $^{18}O_{sw}$ value of -1.0‰ (e.g. Thibault et al., 2016) and applying the temperature relationship of Kim and O'Neil (1997). However, the assumption of constant $\delta^{18}O_{sw}$ may add bias to the temperature reconstructions, as seawater composition may not have been constant or reflect the marine value year-round in the nearshore Ivö Klack setting. Carbon isotope ratios ($\delta^{13}C$) do not always follow the same trends as $\delta^{18}O$ records (**Fig. 6b**). In many parts of *R. diluvianum* shells, there is a clear covariation between the two isotope ratios, suggesting $\delta^{13}C$ is affected by seasonal changes. However, in other parts this correlation is less clear, suggesting that other (non-seasonal) factors play a role in determining the $\delta^{13}C$ of shell material. ~~Superimposed on these changes, a statistically significant~~

~~ontogenetic trend can be discerned in the $\delta^{13}C$ records of 10 out of 12 shells. However, the scale and direction of these trends do not seem consistent between shells.~~

~~3~~4.5 Age models

Modelling the growth of *R. diluvianum* bivalves from seasonal variations in $\delta^{18}O$ profiles yielded age models, growth rate estimates and reconstructions of water temperature variations during the lifetime of the bivalves. Due to the clear seasonal patterns in $\delta^{18}O$ records (**Fig. ~~6~~6a**, **Fig. 7**), modelled $\delta^{18}O$ profiles closely approximated the measured $\delta^{18}O$ profiles (total $R^2 = 0.86$, N = 412, see **S5** and **S9**), lending high confidence to shell age models (see example in **Fig. 7**). Modelling allowed all proxies measured in the shells of *R. diluvianum* to be plotted against shell age, clearly revealing the influence of seasonal variations in environmental parameters on shell chemistry (**S10**). The age models reveal clear, statistically significant ($p < 0.05$) ontogenetic trends in Mg/Li, Sr/Li and $\delta^{13}C$ in nearly all specimens of *R. diluvianum* (see **Table 1**). In 3 out of 5 shells, $\delta^{13}C$ increases with age (see **Fig. 6b** and **Table 1**) with ontogenetically older specimens (e.g. *R. diluvianum* #2) yielding overall higher $\delta^{13}C$ values (**Fig. 6b**). The distribution of slopes of ontogenetic trends in Li/Ca cannot be distinguished from random variation. Therefore, no predictable ontogenetic trends were found for Li-proxies in *R. diluvianum* shells.

~~When plotting all proxies on the same time axis, clear ontogenetic trends emerge in Mg/Li, Sr/Li and $\delta^{13}C$ in nearly all specimens of *R. diluvianum*. Trends and variations in Mg/Li and Sr/Li are strongly correlated, suggesting that variation in both these trace element ratios is largely driven by variations in Li concentrations. Linear regression was applied to isolate ontogenetic trends in $\delta^{13}C$ and Li/Ca ratios (**S11-S12**). While most of these ontogenetic trends are statistically significant ($p < 0.05$), they are highly variable between specimens, both in terms of direction and magnitude. The distribution of slopes of ontogenetic trends in Li/Ca and $\delta^{13}C$ cannot be distinguished from random variation (see **Table 1**). Therefore, no predictable ontogenetic trends were found for $\delta^{13}C$ and Li-proxies in *R. diluvianum* shells.~~

	Li/Ca			$\delta^{13}C$		
	slope (mol/(mol*yr))	R2	p-value	slope (‰/yr)	R2	p-value
***R. diluvianum* 1**	-1.29E-06	0.053	4.32E-08	0.346	0.426	8.86E-07
***R. diluvianum* 2**	3.74E-07	0.101	2.68E-05	0.169	0.440	8.19E-08
***R. diluvianum* 3**	3.86E-07	0.004	5.32E-03	-0.004	0.001	8.09E-01
***R. diluvianum* 4**	-1.07E-06	0.025	8.78E-04	0.023	0.009	3.99E-01
***R. diluvianum* 5**	-1.94E-06	0.030	6.30E-14	0.136	0.492	5.53E-11
***R. diluvianum* 6**	-2.32E-06	0.117	8.75E-15			
***R. diluvianum* 7**	-7.49E-07	0.029	4.77E-02			
***R. diluvianum* 8**	-1.19E-07	0.003	2.90E-01			
***R. diluvianum* 9**	-4.63E-07	0.010	5.65E-02			
***R. diluvianum* 10**	1.59E-06	0.015	1.61E-02			
***R. diluvianum* 11**	-1.87E-06	0.199	4.25E-12			
***R. diluvianum* 12**	-4.55E-07	0.003	4.19E-01			
	$p(\chi^2)$	0.976		$p(\chi^2)$	1.000	
	$p(\chi^2)$ weighed by R2	0.976		$p(\chi^2)$ weighed by R2	1.000	
	$p(\chi^2)$ weighed by p-value	0.961		$p(\chi^2)$ weighed by p-value	0.998	

Table 1: *Overview of the slopes of ontogenetic trends in Li/Ca and $\delta^{13}C$ records. P-values on the bottom of the table show that the distribution of Li/Ca slopes is statistically indistinguishable from random.*

942

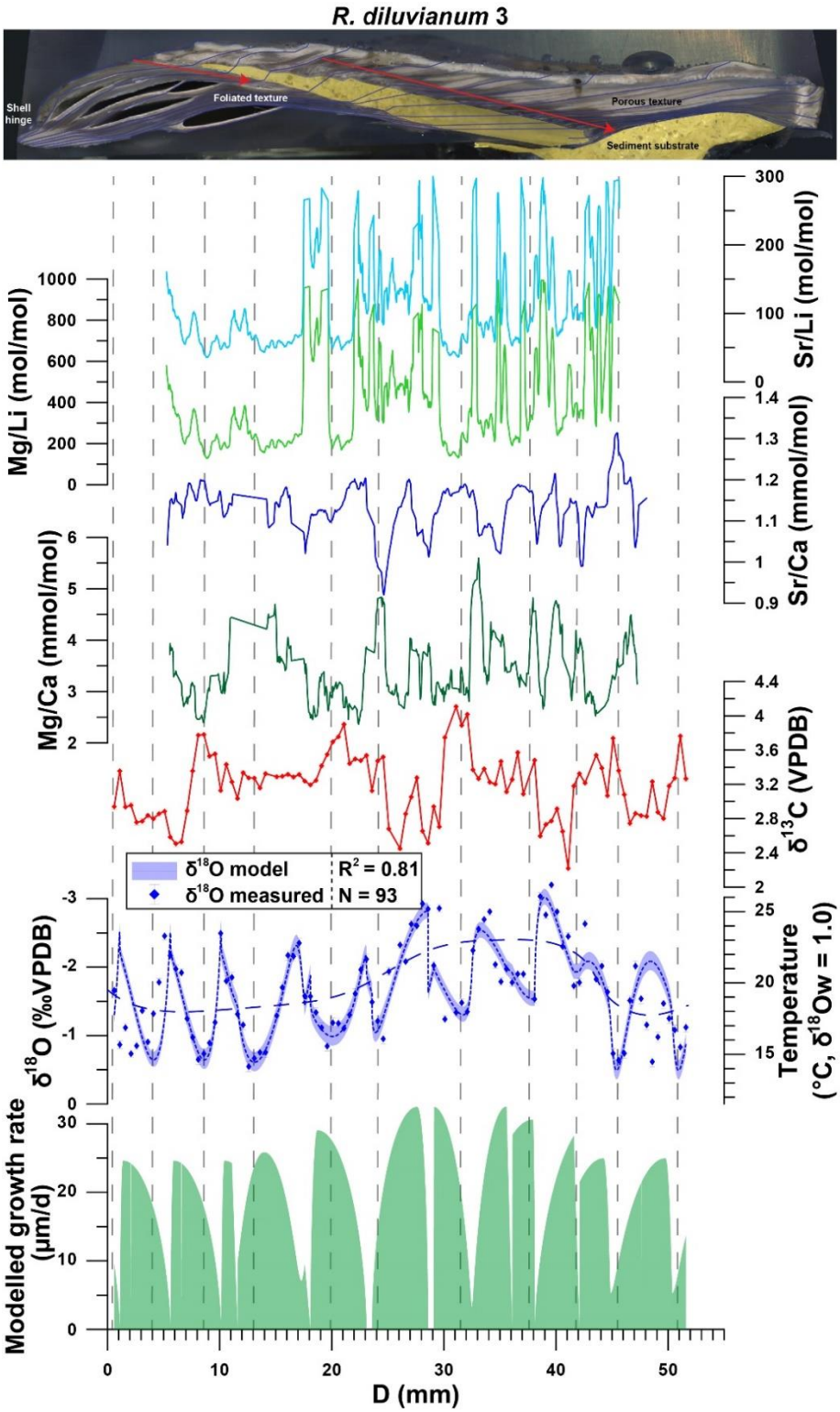

Figure 67: Example of multi-proxy records measured in *R. diluvianum* specimen 3 plotted against distance in growth direction (see image on top and **Fig. 3** for reference). From top to bottom, records of Sr/Li (light blue), Mg/Li (light green), Sr/Ca (dark blue), Mg/Ca (dark green), $\delta^{13}C$ (red), $\delta^{18}O$ (blue dots with error bars) and modelled growth rate (light green fill) are plotted. The shaded blue curve plotted underneath the $\delta^{18}O$ record illustrates the result of growth and $\delta^{18}O$ modelling and its propagated error (vertical thickness of curve, 2SD). The dashed blue curve plotted on top of the $\delta^{18}O$ record shows the observed multi-annual trend in the data. Vertical dashed lines separate growth years. Multi-proxy plots for all specimens are given in **S10**.

943

944

5. Discussion

5.1 Preservation

The relative lack of burial and tectonic activity in the Kristianstad Basin has provided ideal circumstances for the nearly immaculate preservation of *R. diluvianum* shells in the Ivö Klack locality (Kominz et al., 2008; Surlyk and Sørensen, 2010). The excellent state of these shells is evident by the preservation of original (porous and foliated) microstructures that closely resemble those reported for several species of modern ostreid shells (Carriker et al., 1979; Surge et al., 2001; Ullmann et al., 2010; 2013; Zimmt et al., 2018; **Fig. 2-3**). High magnification SEM images demonstrate the excellent preservation of foliated and vesicular calcite structures in *R. diluvianum* shells (**Fig. 3b-d**). The preservation state of *R. diluvianum* shells meets the SEM-based preservation criteria for robust stable isotope analysis set by Cochran et al. (2010). MicroXRF mapping reveals that the foliated calcite in the shells is characterized by high Sr concentrations and low concentrations of Mn, Fe and Si, elements which are generally associated with diagenetic alteration (e.g. Brand and Veizer, 1980; Al-Aasm and Veizer, 1986a; Immenhauser et al., 2005; **Fig. 3b-h**). Trends in bulk Mn and Sr concentrations observed in all fossil species from Ivö Klack (**Fig. 5b;** including less well-preserved parts) likely point towards a diagenetic process affecting a less well-preserved subset of the data. The lack of covariation between Mn concentration and $\delta^{18}O$ shows that there is little evidence for meteoric diagenesis in these shells (**Fig. 5d**; Ullmann and Korte, 2015). Instead, these patterns are best explained by early marine cementation of porous carbonate structures from sea water with similar temperature and $\delta^{18}O$ as the living environment (see also Sørensen et al., 2015).

Typically, a Mn concentration threshold of 100 µg/g is applied below which Cretaceous low-magnesium carbonates are assumed suitable for chemical analysis (Steuber et al., 2005; Huck et al., 2011). Strontium concentrations above 1000 µg/g have also been used as markers for good preservation, since diagenetic processes can cause strontium to leach out of carbonates (e.g. Brand and Veizer, 1980; Huck et al., 2011; Ullmann and Korte, 2015). Previous studies of belemnites in Kristianstad Basin proposed a molar Sr/Mn threshold of 100 for belemnite rostra (Sørensen et al., 2015). However, the height of thresholds used for diagenetic screening differs widely in the literature due to variety between species, fossil matrices and burial histories (e.g. Veizer, 1983; Steuber et al., 1999; Ullmann and Korte, 2015; de Winter and Claeys, 2016).

Applying these thresholds risks introducing biases to chemical datasets from fossil shells and may not be an ideal method for diagenetic screening. Furthermore, large variation in the *in vivo* incorporation of Mn and Sr in mollusk shell carbonate and a strong dependence on the diagenetic setting can make the interpretation of shell preservation from trace element ratios alone highly ambiguous (Ullmann and Korte, 2015). The complex patterns in multi-proxy datasets in this study (**Fig. 5**) merit great care in applying simple, general thresholds for grouping different processes of carbonate diagenesis. Therefore, in this study, a multi-proxy approach is applied for diagenetic screening in which data is excluded based on a combination of Si, Ca, Mn, Fe and Sr concentrations, $\delta^{18}O$ values as well as SEM and visual observations of the shell structure at the location of measurement.

5.2 Dating the Ivö Klack locality

While previous attempts at dating Campanian strata mainly focused on relative dating using magneto- and biostratigraphy (Montgomery et al., 1998; Jarvis et al., 2002; Voigt et al., 2010), integration of cyclostratigraphic approaches in this integrated stratigraphic framework has recently allowed to constrain the age of the Campanian deposits more precisely (Voigt and Schönfield, 2010; Thibault et al., 2012; Wendler, 2013; Thibault et al. 2016). Unfortunately, these rarely cover the time interval in which the Ivö Klack sediments were deposited (e.g. Wendler, 2013; Perdiou et al., 2016). Strontium isotope dating places the Ivö Klack deposits at 78.14 ± 0.26 Ma (**Fig. 4**). When plotting the obtained age of 78.14 Ma on the compilation by Wendler (2013), the age of the Ivö Klack falls slightly above the early/late Campanian subdivision (which is placed at ~78.5 Ma), while the *B. mammilatus* biozone is defined as late early Campanian. Influx of radiogenic strontium-rich weathering products from the nearby Transscandinavian Igneous Belt may bias age estimates from strontium isotope ratios (Högdahl et al., 2004). However, studies of modern strontium isotope ratio variability (Palmer and Edmond, 1989) and the potential bias of strontium isotope ratios in shallow-water carbonates (Kuznetsov et al., 2012; El Meknassi et al., 2018) show that the effect of such inputs on strontium isotope dating results is generally negligible, except in semi-confined shallow-marine basins characterized by considerable freshwater input and low salinities (<7 psu). No evidence exists for such exceptional conditions at Ivö Klack (see **2.1**). We therefore conclude that our strontium isotope age estimate, together with biostratigraphic constraints, places the Ivö Klack locality in the earliest late Campanian. The refined dating of the Ivö Klack deposits and fossils allows the results of

sclerochronological investigations presented in this work to be placed in the context of longer-term climate reconstructions with improved precision.

~~3~~5.3.~~6~~ Trace element ~~seasonality~~variability

Extracted ranges in seasonal scale periodic variability in Mg/Ca, Sr/Ca, Mg/Li and Sr/Li in all 12 *R. diluvianum* shells (**Fig. 8**) show that it is not straightforward to interpret these records in terms of temperature changes. Some of this difficulty arises from the large inter-shell variability in trace element ranges, mostly expressed in strong positive correlations between Sr/Li and Mg/Ca (R^2 = 0.76) and between Sr/Li and Mg/Li (R^2 = 0.93). The benthic foraminifera proxy transfer function for Mg/Li (Bryan and Marchitto, 2008) does not work for *R. diluvianum* (temperatures >50°C), presumably due to typically lower Mg concentrations in foraminifera compared to bivalves (Yoshimura et al., 2011). Bivalve-specific temperature relationships of Mg/Ca (Surge and Lohmann, 2008; based on *Crassostrea virginica*), Sr/Li (Füllenbach et al., 2015; based on *Cerastoderma edule*) and Mg/Li (Dellinger et al., 2018; based on *Mytilus edulis*) yield temperatures in the same range as those reconstructed from ~~local bulk carbonate~~ stable oxygen isotope measurements (10-20°C~~; e.g. Thibault et al., 2016~~). ~~A comparison of the amplitude of periodic variations in Mg/Ca, Sr/Ca, Mg/Li and Sr/Li in 12 *R. diluvianum* shells (**Fig. 7**), together with a tentative interpretation in terms of temperature seasonality, reveals that it is not straightforward to apply the transfer functions previously proposed for these proxies on fossil bivalve shells. Results reveal a strong positive inter-shell correlation between Sr/Li and Mg/Ca (R^2 = 0.76) and between Sr/Li and Mg/Li (R^2 = 0.93), while positive correlations between Sr/Ca and Mg/Ca (R^2 = 0.19) as well as between Sr/Ca and Mg/Li (R^2 = 0.20) are weak. The Mg/Li temperature regressions based on benthic foraminifera (Bryan and Marchitto, 2008) yield unrealistically high-water temperatures (> 50°C), presumably due to typically lower Mg concentrations in foraminifera compared to bivalves (Yoshimura et al., 2011). The Mg/Ca and Sr/Li temperature relationships (Surge and Lohmann, 2008; *C. virginica*; and Füllenbach et al., 2015; *Cerastoderma edule*; respectively) and a Mg/Li temperature regression based on the calcitic bivalve *Mytilus edulis* (Dellinger et al., 2018) yield temperatures in the same range as those reconstructed from local bulk carbonate stable isotope measurements (10-20°C; e.g. Thibault et al., 2016)~~, but~~However, Sr/Li-based temperature trends~~s display a pattern~~are opposite to those based on Mg-proxies~~. ~~, This seems to suggest that, if trace element concentrations in *R. diluvianum* are linked to temperature, the temperature relationship of Mg-based proxies~~

~~and the Sr/Li proxy are discordant and~~suggesting that they cannot both be applicable to *R. diluvianum*. Poorly constrained changes in seawater chemistry (Mg/Ca and Sr/Ca ratios of ocean water) also hinder these trace element-based reconstructions (Lear et al., 2003; Coggron et al., 2010; Rausch et al., 2013). The strong Mg/Li-Sr/Li correlation indicates that both proxies are likely strongly affected by the specimen-specific ontogenetic trends in Li/Ca described in **Table 1**. This, together with the large inter-specimen variability shows that both Li-proxies cannot be used as temperature proxies in *R. diluvianum*. An annual stack of all proxies shows that the positive correlation between Mg/Ca and $\delta^{18}O$ (**Fig. 9**) is opposite to the temperature-relationships found in modern oyster species (Surge and Lohmann, 2008; Mouchi et al., 2013; Ullmann et al., 2013). This together with the reduced seasonal variability (1.2 mmol/mol versus 4-10 mmol/mol in modern oysters; Surge and Lohmann, 2008; Mouchi et al., 2013) and the large (>3 mmol/mol; **Fig. 8**) inter-specimen variability both in mean value and seasonal Mg/Ca range rules out Mg/Ca as a reliable temperature proxy in *R. diluvianum*. This result demonstrates that earlier successful attempts to establish calibration curves for Li- and Mg-based temperature proxies (e.g. Füllenbach et al., 2015; Dellinger et al., 2018) are probably strictly limited to these bivalve species or close relatives. The same conclusion was also drawn by Dellinger et al. (2018) based on Li/Mg and Li isotope ratio measurements in biogenic carbonates. The lack of Mg/Li or Sr/Li calibrations in modern oyster shells limits the interpretation of the results of this stud. Establishing such calibrations using modern oysters in cultured experiments may allow these proxies to be used for reconstructions from fossil oyster shells in the future.

While not a likely candidate for reconstructing temperature (Gillikin et al., 2005; Schöne et al., 2013; Ullmann et al., 2013), seasonal Sr/Ca fluctuations and relationships between Sr/Ca and $\delta^{18}O$ are consistent between individuals (**Fig. 8-9**; see also **S6**). This allows Sr/Ca ratios to be used together with microstructural observations of growth increments as basis for seasonal-scale age models in shells for which no $\delta^{18}O$ measurements were done. Both mean Sr/Ca values and seasonal variability in *R. diluvianum* are consistent with those observed in the same microstructure in modern *Crassostrea gigas* growing in a similar environment (0.8-1.0 mmol/mol; Ullmann et al., 2013), suggesting a consistent incorporation of Sr by different oyster taxa over time. It must be noted that one should be cautious when directly comparing trace element concentrations in biogenic calcite between different time periods, as the seawater composition of Late Cretaceous oceans (e.g. concentrations of Mg, Ca, Sr and especially Li) may have been different from

that of the present-day ocean (Stanley and Hardie, 1998; Coggon et al., 2010; Rausch et al., 2013). Local enrichments in seawater Sr concentrations at Ivö Klack driving increased Sr composition in *R. diluvianum* are unlikely, since Sr/Ca ratios exhibit only small (2-3%) lateral variability in the world's oceans (De Villiers, 1999). Because Sr/Ca ratios in Late Cretaceous oceans were twice as low as in the modern ocean, one would expect, for example, that Sr concentrations in Late Cretaceous biogenic carbonate would be twice as low as those in carbonates formed in the modern ocean, if the partition coefficient between seawater concentrations and shell concentrations remains constant (Stanley and Hardie, 1998; de Winter et al., 2017a). The fact that this reduction in Sr concentrations relative to the modern ocean is not observed in *R. diluvianum* may entail that there is a fixed physiological limit to oyster's discrimination against building Sr into their shells that is independent of ambient Sr concentrations.

~~These results raise difficulties similar to those that arose in earlier attempts to apply trace element ratios for water temperature reconstructions in fossil mollusks (Steuber, 1999; Weiner and Dove, 2003; de Winter et al., 2017a). The interpretation of these records is further complicated by large intra-specific variability in the incorporation of Mg into biogenic carbonates (e.g. Schöne et al., 2010) and the lack of constraints of seawater compositions in the Late Cretaceous (e.g. Stanley and Hardie, 1998; especially with respect to Li concentrations). It shows that trace element ratios in these shells can only be interpreted with some degree of confidence when combined with stable isotope records from shells of the same setting and species.~~

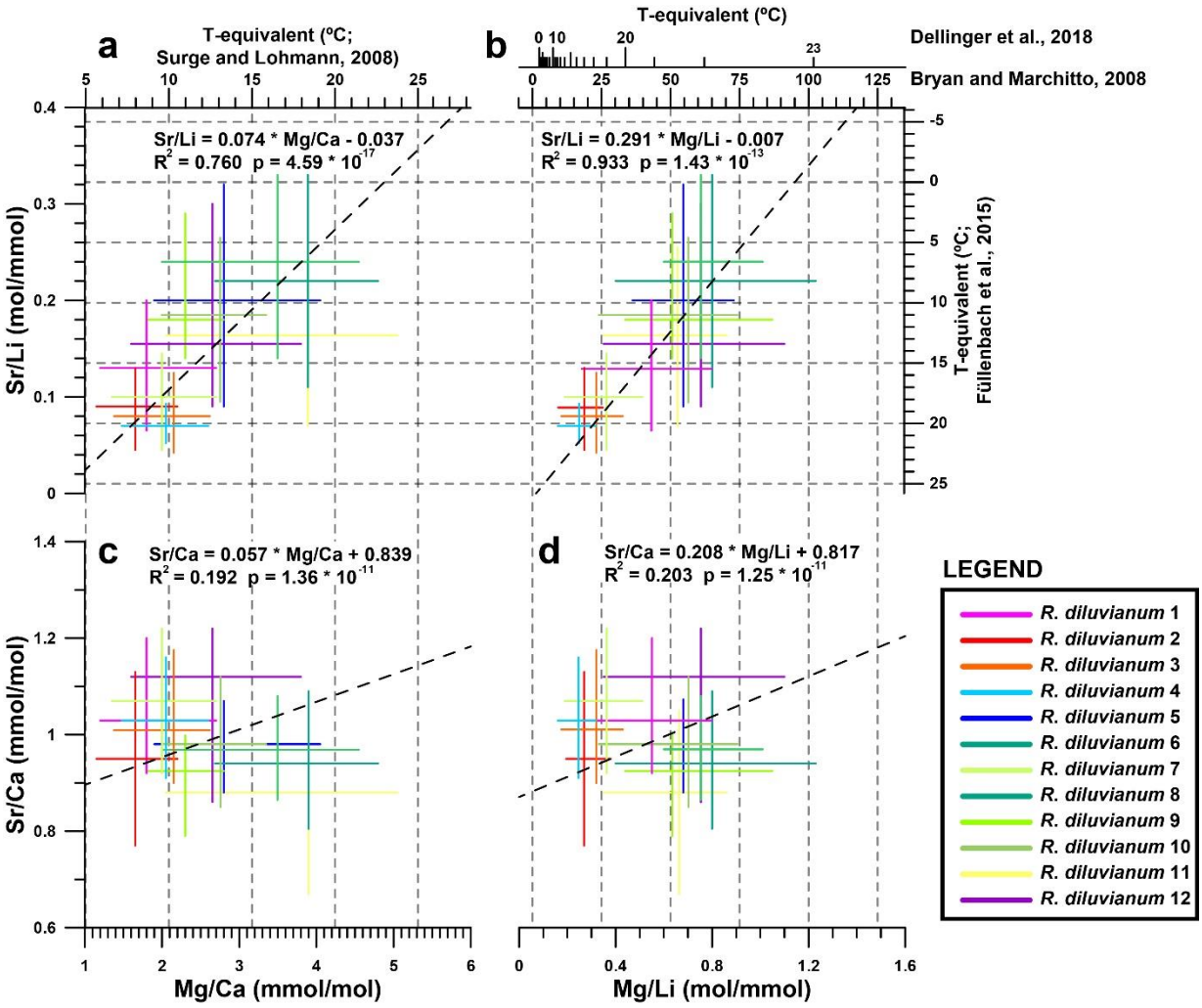

Figure ~~7~~8: Cross plots showing the extent of interpreted seasonality observed in records of four trace element proxies in all 12 *R. diluvianum* specimens. Colors of lines of individual shells correspond to colors indicated in **Fig. 2**. Temperature conversions from previously published regressions of the proxies with temperature are shown on opposite axes with grey dashed lines corresponding

to major tick marks on the temperature scale (**a**) Sr/Li plotted against Mg/Ca showing a strong significant intra-shell correlation. (**b**) Sr/Li plotted against Mg/Li showing a strong significant intra-shell correlation due to dominant variations in Li concentration. Note that two different Mg/Li temperature calibrations were explored. (**c**) Sr/Ca plotted against Mg/Ca showing weak but significant intra-shell correlation. (**d**) Sr/Ca plotted against Mg/Li showing a weakly significant intra-shell correlation. Data for this plot is found in **S13**.

1084

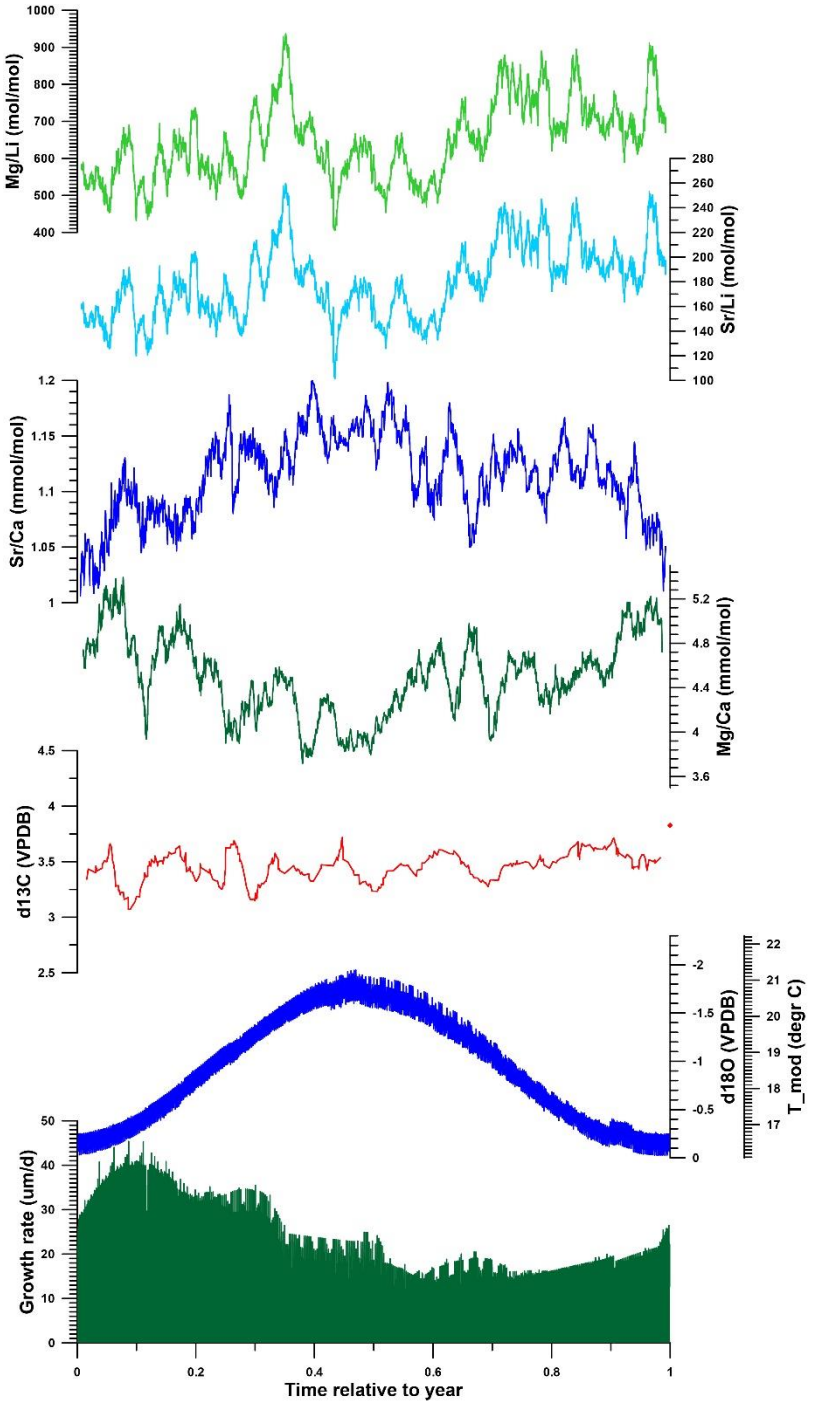

Figure 9: Composite of multi-proxy records from all *R. diluvianum* shells stacked and plotted on a common time axis of 1 year to illustrate the general phase relationships between various proxies in the shells. Records were colored as in **Fig. 7**. Annual stacks plotted in this figure were produced~~/obtained~~ by applying age models on all multi-proxy records, plotting all results against their position relative to the annual cycle and applying 20 point moving averages.

1085

~~3.7~~5.4 Temperature seasonality

~~The seasonal variation in all specimens of *R. diluvianum* was aligned and stacked relative to shell age models (**Fig. 8**). This composite~~An annual stack of all *R. diluvianum* proxy records shows ~~that the~~a $\delta^{18}O_c$-based ~~seasonal temperature range~~temperature variability in Ivö Klack ~~during the late early Campanian was between~~of 16~~°C and -~~21°C when assuming a constant ~~constant seawater~~ $\delta^{18}O_{sw}$ of -1‰VSMOW. However, comparison with $\delta^{18}O$-seasonality in individual specimens shows that the annual stack severely dampens seasonality due to small phase shifts in maximum and minimum temperatures, small uncertainties in the age models between years and specimens, and inter-annual differences and longer-term trends in temperature (see **Fig. 6**). A more accurate estimate of the seasonal extent is obtained by calculating the seasonal range from the coolest winter temperatures (12.6°C in *R. diluvianum* 4; **Fig. 6**; **S10**) with the warmest recorded summer temperature (26°C in *R. diluvianum* 1; **Fig. 6**; **S10** which yields an extreme maximum seasonal sea surface temperature (SST) range of ±13.4°C.

A complication of these reconstructions is the assumption of constant $\delta^{18}O_{sw}$ of -1‰VSMOW, which is unlikely to be completely accurate in the nearshore Ivö Klack locality. –Comparison with data from *Crassostrea gigas* growing in a similar nearshore environment (Ullmann et al., 2010; German North Sea coast, 54°N) show that such an environment away from large river mouths can typically experience seasonal salinity fluctuations of ~4 psu resulting in a dampening of the seasonal $\delta^{18}O_c$ cycle by ~0.5‰VPDB. Such a salinity-effect would reduce our reconstructed 13-26°C seasonal temperature range by ~2°C to 14-25°C.

In addition, mean annual $\delta^{18}O_{sw}$ values can be considerably lighter than the global average seawater composition (e.g. -1‰ to -1.5‰VSMOW compared to global ocean mean of 0‰VSMOW in Ullmann et al., 2010). Considering such a deviation would reduce reconstructed temperatures by 4-6°C to 10-21°C, much colder than open marine reconstructions of the Boreal Chalk Sea by Thibault et al. (2016). This result would be in strong disagreement with a recent study by Tagliavento et al. (2019) in which clumped isotope analyses (which does not rely on the assumption of constant $\delta^{18}O_{sw}$) were used to correct the $\delta^{18}O_c$-based reconstructions of the Boreal Chalk, and which yielded *higher* temperatures (~26°C MAT for open marine

SST) and a correction of $\delta^{18}O_{sw}$ towards 1-1.5‰ heavier values (resulting in a Campanian $\delta^{18}O_{sw}$ of -0.5-0‰VSMOW). Another caveat is that salinity effects on local $\delta^{18}O_{sw}$ strongly depend on the local $\delta^{18}O_{sw}$ of the local freshwater source (riverine or precipitation), which in the present-day higher mid-latitudes is around -7‰VSMOW to -8‰VSMOW (e.g. Ullmann et al., 2010), but this is impossible to constrain at Ivö Klack during the Campanian within the scope of this study.

If local $\delta^{18}O_{sw}$ values at Ivö Klack were indeed 1-1.5‰ reduced with respect to those in the fully marine Boreal Chalk Sea, and marine $\delta^{18}O_{sw}$ was around 0-0.5‰VSMOW rather than the assumed -1‰VSMOW, the effects of these two biases cancel each other out, and the best estimation of the extreme seasonal SST range at Ivö Klack based on this study's data would be 14-25°C with a MAT of 19°C. This MAT is comparable to the MAT of the late early Campanian Boreal Chalk Sea waters of 17-19°C calculated based on coccolith-$\delta^{18}O_c$ (Lowenstam and Epstein, 1954; Jenkyns et al., 2004; Friedrich et al., 2005; Thibault et al., 2016), and slightly warmer than mean annual air temperatures from this paleolatitude based on phosphate-$\delta^{18}O$ reconstructions paleolatitude (±15°C; Amiot et al., 2004). However, Ivö Klack SST's are ~6°C colder than the clumped isotope-based reconstructions from marine chalk samples (Tagliavento et al., 2019). The latter could indicate that coastal SST's and air temperatures were much colder than marine temperatures in the Campanian higher latitudes, but such temperature differences are highly unusual compared to modern climates. Alternatively, this difference could highlight a severe temperature bias in (both phosphate and carbonate) $\delta^{18}O$-based reconstructions, which should be further investigated using independent proxies such as the clumped isotope paleothermometer (e.g. de Winter et al., 2018; Tagliavento et al., 2019).

Modelled growth rates in *R. diluvianum* peak near the end of the low temperature season and average growth rates are lowest shortly after the temperature maximum (**Fig. ~~8~~9**). This phase shift between temperature and growth rate could indicate that growth in *R. diluvianum* in this setting was not limited by low temperatures, as observed in modern mid- to high-latitude oysters (Lartaud et al., 2010). High temperature extremes (>25°C) may have slowed or stopped growth, as recorded in modern low latitude settings (Surge et al., 2001~~), ~~). Heat shock has been shown to limit the growth of modern oysters (*Crassostrea gigas*; Li et al., 2007), ~~but ~~although ~~$\delta^{18}O$ ~~the relatively moderate SST seasonality ~~-~~suggests

that ~~these~~ such very high (>25°C) temperatures were not common at the Ivö Klack locality (**Fig. 6**). In addition, the use of $\delta^{18}O$ records from multiple specimens reduces the effects of growth cessations of individuals on ~~Mg/Ca ratios in *R. diluvianum* exhibit a clear seasonal pattern, which is inversely correlated with temperature, while Mg/Ca ratios in foliate calcite of modern oysters show opposite correlation with temperature (Surge and Lohmann, 2008; Mouchi et al., 2013) or exhibit no correlation at all (Ullmann et al., 2013). Sr/Ca ratios in *R. diluvianum* are positively correlated with seasonal temperature variations. Mg/Li and Sr/Li ratios show no correlation with temperature. Instead, both proxies display elevated values both directly before and after seasonal temperature maxima (**Fig. 8**). Finally, $\delta^{13}C$ values exhibit no observable relationship with temperature seasonality.~~seasonal SST reconstructions and allows the full seasonal range in SST to be resolved.

The reconstructed MAT for Ivö Klack is 7-8 degrees warmer than the present-day mean annual SST in the North and Baltic seas at similar latitude (e.g. 2-18°C monthly seasonality range in Baltic Sea Karlskrona, Sweden, 56°N and 4-18°C monthly seasonality range in North Sea Esbjerg, Denmark, 55°N; IRI/LDEO Climate Data Library, 2020). SST seasonality at Ivö Klack (11°C) is significantly lower than the 14-16°C temperature seasonality that occurs in the present-day Baltic and North seas. Data on temperature seasonality in the Late Cretaceous are scarce, especially in high-latitude settings. However, comparison with data on Cretaceous seasonality between 15°N and 35°N paleolatitude (Steuber et al., 2005) shows that while MAT at 50°N was significantly lower than those at lower latitudes (19°C vs. 25-30°C respectively), the seasonal temperature range during cooler periods in the Late Cretaceous was remarkably similar between latitudes (10-15°C in subtropical latitudes vs. ±14°C in this study). This observation contrasts with the present-day situation in Northern Africa and Europe, in which seasonal temperature ranges are generally much higher in mid- to high-latitudes (30-50°N) than in lower latitudes (10-30°N; Prandle and Lane, 1995; Rayner, 2003; Locarnini et al., 2013; NOAA, 2020). Our SST reconstructions also show that Late Cretaceous latitudinal temperature gradients and mid- to high-latitude seasonality were larger than

previously assumed based on climate model results (Barrera and Johnson, 1999; Hay and Floegel, 2012;

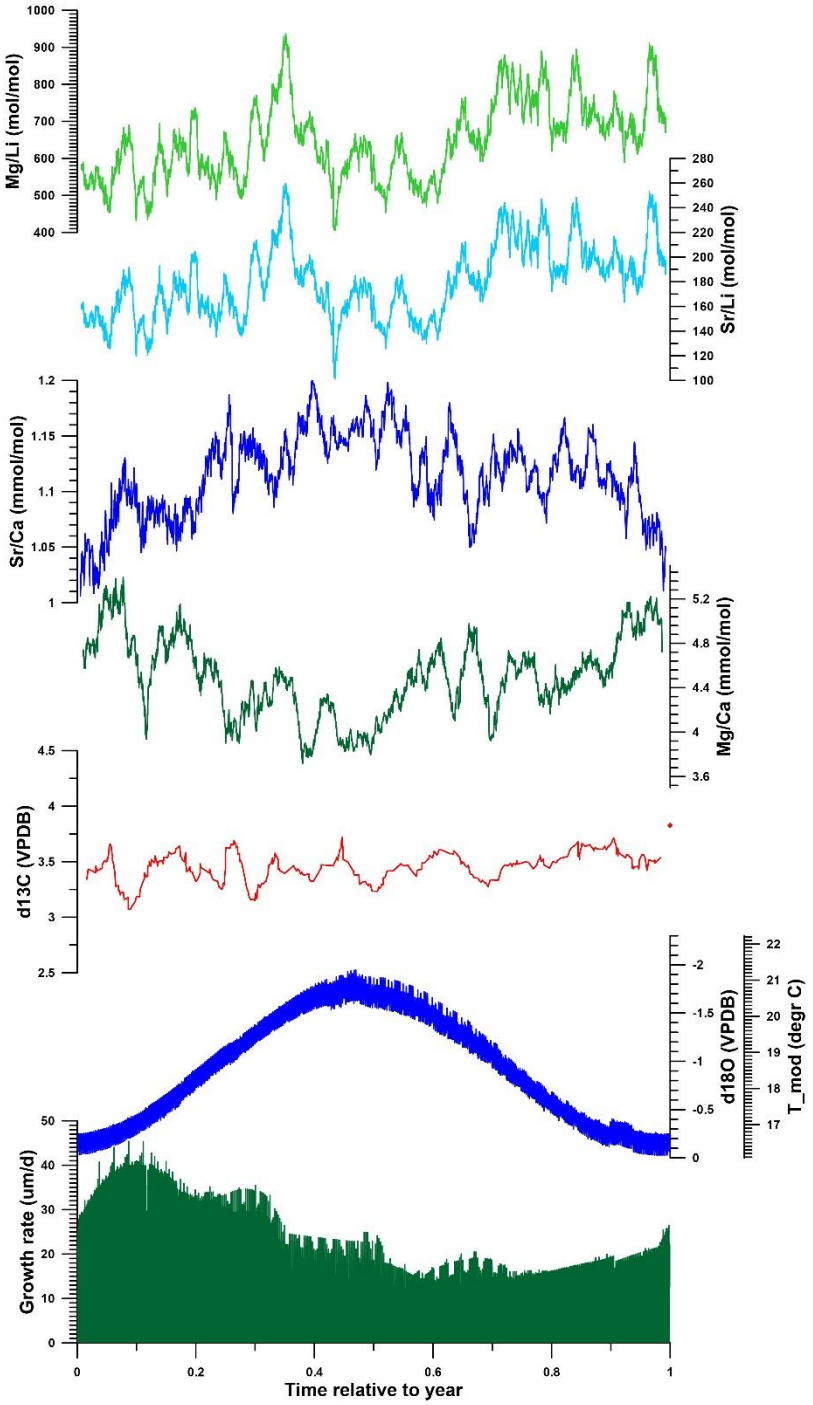

Figure 89: Composite of multi-proxy records from all *R. diluvianum* shells stacked and plotted on a common time axis of 1 year to illustrate the general phase relationships between various proxies in the shells. Records were colored as in **Fig. 67**. Annual stacks plotted in this figure were produced/obtained by applying age models on all multi-proxy records, plotting all results against their position relative to the annual cycle and applying 20 point moving averages.

Upchurch et al., 2015).

~~3.8~~5.5 Shell growth and ontogeny

5.5.1. Growth curves

~~Plots of modelled shell height against age allow to compare growth patterns of individual *R. diluvianum* (**Fig. 9**). Individual g~~Growth curves of individual *R. diluvianum* specimens clearly converge to a general growth development curve for the species (**Fig. 10**). Considering that these growth curves are based on $\delta^{18}O$ and Sr/Ca~~the isotope~~ transects ~~used to establish these growth curves were measured~~ in different stages of life in different specimens (large age variation; see **Fig. 8**), individual growth curves are remarkably similar. The growth of *R. diluvianum* takes the typical shape of the asymptotic Von Bertalanffy curve, in which shell height (H_t) development with age (t) is related to a theoretical adult size H_{max} and a constant k in the equation: $H_t[mm] = H_{max} * \left(1 - e^{k*(t[yr]-t_0)}\right)$, with t_0 representing the time at which the growth period started (always zero in this case; Von Bertalanffy, 1957). When this formula is regressed over all modelled growth data of all shells (1 data point per day, 15146 points in total), the fit with an H_{max} of ±120.3 mm and a K value of ±0.32 is very good (R^2 = 0.79; see **Fig. ~~9~~10**).

The consistency in growth curves between individuals of *R. diluvianum* is surprising as modern oyster species are known to exhibit large variations in growth rates and shell shapes as a function of their colonial lifestyle, which often limits the growth of their shells in several directions (Galtsoff, 1964; Palmer and Carriker, 1979). The strong resemblance of growth between individuals and the close fit of the idealized Von Bertalanffy growth model suggests that growth of *R. diluvianum* at Ivö Klack was relatively unrestricted in space. This hypothesis is consistent with the apparent mode of life of *R. diluvianum* in Ivö Klack cemented next to each other in loose groups, subject to strong wave action and turbulence, but with little competition for space due to the high-energy environment (Surlyk and Christensen, 1974; Sørensen et al., 2012). The shape of the growth curve of *R. diluvianum* resembles that of modern Chesapeake Bay oysters (*Crassostrea virginica*), which exhibit a slightly larger modelled maximum height (150 mm) and a slightly smaller K-value (0.28). A larger subset of *R. diluvianum* specimens studied by Sørensen et al. (2012) demonstrates that these bivalves could grow up to 160 mm in height. The curvature of the growth of *R. diluvianum* (K -value) is also similar to that found for other modern shallow marine bivalve species (e.g.

Macoma balthica, K = 0.2-0.4; Bachelet, 1980; *Pinna nobilis*, K = 0.33-0.37; Richardson et al., 2004) and significantly higher than in growth curves of deep shelf-dwelling bivalves (e.g. *Placopecten magellanicus*, K = 0.16-0.24; MacDonald and Thompson, 1985; Hart and Chute, 2009) or bivalves from cold habitats (e.g. North Atlantic *Arctica islandica*, K = 0.06; Strahl et al., 2007). This reflects the high growth rates (steeper growth curves, higher K-values) of shallow marine bivalves compared to species living in more unfavorable or restricting (colder or deeper) habitats, with *R. diluvianum* clearly being part of the former group.

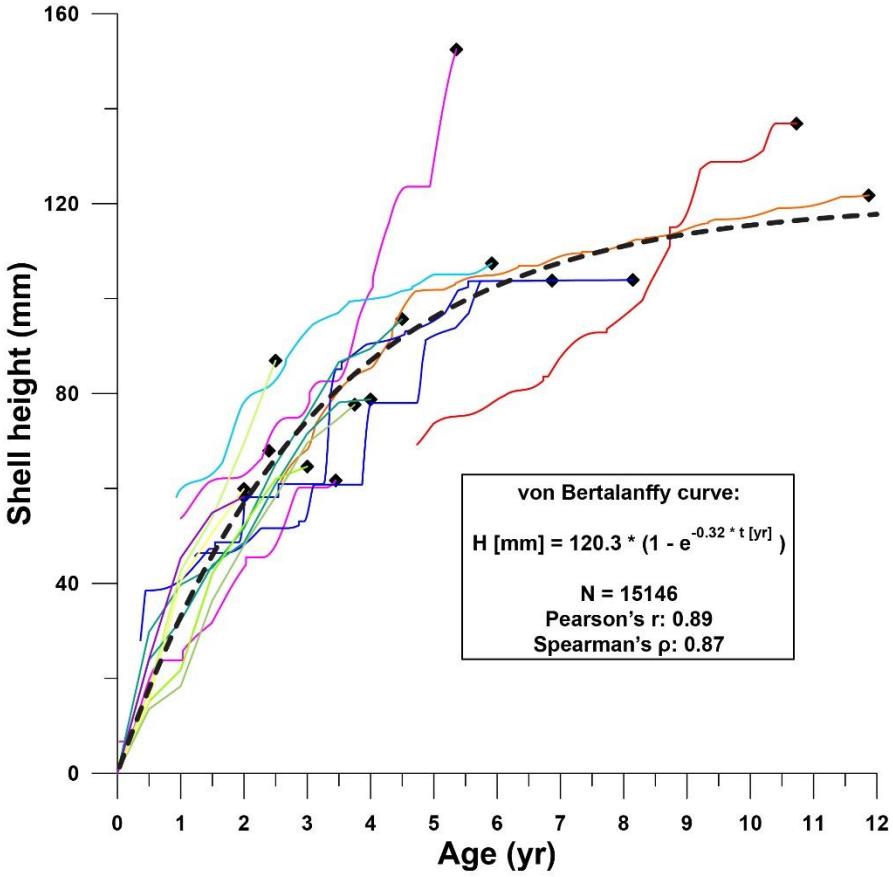

Figure 910: Shell height plotted against age for all *R. diluvianum* records (see **Fig.** ~~7~~ **8** for color legend of lines representing individuals). The similarity between growth curves of different specimens allows a Von Bertalanffy curve to be fitted to the data with high confidence. Sinusoidal patterns superimposed on all growth curves are caused by seasonal variability in growth rate (see **Fig. 6-** ~~6~~ **7**~~for an example~~). Data found in **S9**.

5.5.2 Seasonal growth

~~3.9 Statistics in seasonal growth and ecology~~

To study variability in minimum growth temperature (**Fig. 11a**), length of the growth season and time of year on which maximum growth occurs (**Fig. 11b**), we isolated individual growth years from all age models of the five shells in which $\delta^{18}O$ curves were measured (**Fig. 11**). ~~The seasonality stack of growth rates shown in **Fig. 8** suggests a potential year-round growth in *R. diluvianum*, but this is a bias induced by the way the annual stack is plotted. To better understand the growth and life history of *R. diluvianum* oysters, it is important to consider the variability between individual years of growth in the different individuals. Using oxygen isotope records, year-long "seasonal" cycles and subsequently derived growth rates from our 12 specimens of *R. diluvianum*, we isolated statistics of individual growth seasons in order to visualize the potential relationship between growth rate, temperature and time of year (**Fig. 10**).~~ The onset and end of each growth year correspond to maxima in $\delta^{18}O$ values (minima in temperatures). ~~Isolating all 58 individual growth years in specimens used in this study based on the temperature seasonality modelled on $\delta^{18}O$ records allowed a comparison of statistics such as seasonal minima and maxima in growth, the length of the growth season and the extent of seasonality to be evaluated (**Fig. 10**).~~ The onset of the first growth year in each shell at its precise position relative to the seasonal temperature cycle showed in which season spawning occurred (~~**Fig. 10c**~~**Fig. 11b**). ~~Finally, evaluation of the distribution of growth maxima and minima along the seasonal cycle and regression analyses between these parameters reconstructed from the growth models shed light on the relationships between growth parameters in *R. diluvianum* and seasonality~~ All data used to create plots in ~~**Fig. 10**~~**Fig. 11** ~~is~~ are provided in **S14**. Relationships between these growth parameters are summarized in **Table 2**.

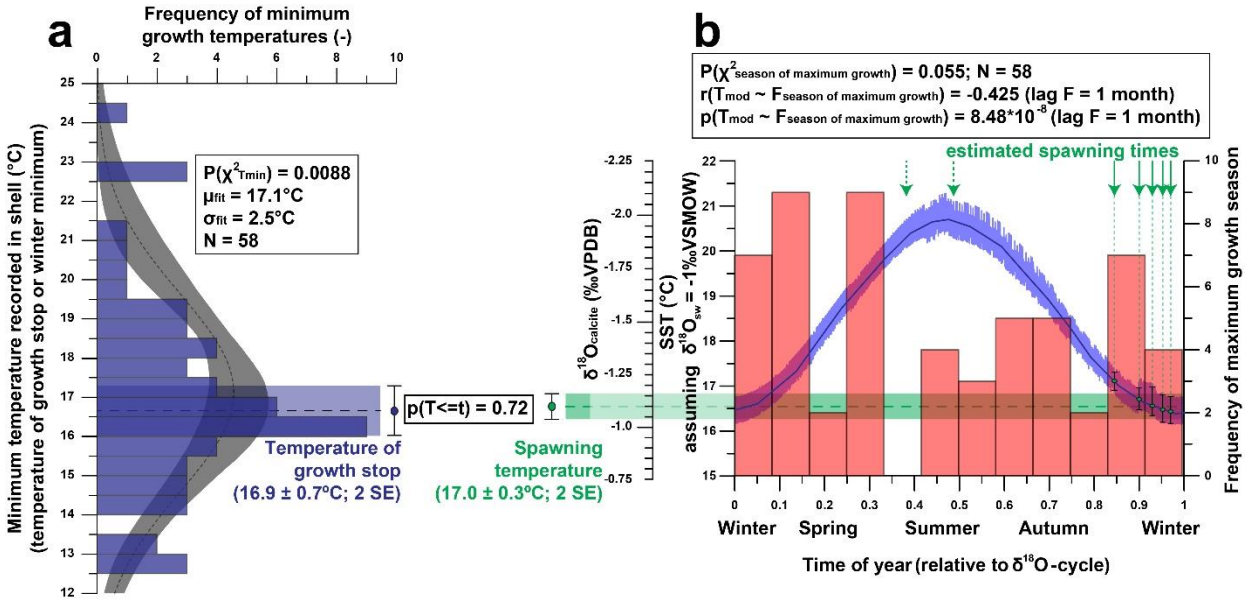

Figure ~~10~~6: Overview of statistical evaluation of growth parameters of *R. diluvianum* derived from age modelling in shells 1-5. (**a**) Histogram of minimum temperatures of growth (equivalent to the time at which growth stops or the minimum yearly temperature) in *R. diluvianum* showing that the temperature on which growth slows coincides with that of the spawning season (p = 0.717). ~~(b) Strong significant positive correlation between MAT and temperature of the slowest growth season shows that the season of minimum growth is not strictly forced by minimum temperatures but rather by timing relative to the annual $\delta^{18}O$ cycle.~~ (**cb**) Histogram of the season of maximum growth relative to the $\delta^{18}O$ seasonality cycle shows no significant concentration towards a favorable growing season while moments of first growth (spawning) are significantly concentrated towards the low-$\delta^{18}O$ season.

N = 58	Total annual growth (µm)	Maximum growth rate (µm/d)	Length of season (d)	Minimum growth temperature (°C)	Temperature seasonality (°C)	Average temperature (°C)
Temperature seasonality (°C)	R^2 0.024 p $2.16*10^{-11}$	R^2 0.053 p $6.73*10^{-10}$	R^2 0.403 p $2.15*10^{-22}$			
Average temperature (°C)	R^2 0.020 p $2.29*10^{-11}$	R^2 0.027 p $6.95*10^{-7}$	R^2 0.008 p $2.87*10^{-21}$	R^2 0.565 p $3.44*10^{-7}$		
Age (yr)	R^2 0.000 p $1.11*10^{-9}$	R^2 0.062 p $9.74*10^{-12}$	R^2 0.002 p $1.59*10^{-22}$	R^2 0.002 p $1.05*10^{-30}$	R^2 0.059 p $4.59*10^{-1}$	R^2 0.000 p $1.09*10^{-35}$

Table 2: Overview of statistical evaluation of growth parameters of *R. diluvianum* derived from age modelling in shells 1-5. Coefficients of determination (R^2) and p-values were determined for relationships between temperature seasonality, average temperature, age of the bivalve, length of the season, minimum growth temperatures and annual average and maximum growth rates. Values in green indicate strong correlations while values in red indicate the absence of a correlation. Data reported in **S14**.

The growing season is shorter than 365 days in all but five modelled years, demonstrating that growth stops or slowdowns did occur in *R. diluvianum*. Minimum growth temperatures (temperatures at which growth stops) are concentrated around 17°C (χ^2 = 0.0088; **Fig. 11a**) and correlate strongly to MAT (R^2=0.57; **Table 2**), suggesting that growth halts in *R. diluvianum* are not forced by an absolute temperature threshold, but rather by timing relative to the seasonality (circadian rhythm). If there would be a fixed temperature threshold (e.g. 6°C or 10°C for *Crassostrea gigas*; Lartaud et al., 2010; Ullmann et al., 2010) the length of the growth season should positively correlate with annual mean temperature, but this is not the case (R^2<0.1). Other authors have suggested growth in modern *C. gigas* does not actually cease completely but rather slows down significantly, which may also have been the case in *R. diluvianum*. On average, the moment of minimum growth in *R. diluvianum* occurs right after the highest temperatures of the year are reached (early autumn, **Fig. 9**).

The spawning season is concentrated in the two last months before the $\delta^{18}O$ maximum (first half of winter) when modelled water temperatures are ±17°C (**Fig. 11b**). Note that only three of the five shells allowed sampling of the first month of growth, and extrapolated records for the other two shells are likely unreliable. Comparing **Fig. 11a** and **Fig. 11b** shows that growth halts and spawning occur at similar temperatures (16.9 ± 0.7°C and 17.0 ± 0.3°C respectively, p = 0.72), suggesting that these events occur simultaneously or on either side of a seasonal growth halt (if it occurs). The timing of spawning in *R. diluvianum* differs from that in modern oysters, which generally spawn during the spring season, with the young oyster spat settling in in the summer (e.g. for *Crassostrea gigas*: Fan et al., 2011). In the case of modern oysters, it is known that reproduction requires a relatively warm minimum temperatures (ideally around 22°C for *C. gigas*; Cognie et al., 2006), and that a combination of salinity and temperature conditions is important (Fan et al., 2011), while extreme temperatures (>28°C; Surge et al., 2001) can induce shock. Perhaps the ideal conditions of *R. diluvianum* are lower (~17°C) or the ideal combination of temperature and salinity is met specifically in the autumn season.

Figure 11b shows that the distribution of months with fastest growth rate is random ($p(\chi^2)$ = 0.055, <95% confidence). However, in 27 of the 58 years, the growth peak occurs in the season with decreasing $\delta^{18}O$ values ("spring season"). **Table 2** shows that the extent of temperature seasonality (difference between

minimum and maximum $\delta^{18}O$ converted to temperature) significantly influences the length of the growing season ($R^2 = 0.40$). However, total annual growth and maximum growth rates are independent of SST (both seasonal extent and MAT) and ontogenetic age of the organism does not predict a significant part of any of the above-mentioned growth and seasonality parameters (**Table 2**). If temperature controlled the growth of *R. diluvianum* shells, larger temperature seasonality would increase the chance of crossing thresholds of temperature tolerance which would shorten the length of the growing season. All this suggests that temperature seasonality may not have been the dominant factor causing growth cessations in *R. diluvianum*. This hypothesis is supported by the observation that temperatures at which growth cessations occur (16.9 ± 0.7°C; **Fig. 11a**) show large variability and do not correspond significantly to the lowest temperatures of the year.

These observations do not necessarily show that *R. diluvianum* tolerated larger temperature differences than modern oyster taxa, because the extent of seasonality (14-25°C) causes neither the lower (~10°C) nor the upper limit of temperature tolerance (~28°C) in modern oysters to be reached. If temperature tolerance of *R. diluvianum* did resemble that of its closest modern relatives, then the mild seasonal temperature cycle at Ivö Klack might have provided the ideal temperature range for its growth. Perhaps these favorable conditions partly explain why biodiversity and abundance of invertebrates at Ivö Klack was so high (Surlyk and Sørensen, 2010).

5.5.3 Productivity

Shell growth in *R. diluvianum* may not have been governed by temperature, but rather by changes in productivity. The observation that peak growth rates and spawning both occur during the early spring season (**Fig. 11b**) supports this hypothesis. Spring productivity blooms caused by increases in nutrient-rich freshwater from onshore (Arthur et al., 1983; Krantz et al., 1987) or due to storm-induced mixing of more nutrient-rich deeper waters are common in present-day mid- and high-latitude marine ecosystems (e.g. Waniek, 2003; Danielsson et al., 2008). An increase in seasonal freshwater influx would cause longer growth cessations to occur in the spring season, reducing the length of the growing season while also dampening the reconstructed temperature seasonality (see **5.5.2**), which explains the correlation found between these two parameters (**Table 2**). At the same time, this freshwater input would increase

reconstructed MAT by increasing $\delta^{18}O$ values in *R. diluvianum* shells, explaining the weak positive correlation between MAT and length of the growing season (**Table 2**).

The occurrence of spring blooms is supported by weak 0.5-1.0‰ seasonal variability in $\delta^{13}C$ (**Fig. 6**). Seasonal changes in productivity and/or salinity will cause changes in DIC in the environment, which are apparent in the $\delta^{13}C$ of the shell above the ontogenetic trends and the effect of respiration on $\delta^{13}C$ (see **2.4**; **Table 1**). The fact that a clear seasonality in $\delta^{13}C$ is absent from the stack in **Fig. 9** shows that these productivity peaks do not occur at regular times of the season and that their effect on $\delta^{13}C$ is obscured by ontogenetic trends. The 0.5-1.0‰ shifts in $\delta^{13}C$ that appear to be seasonal are much smaller than those in modern oyster records (2-3‰ in low-latitude estuarine *Crassostrea virginica*; Surge et al., 2001; 2003; Surge and Lohmann, 2008). Instead, the determined shifts more closely resemble the 0.5‰ variability in $\delta^{13}C$ observed in modern *Crassostrea gigas* from the same approximate latitude as Ivö Klack in the North Sea (Ullmann et al., 2013). The extreme isotopic shifts in the estuarine *C. virginica* specimens have been shown to be caused by large shifts in freshwater input due to large seasonal variations in rainfall over southern North America (Surge et al., 2003), while smaller variations in *C. gigas* from the North Sea are produced by DIC changes due to seasonal changes in productivity (e.g. spring blooms; Ullmann et al., 2013). The closer resemblance of *R. diluvianum* to the North Sea condition shows that the Ivö Klack paleoenvironment did not experience large seasonal shifts in freshwater input and may have seen productivity peaks in spring season. The latter interpretation is in agreement with the coincidence of negative $\delta^{13}C$ excursions (in parts of the records not affected by ontogenetic trends and respiration) with the low-$\delta^{18}O$ season (winter or spring; **Fig. 6**; **S6**) and the occurrence of spawning and a peak in growth rates in the spring season (much like in wild modern oysters; Berthelin et al., 2000; **Fig. 9**; **Fig. 11a**).

5.5.4 Ontogeny~~4. Discussion~~

~~4.1 Preservation~~

~~The relative lack of burial and tectonic activity in the Kristianstad Basin has provided ideal circumstances for the nearly immaculate preservation of *R. diluvianum* shells in the Ivö Klack locality (Kominz et al., 2008;~~

Surlyk and Sørensen, 2010). The excellent state of these shells is evident by the preservation of original (porous and foliated) microstructures that closely resemble those reported for several species of modern ostreid shells (Carriker et al., 1979; Surge et al., 2001; Ullmann et al., 2010; 2013; Zimmt et al., 2018; Fig. 2-3). High magnification SEM images demonstrate the excellent preservation of foliated and vesicular calcite structures in *R. diluvianum* shells (Fig. 3b-d). The preservation state of *R. diluvianum* shells meets the criteria for robust stable isotope analysis set by Cochran et al. (2010). MicroXRF mapping reveals that the foliated calcite in the shells is characterized by high Sr concentrations and low concentrations of Mn, Fe and Si, elements which are generally associated with diagenetic alteration (e.g. Brand and Veizer, 1980; Al-Aasm and Veizer, 1986a; Immenhauser et al., 2005; Fig. 3b-h). Typically, a Mn concentration threshold of 100 µg/g is applied below which Cretaceous low-magnesium carbonates are assumed suitable for chemical analysis (Steuber et al., 2005; Huck et al., 2011). Strontium concentrations above 1000 µg/g have also been used as markers for good preservation, since diagenetic processes can cause strontium to leach out of carbonates (e.g. Brand and Veizer, 1980; Huck et al., 2011; Ullmann and Korte, 2015). Therefore, previous studies of belemnites in Kristianstad Basin proposed a molar Sr/Mn threshold of 100 (Sørensen et al., 2015). However, maintaining thresholds for diagenetic screening is relatively arbitrary and the height of the thresholds used differs widely in the literature (e.g. Veizer, 1983; Steuber et al., 2002; Ullmann and Korte, 2015; de Winter and Claeys, 2016). Applying these thresholds risks introducing biases to chemical datasets from fossil shells and may not be an ideal method for diagenetic screening. Furthermore, large variation in the *in vivo* incorporation of Mn and Sr in mollusk shell carbonate and a strong dependence on the diagenetic setting can make the interpretation of shell preservation from trace element ratios alone highly ambiguous (Ullmann and Korte, 2015). This conclusion is supported by the trace element and stable isotope data gathered and compiled in this study (Fig. 5). Comparison of data from different fossil species in Ivö Klack with two closely related modern oyster species from different environments indicates that the differences between fossil mollusk species are similar to the differences among modern oyster species. It also shows that pristine carbonate from modern oyster shells can contain up to 200 µg/g Mn accompanied by a wide range in Sr concentrations.

One should be cautious when directly comparing trace element concentrations in biogenic calcite between different time periods, as seawater composition of Late Cretaceous oceans (e.g. concentrations of Mg, Ca,

Sr and especially Li) may have been different from that of the present-day ocean (Stanley and Hardie, 1998; Coggon et al., 2010; Rausch et al., 2013). For this reason, one would expect, for example, that Sr concentrations in Late Cretaceous biogenic carbonate would be twice as low as those in carbonates formed in the modern ocean (Stanley and Hardie, 1998; de Winter et al., 2017a). Trends in Mn and Sr concentrations observed in all fossil species from Ivö Klack (Fig. 5b) likely point towards a diagenetic process affecting a subset of the data. When observing variations in $\delta^{18}O$ (a sensitive proxy for diagenesis and recrystallization; Brand and Veizer, 1980; Al-Aasm and Veizer, 1986b; Fig. 5d), the lack of covariation between Mn concentration and $\delta^{18}O$ shows that there is little evidence for meteoric diagenesis in these shells (Ullmann and Korte, 2015). Instead, these patterns are best explained by early marine cementation of porous carbonate structures from sea water with similar temperature and $\delta^{18}O$ as the living environment (see also Sørensen et al., 2015). These complex patterns merit great care in applying simple, general thresholds for diagenesis. Therefore, in this study, a multi-proxy approach is applied for diagenetic screening in which data is excluded based on a combination of Si, Ca, Mn, Fe and Sr concentrations, $\delta^{18}O$ values as well as SEM and visual observations of the shell structure at the location of measurement.

4.2 Dating of the Ivö Klack locality

Strontium isotope dating places the Ivö Klack deposits at 78.14 ± 0.26 Ma (Fig. 4). Nevertheless, age estimates from strontium isotope analyses could be biased towards a younger age due to the influx of radiogenic strontium-rich weathering products from the nearby Transscandinavian Igneous Belt (Högdal et al., 2004). This may explain the fact that, when plotting the obtained age of 78.14 Ma on the compilation by Wendler (2013), the age of the Ivö Klack falls slightly above the early/late Campanian subdivision (which is placed at ~78.5 Ma), while the *B. mammilatus* biozone is defined as late early Campanian. However, studies of modern strontium isotope ratio variability (Palmer and Edmond, 1989) and the potential bias of strontium isotope ratios in shallow-water carbonates (Kuznetsov et al., 2012; Meknassi et al., 2018) show that the effect of such inputs on strontium isotope dating results is generally negligible, except in semi-confined shallow-marine basins characterized by considerable freshwater input and low salinities (<7 g/kg). No evidence for such exceptional conditions at Ivö Klack exist (see section 4.3). We therefore conclude that

our strontium isotope age estimate, together with biostratigraphic constraints, places the Ivö Klack locality in the latest early Campanian.

The refined dating of the Ivö Klack deposits and fossils allows the results of sclerochronological investigations presented in this work to be placed in the context of longer-term climate reconstructions with improved precision. While previous attempts at dating Campanian strata mainly focused on relative dating using magneto- and biostratigraphy (Montgomery et al., 1998; Jarvis et al., 2002; Voigt et al., 2010), integration of cyclostratigraphic approaches in this integrated stratigraphic framework has recently allowed to constrain the age of the Campanian deposits more precisely (Voigt and Schönfield, 2010; Thibault et al., 2012; Wendler, 2013; Thibault et al. 2016). Unfortunately, these attempts rarely cover the time interval in which the Ivö Klack sediments were deposited (latest Early Campanian; e.g. Wendler, 2013; Perdiou et al., 2016). Given the length of individual magnetochrons, carbon isotope shifts and biozones, the accuracy of dating obtained by strontium isotope dating cannot, at the moment, be matched by the abovementioned integrated stratigraphical approaches (Wagreich et al., 2012). For short, nearshore sections that cannot be replaced within a long-term stratigraphic framework (such as Ivö Klack), strontium isotope stratigraphy on well-preserved samples remains the most reliable dating method at present.

4.3 Ontogeny, metabolism and environment

The complex relationship between $\delta^{13}C$ and $\delta^{18}O$ records in *R. diluvianum* suggests that multiple factors influence the incorporation of carbon into the shell calcite. In marine mollusks, dissolved inorganic carbon (DIC) in the ambient sea water contributes to the majority (90%) of carbon used for shell mineralization (McConnaughey, 2003; Gillikin et al., 2007). However, changes in respiration rates can alter the carbon budget of shell carbonate by adding or removing isotopically light respired carbon in the form of CO_2 (Lorrain et al., 2004). Of course, environmental changes in DIC can also have a strong influence on this carbon budget, especially when bivalves grow in nearshore or estuarine conditions with large (seasonal) variations in environmental $\delta^{13}C$ of DIC and organic carbon (Gillikin et al., 2006). Conceptual models exist that attempt to correlate shell $\delta^{13}C$ in modern mollusks to environmental and physiological variations, but these require knowledge of ambient CO_2 pressures and $\delta^{13}C$ values of DIC, gas ventilation rates in the animal and CO_2 and O_2 permeabilities of membranes (McConnaughey et al., 1997). Since these boundary

~~conditions are not available in fossil bivalve studies, the following discussion will remain limited to qualitative interpretations of $\delta^{13}C$ trends.~~

A part of the variation in $\delta^{13}C$ ~~may be~~is explained by the presence of ontogenetic trends. These trends are known to occur in marine and freshwater bivalves ~~as well as~~including in bivalves with symbionts (Klein et al., 1996b; Watanabe et al., 2004; Gillikin et al., 2007; McConnaughey and Gillikin, 2008). The scale and direction of the~~se~~ trends in $\delta^{13}C$ are not consistent between individual *R. diluvianum* shells, which is also the case in other bivalve species (see **section ~~3.5~~4.5**; **Table 1**; McConnaughey and Gillikin, 2008 and references therein). Studies of modern bivalves show that in larger (older) bivalves, the contribution of respired CO_2 to carbon in the shell is larger (up to 40%; Gillikin et al., 2007). This finding explains common trends of reducing $\delta^{13}C$ with age in bivalve shells, since respired carbon is isotopically lighter than environmental DIC. Since ontogenetic trends are likely caused by changes in the amount of respired carbon entering the shell, and the direction of these trends in *R. diluvianum*, the contribution of respired CO_2 to *R. diluvianum* shells likely did not strictly increase with age. While this complicates the interpretation of $\delta^{13}C$ records, the relative contribution of environmental changes to $\delta^{13}C$ variability in *R. diluvianum* shells does appear to be highest on the positive end of the ontogenetic trend.

~~In all $\delta^{13}C$ records we observe that the parts of the record that exceed a $\delta^{13}C$ value of ±3.6‰ exhibit more regular variations of ±0.6‰ that are correlated to the seasonal variability in $\delta^{18}O$ (see **S6**). These periods of covariation between $\delta^{13}C$ and $\delta^{18}O$ do not dominate in the records, as is evident from the lack of seasonality in the annual stack of $\delta^{13}C$ (**Fig. 8**). It is possible that, during parts of the lifetime of *R. diluvianum* when the effect of respiration on $\delta^{13}C$ of the shell is reduced, $\delta^{13}C$ fluctuations reflect a combination of changes in DIC and/or salinity in the environment, which are likely paced to the seasonal cycle. These ±0.6‰ shifts in $\delta^{13}C$ that appear to be seasonal are much smaller than those in modern oyster records (2-3‰ in low-latitude estuarine *Crassostrea virginica*; Surge et al., 2001; 2003; Surge and Lohmann, 2008). Instead, the determined shifts more closely resemble the 0.5‰ variability in $\delta^{13}C$ observed in modern *Crassostrea gigas* from the same approximate latitude as Ivö Klack in the North Sea (Ullmann et al., 2013). The extreme isotopic shifts in the estuarine *C. virginica* specimens have been shown to be caused by large shifts in freshwater input due to large seasonal variations in rainfall over southern North America (Surge et~~

al., 2003), while smaller variations in *C. gigas* from the North Sea are produced by DIC changes due to seasonal changes in productivity (e.g. spring blooms; Ullmann et al., 2013). The closer resemblance of *R. diluvianum* to the North Sea condition evidences that the Ivö Klack paleoenvironment did not experience large seasonal shifts in freshwater input and may have seen productivity peaks in spring season. The latter interpretation is in agreement with the coincidence of negative $\delta^{13}C$ excursions (in parts of the records not affected by ontogenetic trends and respiration) with the low-$\delta^{18}O$ season (winter or spring; **S6**) and the occurrence of spawning and a peak in growth rates in the spring season (much like in wild modern oysters; Berthelin et al., 2000; **Fig. 8,10a**). Large shifts in freshwater input are unlikely to have occurred in the Ivö Klack setting, lending more confidence to the growth and temperature modelling based on $\delta^{18}O$ records, which requires the assumption that changes in $\delta^{18}O_{seawater}$ did not exert dominant control on the $\delta^{18}O$ in shell carbonate.

4.4 Temperature seasonality

Modelling of seasonal changes in growth rate and temperature based on the $\delta^{18}O$ records in *R. diluvianum* yielded a MAT of 18.7°C with an average seasonal range of 5.2°C (**Fig. 8**). The reconstructed MAT is 7-8 degrees warmer than the present-day 10-12°C mean annual sea surface temperature in the North and Baltic seas at the same latitude (50-55°N; IRI/LDEO Climate Data Library, 2018). The MAT found in this study is similar to the MAT of the late early Campanian Boreal Chalk Sea waters of 17-19°C based on long-term reconstructions (Lowenstam and Epstein, 1954; Jenkyns et al., 2004; Friedrich et al., 2005; Thibault et al., 2016) and is slightly warmer than mean annual air temperatures reconstructed at the same paleolatitude (±15°C; Amiot et al., 2004). Averaging seasonality (**Fig. 8**) underestimates the extent of seasonality at Ivö Klack, because not all seasons contributing to the average have long growing seasons, which will reduce the average extent of seasonality. A more accurate estimate of the seasonal extent is obtained by calculating the seasonal range from the coolest winter temperatures (12.6°C in *R. diluvianum* 4; **SI10**) with the warmest recorded summer temperature (26°C in *R. diluvianum* 1; **S10** which yields a maximum seasonal sea surface temperature range of ±13.4°C. This is significantly less than the 16-20°C temperature seasonality that occurs in the present-day Baltic and North seas at the same latitude as Ivö Klack (IRI/LDEO Climate Data Library, 2018). Data on temperature seasonality in the Late Cretaceous is

scarce, especially in high-latitude settings. However, comparison with data on Cretaceous seasonality between 15°N and 35°N paleolatitude (Steuber et al., 2005) shows that while MAT at 50°N was significantly lower than those at lower latitudes (18°C vs. 25-30°C respectively), the seasonal temperature range during cooler periods in the Late Cretaceous was remarkably similar between latitudes (10-15°C in subtropical latitudes vs. ±14°C in this study). This observation contrasts with the present-day situation in Northern Africa and Europe, in which seasonal temperature ranges are generally much higher in mid- to high-latitudes (30-50°N) than in lower latitudes (10-30°N; Prandle and Lane, 1995; Rayner, 2003; Locarnini et al., 2013; NOAA, 2018). Such seasonalities reconstructed from bivalve shells are not consistent with model predictions of an ice-free Cretaceous world, since those models predict both smaller seasonal temperature ranges and a shallower paleotemperature gradient (Barrera and Johnson, 1999; Hay and Floegel, 2012; Upchurch et al., 2015).

4.5 Trace element proxies

4.5.1 Mg/Ca

From the data in **Fig. 8,** it is evident that there is a positive correlation between Mg/Ca and $\delta^{18}O$, or a negative correlation between Mg/Ca and temperature. This correlation is opposite to the temperature-relationships found in modern oyster species (Surge and Lohmann, 2008; Mouchi et al., 2013; Ullmann et al., 2013). Furthermore, the difference between seasonally high and low Mg/Ca values is small (1.2 mmol/mol) compared to seasonal variability observed in modern oysters (4-10 mmol/mol; Surge and Lohmann, 2008; Mouchi et al., 2013) and the variability between specimens of *R. diluvianum* (>3 mmol/mol; **Fig. 7**). This dampening of the Mg/Ca cycle likely results from phase shifts between seasonal Mg/Ca cycles in different specimens, causing seasonal cyclicity in different years and individuals to partly cancel each other out in the annual stacks in **Fig. 8** (see **SI10**). These inconsistencies and the inverse temperature correlation compared to modern oyster species demonstrate that it is unlikely that Mg/Ca ratios in *R. diluvianum* are predominantly controlled by water temperatures. Mg/Ca ratios can therefore not be used as reliable temperature proxies in this species.

4.5.2 Sr/Ca

Previous studies on modern bivalve species indicate that Sr/Ca ratios are not a likely candidate for reconstructing temperature (Gillikin et al., 2005; Schöne et al., 2013; Ullmann et al., 2013). However, the negative seasonal correlation between $\delta^{18}O$ and Sr/Ca ratios (**Fig. 8**) suggests that there is at least some seasonal parameter influencing Sr incorporation into *R. diluvianum* shells. This correlation cannot be explained by classic diagenetic alteration of the shell, since this process would cause more negative $\delta^{18}O$ values to coincide with lower Sr concentrations (Brand and Veizer, 1980; Ullmann and Korte, 2015; Sørensen et al., 2015), while the opposite is observed here. Unlike the Mg/Ca seasonality, comparison between Sr/Ca variability in **Fig. 7** and **Fig. 8** shows that the seasonal variability in Sr/Ca is much less dampened by inter-specimen variability and that phase relationships between Sr/Ca and $\delta^{18}O$ are consistent between individuals (see also **S6**). The variability in Sr/Ca observed in foliate calcite in *R. diluvianum* resembles seasonal variability in the same microstructure in modern *Crassostrea gigas* oysters grown in a similar, though cooler, environment (see discussion in **section 4.3**) both in relation to the $\delta^{18}O$ cycle and in absolute Sr/Ca values (0.8-1.0 mmol/mol; Ullmann et al., 2013). This resemblance would support a similar explanation for *R. diluvianum* as was attributed to Sr/Ca ratios in *C. gigas*, namely that the proxy reflects seasonal changes in ambient sea water chemistry. There is some uncertainty as to whether sea water Sr/Ca ratios in the Late Cretaceous were lower than (Stanley and Hardie, 1998; Coggon et al., 2010) or similar to (Steuber and Veizer, 2002; Lear et al., 2003) those in the modern ocean. Local enrichments in seawater Sr concentrations at Ivö Klack driving increased Sr composition in *R. diluvianum* are unlikely, since Sr/Ca ratios exhibit only small (2-3%) lateral variability in the world's oceans (De Villiers, 1999). Therefore, the similarity in absolute calcite Sr/Ca ratios between modern *C. gigas* and Campanian *R. diluvianum* may demonstrate that *R. diluvianum* incorporated more Sr into its shell than modern oysters compensating for lower ambient Sr concentrations.

4.5.3 Li-proxies

While tentative temperature reconstructions based on Sr/Li and Mg/Li ratios (**Fig. 7**) appear consistent with those found using $\delta^{18}O$, the stack in **Figure 8** shows that these ratios do not correlate with the seasonal $\delta^{18}O$ cycle. Instead, it seems as if both Mg/Li and Sr/Li follow the same pattern with two maxima per annual cycle. This, together with the strong covariation between Mg/Li and Sr/Li, is inconsistent with the

temperature dependence of these proxies (see **Fig. 7**). Instead, this covariation points to strong variations in Li concentrations in the shells as drivers for the observed variability. The negative correlation between Sr/Ca and Mg/Ca found in **Fig. 8** contradicts the inter-shell correlation between Mg/Li and Sr/Li found in **Fig. 7**. This shows that, when comparing proxy records between shells, it is important to apply reliable age models to correctly align the records such as the growth and age modelling approach applied in this study. The age model-based approach reliably visualizes correlations between proxies on a seasonal scale, while the approach of comparing seasonal averages and ranges of proxies (**Fig. 7**) puts more emphasis on absolute inter-shell differences in the expression of proxies. While the latter may be useful in detecting specimen-specific vital effects in trace element proxies (Freitas et al., 2008), the seasonally aligned comparison in **Fig. 8** more reliably reveals relationships between proxies and can be used to infer temperature dependence.

The inter-specimen comparison (**Fig. 7**) and the presence of randomly distributed ontogenetic trends in Li/Ca (see **section 3.5**) suggests that a large part of the variability in Mg/Li and Sr/Li is controlled by mechanisms that are local or even specimen-specific. The apparent occurrence of two peaks per year in these records (**Fig. 8**) shows that sub-annual changes in environment may contribute to the variability in Li proxies in *R. diluvianum*. Riverine input can be a large source contributing to the dissolved Li budget in shallow marine systems (Huh et al., 1998; Misra and Froelich, 2012). Therefore, synchronous fluctuations in Mg/Li and Sr/Li ratios observed in **Fig. 8** may reflect changes in riverine input over the year. However, stable isotope ratios in *R. diluvianum* show no sign of large fluctuations in freshwater input (see **section 4.3**), so the effect of these potential influxes on the local Li budget must have been limited. Furthermore, dissolved Li in modern rivers strongly covaries with Mg and Sr, causing an increase in freshwater input to have a limited effect on Mg/Li and Sr/Li ratios (Huh et al., 1998; Brunskill et al., 2003). The observation that the inter-species variability in these proxies is much larger than the sub-annual variability (50-300 mol/mol for Sr/Li and 350-1000 mol/mol for Mg/Li between specimens compared to 120-260 mol/mol for Sr/Li and 450-900 mol/mol for Mg/Li within a year) indicates that the effect of sub-annual environmental change is likely to be small, and specimen-specific effects dominate. These complications prevent the use of Mg/Li and Sr/Li proxies for temperature reconstructions in *R. diluvianum*.

~~The complexity of interpreting trace element proxies in this study shows that the incorporation of Mg and Li into *R. diluvianum* was likely heavily biologically regulated. This result demonstrates that earlier successful attempts to establish calibration curves for Li- and Mg-based temperature proxies (e.g. Füllenbach et al., 2015; Dellinger et al., 2018) are probably strictly limited to bivalve species or close relatives. The same conclusion was also drawn by Dellinger et al. (2018) based on Li/Mg and Li isotope ratio measurements in biogenic carbonates. The lack of Mg/Li or Sr/Li calibrations in modern oyster shells limits the interpretation of results in this study and establishing such calibrations using modern oysters in cultured experiments may allow these proxies to be used for reconstructions from fossil oyster shells in the future.~~

~~4.6 Growth and life cycle~~

~~Modelling the growth of *R. diluvianum* shells based on $\delta^{18}O$ profiles (Judd et al., 2018) yields a lot of information about the growth and life cycle of these oysters (**Fig. 9-10**). One of the most interesting results is the remarkable similarity in growth patterns between individuals of *R. diluvianum* (**Fig. 9**). Except for the final parts of growth curves of some of the older shells, all shells show similar development of shell height with age. This development is well approximated by a Von Bertalanffy curve with a K value of 0.32 and a theoretical full-grown shell height (H_{max}) of 120.3 mm ($r = 0.89$; $\rho = 0.87$; Von Bertalanffy, 1957; **Fig. 9**). The consistency in growth curves between individuals of *R. diluvianum* is somewhat surprising given the fact that modern oyster species are known to exhibit large variations in growth rates and shell shapes as a function of their colonial lifestyle, which often limits the growth of their shells in several directions (Galtsoff, 1964; Palmer and Carriker, 1979). The strong resemblance of growth between individuals and the close fit of the idealized Von Bertalanffy growth model suggests that growth of *R. diluvianum* at Ivö Klack was relatively unrestricted in space. This hypothesis is consistent with the apparent mode of life of *R. diluvianum* in Ivö Klack cemented together in groups, subject to strong wave action and turbulence, but with little competition for space due to the high-energy environment (Surlyk and Christensen, 1974; Sørensen et al., 2012). The shape of the growth curve of *R. diluvianum* is fairly consistent with that of modern Chesapeake Bay oysters (*Crassostrea virginica*), which exhibit a slightly larger modelled maximum height (150 mm) and a slightly smaller K-value (0.28). A larger subset of *R. diluvianum* specimens studied by Sørensen et al.~~

(2012) demonstrates that these bivalves could grow up to 160 mm in height. The curvature of the growth of *R. diluvianum* (K -value) is also similar to that found for other modern shallow marine bivalve species (e.g. *Macoma balthica*, K = 0.2-0.4; Bachelet, 1980; *Pinna nobilis*, K = 0.33-0.37; Richardson et al., 2004) and significantly higher than in growth curves of deep marine bivalves (e.g. *Placopecten magellanicus*, K = 0.16-0.24; MacDonald and Thompson, 1985; Hart and Chute, 2009) or bivalves from cold habitats (e.g. North Atlantic *Arctica islandica*, K = 0.06; Strahl et al., 2007). This reflects the high growth rates (steeper growth curves, higher K-values) of shallow marine bivalves compared to species living in more unfavorable or restricting (colder or deeper) habitats, with *R. diluvianum* clearly being part of the former group.

Figure 10 and **Table 2** illustrate statistics of growth and seasonality for a total of 58 years of growth in the complete dataset. This data indicates that the growing season is shorter than 365 days in all but five modelled years, demonstrating that growth stops did occur in *R. diluvianum*. Minimum growth temperatures (temperatures by which growth stops) are concentrated around 17°C (χ^2 = 0.0088; **Fig. 10a**) and correlate strongly to MAT (Pearson's r = 0.752; **Fig. 10b**), suggesting that while potential growth halts in *R. diluvianum* occur systematically at a certain time interval of the year (first half of "winter"), they are not forced by an absolute temperature threshold, but rather by timing relative to the seasonality (circadian rhythm). On average, the moment of minimum growth occurs right after the highest temperatures of the year are reached (early autumn, **Fig. 8**).

The spawning season (onset of the first growth year, see **3.9**) is concentrated in the two last months before the $\delta^{18}O$ maximum (first half of "winter") when modelled water temperatures are ±17°C (**Fig. 10c**). Note that only three of the five shells allowed sampling of the first month of growth, and extrapolated records for the other two shells yielded spawning around the $\delta^{18}O$ minimum ("summer"). The offset of these estimates likely results from uncertainty introduced due to extrapolation of the records of these two remaining shells, showing that these estimates are likely unreliable. Comparing **Fig. 10c** and **Fig. 10a** shows that growth halts and spawning occur at similar temperatures (16.85 ± 0.67°C and 16.98 ± 0.34°C respectively, p = 0.717), suggesting that these events occur simultaneously or on either side of a seasonal growth halt (if it occurs).

Figure 10c shows that the distribution of months with fastest growth rate is random ($p(\chi^2) = 0.055$, <95% confidence). However, in 27 of the 58 years, the growth peak occurs in the season with decreasing $\delta^{18}O$ values ("spring season"), just after the moment of spawning (winter season; **Fig. 10a-b**). **Table 2** shows that the extent of temperature seasonality (difference between minimum and maximum $\delta^{18}O$ converted to temperature) significantly influences the length of the growing season (strong correlation), the maximum growth in that year and the total annual growth (weak correlations). MAT is a weak but significant driver of annual growth, maximum growth and length of growing season. Ontogenetic age of the organism does not predict a significant part of any of the above mentioned growth and seasonality parameters (**Table 2**). All this suggests that temperature seasonality may not have been the dominant factor causing growth cessations in *R. diluvianum*. This hypothesis is supported by the observation that temperatures at which growth cessations occur (16.85 ± 0.67°C; **Fig. 10b**) show large variability and do not correspond significantly to the lowest temperatures of the year.

This pattern is decidedly different from that observed in modern *Crassostrea gigas* shells, which generally stop growing their shell at temperatures below ±10°C (Surge et al., 2001; Lartaud et al., 2010; Ullmann et al., 2013). In contrast, lower latitude *Crassostrea virginica* from estuarine environments cease shell growth at temperature maxima (>28°C; Surge et al., 2001). Other bivalves are known to have more flexible temperature thresholds for shell precipitation (Ivany, 2012), but a lack of correlation between shell age and length of season or minimum growth temperature (**Table 2**) demonstrates that there is no evidence for this in *R. diluvianum*. These observations do not necessarily show that *R. diluvianum* tolerated larger temperature differences than these modern taxa, because the maximum extent of seasonality between 12.6°C and 26°C reconstructed from $\delta^{18}O$ records in this study (see **section 4.3**) causes neither the lower nor the upper limit of temperature tolerance in modern oysters to be reached. If temperature tolerance of *R. diluvianum* did resemble that of its closest modern relatives, then the mild seasonal temperature cycle at Ivö Klack might have provided the ideal temperature conditions for its growth. Perhaps these favorable conditions partly explain why biodiversity and abundance of invertebrates at Ivö Klack was so high (Surlyk and Sørensen, 2010). If this was the case, then shell growth in *R. diluvianum* may not have been governed by temperature, but rather by changes in productivity, as was already hypothesized based on fluctuations in $\delta^{13}C$ (see **section 4.4**). A strong 1:1 correlation between MAT and the temperature by which growth

cessations occur (slope = 0.981; r = 0.752; **Fig. 10c**) supports the hypothesis that absolute temperatures did not limit shell growth, but rather that growth cessations occur consistently in certain parts of the seasonal cycle. The observation that peak growth rates and spawning both occur during the early spring season (**Fig. 10c**) is also consistent with the occurrence of spring blooms of increased productivity (**section 4.3**).

Finally, as **Table 2** shows, the length of the growing season positively correlates with the size of temperature seasonality. This relationship is opposite to what would be expected if temperature controlled the growth of *R. diluvianum* shells, since in that case, larger temperature seasonality would cause intolerable temperature thresholds to be reached during larger parts of the seasonal cycle, which would shorten the length of the growing season. Instead, the correlation in **Table 2** can be explained by a small input of isotopically light freshwater in spring carrying nutrients to initiate the spring bloom (Arthur et al., 1983; Krantz et al., 1987). Such a freshwater contribution would reduce $\delta^{18}O_{seawater}$ in the early spring season and dampen the seasonality in shell $\delta^{18}O$ values. A larger influence of seasonal freshwater input would cause longer growth cessations to occur in the spring season, reducing the length of the growing season while also dampening the reconstructed temperature seasonality, which explains the correlation found between these two parameters. At the same time, this freshwater input would increase reconstructed MAT by increasing $\delta^{18}O$ values in *R. diluvianum* shells, explaining the weak positive correlation between MAT and length of the growing season (**Table 2**). While seasonal changes in salinity and seawater $\delta^{18}O$ must have remained limited at Ivö Klack (see **section 4.3**), from the discussion above we conclude that seasonal differences in productivity, potentially forced by input of nutrient-rich freshwater, are likely to have been a major factor influencing shell growth in *R. diluvianum* at Ivö Klack. In this case, dampening of the seasonal $\delta^{18}O$ cycle may cause temperature seasonality reconstructions in this study to underestimate the real extent of seasonality.

5. Conclusions

The highly biodiverse marine invertebrate community at Ivö Klack in the Kristianstad Basin in southern Sweden offers a unique opportunity to recover a wealth of information about Campanian climate and environment in high latitudes and the ecology and life of extinct invertebrate species that lived under these

conditions. The lack of burial and tectonic activity in the region favored *Rastellum diluvianum* fossil shells from Ivö Klack to be well preserved, as is evident from the excellent preservation of growth structures typical for ostreid shells as well as from limited evidence for geochemical changes associated with diagenetic alteration. This excellent preservation allows the shells of *R. diluvianum* to be used to accurately and precisely constrain the age of the Ivö Klack locality using strontium isotope stratigraphy (78.14 ± 0.26 Ma; $^{87}Sr/^{86}Sr = 0.707552 \pm 0.000112$). Furthermore, *R. diluvianum* shells reveal sub-annual scale variability in temperature, local environment and growth rates through ~~our~~ a multi-proxy geochemical approach. The combination of trace element and stable isotope measurements with growth modelling based on $\delta^{18}O$ records in the shells allow all measured proxies to be aligned on the same time axis. Application of transfer functions for potential Mg/Ca, Mg/Li and Sr/Li temperature proxies established in modern invertebrates yields temperatures consistent with those calculated from $\delta^{18}O$ records. However, close examination of the seasonal phase relationships between these proxies reveals that the sub-annual variability in these trace element ratios is not controlled by temperature changes alone. This observation supports previous studies that found the expression of trace element proxies to be highly variable among species and even among different specimens of the same species. If trace element proxies are to be used for seasonality reconstructions in pre-Qua~~r~~ternary times, a more robust, non-species-specific model for the incorporation of trace elements by bivalves is required. Establishing such a model requires culture experiments with different bivalve species in which multiple parameters influencing trace element composition can be controlled (e.g. temperature, salinity, food intake and microstructure).

Stable isotope records in *R. diluvianum* shells reveal a MAT of ~~17-~~19°C with a ~~maximal~~ seasonal water temperature range of ±~~14~~11°C (14-25°C~~12.6°C - 26°C~~) at Ivö Klack. This value for MAT is ~~consistent with long-term temperature reconstructions in the Campanian Boreal Chalk Sea~~lower than full marine SST of Boreal Chalk recently reevaluated with the clumped isotope thermometer. The difference highlights potential biases in temperature reconstructions based on $\delta^{18}O$ values and argue for reevaluations of these proxy records with more accurate techniques such as clumped isotope analysis. Comparing the seasonal temperature range reconstructed from *R. diluvianum* shells with other Late Cretaceous seasonality records from lower latitudes reveals that both latitudinal gradients and ~~temperature~~ SST seasonality outside the tropics were much ~~was remarkably similar across latitudes~~higher than predicted by. ~~These reconstructions~~

contradict results from climate models, which predict smaller temperature seasonalities. This disagreement between data and models clearly illustrates the disadvantage of the lack of data on Late Cretaceous seasonality outside the (sub-)tropical latitudes and highlights how important such reconstructions are for improving our understanding of the dynamics in temperature variability in both space and time during greenhouse climates.

Finally, the coupled modelling and multi-proxy approach applied in this study sheds light on the effects of environmental changes on the life cycle and sub-annual growth of *R. diluvianum* shells. This study reveals that growth curves of *R. diluvianum* strongly resemble those in modern shallow marine bivalves that grow in coastal high latitude environments. However, changes in growth rate of our Boreal oysters seem unrelated to temperature, in contrast to modern, high-latitude oysters that tend to lower their growth rate and cease mineralization below a certain cold threshold. We conclude that growth cessations and sub-annual changes in growth rate in *R. diluvianum* were most likely not caused by intolerable temperatures, but rather by circadian rhythm tied to the seasonal cycle and seasonal changes in sea surface productivity, driven by nutrient-rich freshwater inputs.

Acknowledgements

The authors would like to thank dr. Johan Vellekoop and dr. Andrew Johnson for their review that helped improve the manuscript, as well as editor dr Aninda Mazumdar for guiding the review process. This work was made possible with help of an IWT doctoral fellowship (IWT700) awarded to Niels de Winter. Instrumentation at the VUB was funded by Hercules infrastructure grants (HERC09 and HERC461309). The authors acknowledge financial and logistic support from the Flemish Research Foundation (FWO, research project G017217N) and Teledyne CETAC Technologies (Omaha, NE, USA) as well as support from VUB Strategic Research (BAS48). Stijn Goolaerts is funded by a Belspo Brain project (BR/175/A2/CHICXULUB). Nicolas Thibault is funded by Carlsbergfondet grant CF16-0457. The authors would like to thank David Verstraeten for his help with stable isotope analyses. We thank Bart Lippens for assisting sample preparation and Joke Belza for help with the LA-ICP-MS analyses. Thanks are due to Julien Cilis (RBINS) for his assistance with SEM imaging. The authors wish

to thank Emily Judd for discussions about her growth rate model for bivalve shells and Roger Barlow for his assistance with combining strontium isotope measurements with asymmetric error distributions.

Supplementary files

All supplementary files are stored in the open access online database Zenodo and can be accessed using the following link: https://doi.org/10.5281/zenodo.3699542~~https://zenodo.org/record/2581305~~

S1: High resolution (6400 dpi) scans of cross sections through the 12 shells of *Rastellum diluvianum* used in this study.

S2: Compilation of µXRF maps of cross sections through the 12 shells of *Rastellum diluvianum* used in this study.

S3: Compilation of XRF line scans measured through the foliated calcite of *Rastellum diluvianum* shells.

S4: Compilation of LA-ICP-MS data collected within the context of this study.

S5: Compilation of IRMS data used in this study.

S6: Composite figures of XRF linescan data through the shells of *Rastellum diluvianum*.

S7: Source code of the bivalve growth model adapted from Judd et al. (2018) including temperature equations for calcite.

S8: Compilation of strontium isotope data and ages used in this study.

S9: Compilation of the results from growth modelling on 5 *Rastellum diluvianum* shells.

S10: Compilation figures of proxy record data plotted on time axis for all 5 shells for which modelling was carried out.

S11: Plot of ontogenetic trends in $\delta^{13}C$ and Li/Ca proxies including statistics on the spread of the slopes of these trends.

S12: Data on trends in $\delta^{13}C$ and Li/Ca.

S13: Data used to create seasonality crossplots shown in **Fig. 7**.

S14: Data on statistics of the growth rates, seasonality and spawning season of all 5 bivalves for which modelling was done.

~~IRI/LDEO Climate Data Library URL http://iridl.ldeo.columbia.edu (accessed 01/11/19).~~

~~NOAA Earth System Research Laboratory: NOAA Optimum Interpolation (IO) Sea Surface Temperature (SST) http://www.esrl.noaa.gov/psd/data/gridded/data.noaa.oisst.v2.html (accessed 01/21/19).~~

References

Al-Aasm, I. S. and Veizer, J.: Diagenetic stabilization of aragonite and low-Mg calcite, II. Stable isotopes in rudists, Journal of Sedimentary Research, 56(6), 763–770, 1986a.

Al-Aasm, I. S. and Veizer, J.: Diagenetic stabilization of aragonite and low-Mg calcite, I. Trace elements in rudists, Journal of Sedimentary Research, 56(1), 138–152, 1986.

Alberti, M., Fürsich, F. T., Abdelhady, A. A. and Andersen, N.: Middle to Late Jurassic equatorial seawater temperatures and latitudinal temperature gradients based on stable isotopes of brachiopods and oysters from Gebel Maghara, Egypt, Palaeogeography, Palaeoclimatology, Palaeoecology, 468, 301–313, doi:10.1016/j.palaeo.2016.11.052, 2017.

Amiot, R., Lécuyer, C., Buffetaut, E., Fluteau, F., Legendre, S. and Martineau, F.: Latitudinal temperature gradient during the Cretaceous Upper Campanian–Middle Maastrichtian: δ18O record of continental vertebrates, Earth and Planetary Science Letters, 226(1), 255–272, doi:10.1016/j.epsl.2004.07.015, 2004.

Andreasson, F. P. and Schmitz, B.: Winter and summer temperatures of the early middle Eocene of France from Turritella 18O profiles, , 4, 1996.

Arthur, M. A., Williams, D. F. and Jones, D. S.: Seasonal temperature-salinity changes and thermocline development in the mid-Atlantic Bight as recorded by the isotopic composition of bivalves, Geology, 11(11), 655–659, doi:10.1130/0091-7613(1983)11<655:STCATD>2.0.CO;2, 1983.

Bachelet, G.: Growth and recruitment of the tellinid bivalve Macoma balthica at the southern limit of its geographical distribution, the Gironde estuary (SW France), Marine Biology, 59(2), 105–117, 1980.

Barlow, R.: Asymmetric systematic errors, arXiv preprint physics/0306138, 2003.

Barrera, E. and Johnson, C. C.: Evolution of the Cretaceous Ocean-climate System, Geological Society of America., 1999.

Berthelin, C., Kellner, K. and Mathieu, M.: Storage metabolism in the Pacific oyster (Crassostrea gigas) in relation to summer mortalities and reproductive cycle (West Coast of France), Comparative Biochemistry and Physiology Part B: Biochemistry and Molecular Biology, 125(3), 359–369, doi:10.1016/S0305-0491(99)00187-X, 2000.

Brand, U. and Veizer, J.: Chemical diagenesis of a multicomponent carbonate system–1: Trace elements, Journal of Sedimentary Research, 50(4), 1219–1236, 1980.

Brand, U. and Veizer, J.: Chemical diagenesis of a multicomponent carbonate system-2: stable isotopes, Journal of Sedimentary Research, 51(3), 987–997, 1981.

Bryan, S. P. and Marchitto, T. M.: Mg/Ca–temperature proxy in benthic foraminifera: New calibrations from the Florida Straits and a hypothesis regarding Mg/Li, Paleoceanography, 23(2), PA2220, doi:10.1029/2007PA001553, 2008.

Burgener, L., Hyland, E., Huntington, K. W., Kelson, J. R. and Sewall, J. O.: Revisiting the equable climate problem during the Late Cretaceous greenhouse using paleosol carbonate clumped isotope temperatures from the Campanian of the Western Interior Basin, USA, Palaeogeography, Palaeoclimatology, Palaeoecology, 516, 244–267, doi:10.1016/j.palaeo.2018.12.004, 2018.

Butler, P. G., Wanamaker, A. D., Scourse, J. D., Richardson, C. A. and Reynolds, D. J.: Variability of marine climate on the North Icelandic Shelf in a 1357-year proxy archive based on growth increments in the bivalve Arctica islandica, Palaeogeography, Palaeoclimatology, Palaeoecology, 373, 141–151, doi:10.1016/j.palaeo.2012.01.016, 2013.

Carriker, M. R., Palmer, R. E. and Prezant, R. S.: Functional ultramorphology of the dissoconch valves of the oyster Crassostrea virginica, in Proceedings of the National Shellfisheries Association, vol. 70, pp. 139–183. [online] Available from: https://www.researchgate.net/profile/Robert_Prezant2/publication/236964411_Functional_ultramorphology_of_the_dissoconch_valves_of_the_oyster_Crassostrea_virginica/links/53dfd2260cf2a768e49be892.pdf, 1979.

Carriker, M. R., Swann, C. P., Prezant, R. S. and Counts, C. L.: Chemical elements in the aragonitic and calcitic microstructural groups of shell of the oysterCrassostrea virginica: A proton probe study, Marine Biology, 109(2), 287–297, 1991.

Christensen, W. K.: Upper Cretaceous belemnites from the Kristianstad area in Scania, Fossils and Strata., 1975.

Christensen, W. K.: The Albian to Maastrichtian of southern Sweden and Bornholm, Denmark: a review, Cretaceous Research, 5(4), 313–327, 1984.

Christensen, W. K.: Paleobiogeography and migration in the Late Cretaceous belemnite family Belemnitellidae, Acta palaeontologica polonica, 42(4), 457–495, 1997.

Clarke, L. J. and Jenkyns, H. C.: New oxygen isotope evidence for long-term Cretaceous climatic change in the Southern Hemisphere, Geology, 27(8), 699–702, 1999.

Cochran, J. K., Kallenberg, K., Landman, N. H., Harries, P. J., Weinreb, D., Turekian, K. K., Beck, A. J. and Cobban, W. A.: Effect of diagenesis on the Sr, O, and C isotope composition of late Cretaceous mollusks from the Western Interior Seaway of North America, American Journal of Science, 310(2), 69–88, doi:10.2475/02.2010.01, 2010.

Coggon, R. M., Teagle, D. A., Smith-Duque, C. E., Alt, J. C. and Cooper, M. J.: Reconstructing past seawater Mg/Ca and Sr/Ca from mid-ocean ridge flank calcium carbonate veins, Science, 327(5969), 1114–1117, 2010.

Cognie, B., Haure, J. and Barillé, L.: Spatial distribution in a temperate coastal ecosystem of the wild stock of the farmed oyster Crassostrea gigas (Thunberg), Aquaculture, 259(1–4), 249–259, 2006.

Csiki-Sava, Z., Buffetaut, E., Ősi, A., Pereda-Suberbiola, X. and Brusatte, S. L.: Island life in the Cretaceous - faunal composition, biogeography, evolution, and extinction of land-living vertebrates on the Late Cretaceous European archipelago, Zookeys, (469), 1–161, doi:10.3897/zookeys.469.8439, 2015.

Dalbeck, P., England, J., Cusack, M., Lee, M. R. and Fallick, A. E.: Crystallography and chemistry of the calcium carbonate polymorph switch in M. edulis shells, European Journal of Mineralogy, 18(5), 601–609, doi:10.1127/0935-1221/2006/0018-0601, 2006.

Danielsson, \AAsa, Papush, L. and Rahm, L.: Alterations in nutrient limitations—scenarios of a changing Baltic Sea, Journal of Marine Systems, 73(3–4), 263–283, 2008.

De Villiers, S.: Seawater strontium and Sr/Ca variability in the Atlantic and Pacific oceans, Earth and Planetary Science Letters, 171(4), 623–634, 1999.

DeConto, R. M., Hay, W. W., Thompson, S. L. and Bergengren, J.: Late Cretaceous climate and vegetation interactions: cold continental interior paradox, SPECIAL PAPERS-GEOLOGICAL SOCIETY OF AMERICA, 391–406, 1999.
Dellinger, M., West, A. J., Paris, G., Adkins, J. F., von Strandmann, P. A. P., Ullmann, C. V., Eagle, R. A., Freitas, P., Bagard, M.-L. and Ries, J. B.: The Li isotope composition of marine biogenic carbonates: Patterns and Mechanisms, Geochimica et Cosmochimica Acta, 236, 315–335, 2018.
Donnadieu, Y., Pucéat, E., Moiroud, M., Guillocheau, F. and Deconinck, J.-F.: A better-ventilated ocean triggered by Late Cretaceous changes in continental configuration, Nature Communications, 7, 10316, doi:10.1038/ncomms10316, 2016.
El Meknassi, S., Dera, G., Cardone, T., De Rafélis, M., Brahmi, C. and Chavagnac, V.: Sr isotope ratios of modern carbonate shells: Good and bad news for chemostratigraphy, Geology, 46(11), 1003–1006, 2018.
Fan, C., Koeniger, P., Wang, H. and Frechen, M.: Ligamental increments of the mid-Holocene Pacific oyster Crassostrea gigas are reliable independent proxies for seasonality in the western Bohai Sea, China, Palaeogeography, palaeoclimatology, palaeoecology, 299(3–4), 437–448, 2011.
Freitas, P. S., Clarke, L. J., Kennedy, H. A. and Richardson, C. A.: Inter-and intra-specimen variability masks reliable temperature control on shell Mg/Ca ratios in laboratory and field cultured Mytilus edulis and Pecten maximus (bivalvia), Biogeosciences Discussions, 5(1), 531–572, 2008.
Friedrich, O., Herrle, J. O. and Hemleben, C.: Climatic changes in the late Campanian—early Maastrichtian: Micropaleontological and stable isotopic evidence from an epicontinental sea, Journal of Foraminiferal Research, 35(3), 228–247, 2005.
Friedrich, O., Herrle, J. O., Wilson, P. A., Cooper, M. J., Erbacher, J. and Hemleben, C.: Early Maastrichtian carbon cycle perturbation and cooling event: Implications from the South Atlantic Ocean, Paleoceanography, 24(2), PA2211, doi:10.1029/2008PA001654, 2009.
Friedrich, O., Norris, R. D. and Erbacher, J.: Evolution of middle to Late Cretaceous oceans—a 55 my record of Earth's temperature and carbon cycle, Geology, 40(2), 107–110, 2012.
Füllenbach, C. S., Schöne, B. R. and Mertz-Kraus, R.: Strontium/lithium ratio in aragonitic shells of Cerastoderma edule (Bivalvia)—A new potential temperature proxy for brackish environments, Chemical Geology, 417, 341–355, 2015.
Galtsoff, P. S.: The American Oyster: US Fish and Wildlife Service, Fishery Bulletin, 64, 480, 1964.
Gillikin, D. P., Lorrain, A., Navez, J., Taylor, J. W., André, L., Keppens, E., Baeyens, W. and Dehairs, F.: Strong biological controls on Sr/Ca ratios in aragonitic marine bivalve shells, Geochemistry, Geophysics, Geosystems, 6(5), Q05009, 2005.
Gillikin, D. P., Lorrain, A., Bouillon, S., Willenz, P. and Dehairs, F.: Stable carbon isotopic composition of Mytilus edulis shells: relation to metabolism, salinity, δ 13 C DIC and phytoplankton, Organic Geochemistry, 37(10), 1371–1382, 2006.
Gillikin, D. P., Lorrain, A., Meng, L. and Dehairs, F.: A large metabolic carbon contribution to the δ 13 C record in marine aragonitic bivalve shells, Geochimica et Cosmochimica Acta, 71(12), 2936–2946, 2007.
Hart, D. R. and Chute, A. S.: Verification of Atlantic sea scallop (Placopecten magellanicus) shell growth rings by tracking cohorts in fishery closed areas, Canadian Journal of Fisheries and Aquatic Sciences, 66(5), 751–758, 2009.
Hay, W. W. and Floegel, S.: New thoughts about the Cretaceous climate and oceans, Earth-Science Reviews, 115(4), 262–272, 2012.
van Hinsbergen, D. J., de Groot, L. V., van Schaik, S. J., Spakman, W., Bijl, P. K., Sluijs, A., Langereis, C. G. and Brinkhuis, H.: A paleolatitude calculator for paleoclimate studies, PloS one, 10(6), e0126946, 2015.
Högdahl, K., Andersson, U. B. and Eklund, O.: The Transscandinavian Igneous Belt (TIB) in Sweden: a review of its character and evolution, Geological survey of Finland Espoo., 2004.
Huber, B. T., Norris, R. D. and MacLeod, K. G.: Deep-sea paleotemperature record of extreme warmth during the Cretaceous, Geology, 30(2), 123–126, 2002.
Huck, S., Heimhofer, U., Rameil, N., Bodin, S. and Immenhauser, A.: Strontium and carbon-isotope chronostratigraphy of Barremian–Aptian shoal-water carbonates: Northern Tethyan platform drowning predates OAE 1a, Earth and Planetary Science Letters, 304(3–4), 547–558, doi:10.1016/j.epsl.2011.02.031, 2011.
Huyghe, D., Lartaud, F., Emmanuel, L., Merle, D. and Renard, M.: Palaeogene climate evolution in the Paris Basin from oxygen stable isotope (δ18O) compositions of marine molluscs, Journal of the Geological Society, 172(5), 576–587, 2015.
Huyghe, D., de Rafelis, M., Ropert, M., Mouchi, V., Emmanuel, L., Renard, M. and Lartaud, F.: New insights into oyster high-resolution hinge growth patterns, Mar Biol, 166(4), 48, doi:10.1007/s00227-019-3496-2, 2019.
Immenhauser, A., Nägler, T. F., Steuber, T. and Hippler, D.: A critical assessment of mollusk 18 O/16 O, Mg/Ca, and 44 Ca/40 Ca ratios as proxies for Cretaceous seawater temperature seasonality, Palaeogeography, Palaeoclimatology, Palaeoecology, 215(3), 221–237, 2005.
IPCC: IPCC, 2013: Climate Change 2013: The Physical Science Basis. Contribution of Working Group I to the Fifth Assessment Report of the Intergovernmental Panel on Climate Change, 1535 pp, Cambridge Univ. Press, Cambridge, UK, and New York., 2013.
IRI/LDEO Climate Data Library URL http://iridl.ldeo.columbia.edu (accessed 06/03/20).
Ivany, L. C.: Reconstructing paleoseasonality from accretionary skeletal carbonates—challenges and opportunities, The Paleontological Society Papers, 18, 133–166, 2012.
Ivany, L. C. and Runnegar, B.: Early Permian seasonality from bivalve δ18O and implications for the oxygen isotopic composition of seawater, Geology, 38(11), 1027–1030, 2010.
Jablonski, D., Huang, S., Roy, K. and Valentine, J. W.: Shaping the latitudinal diversity gradient: new perspectives from a synthesis of paleobiology and biogeography, The American Naturalist, 189(1), 1–12, 2017.
Jarvis, I., Mabrouk, A., Moody, R. T. and de Cabrera, S.: Late Cretaceous (Campanian) carbon isotope events, sea-level change and correlation of the Tethyan and Boreal realms, Palaeogeography, Palaeoclimatology, Palaeoecology, 188(3), 215–248, 2002.
Jenkyns, H. C., Gale, A. S. and Corfield, R. M.: Carbon-and oxygen-isotope stratigraphy of the English Chalk and Italian Scaglia and its palaeoclimatic significance, Geological Magazine, 131(1), 1–34, 1994.
Jenkyns, H. C., Forster, A., Schouten, S. and Damsté, J. S. S.: High temperatures in the late Cretaceous Arctic Ocean, Nature, 432(7019), 888, 2004.
Jones, D. S.: Sclerochronology: reading the record of the molluscan shell: annual growth increments in the shells of bivalve molluscs record marine climatic changes and reveal surprising longevity, American Scientist, 71(4), 384–391, 1983.

Judd, E. J., Wilkinson, B. H. and Ivany, L. C.: The life and time of clams: Derivation of intra-annual growth rates from high-resolution oxygen isotope profiles, Palaeogeography, Palaeoclimatology, Palaeoecology, 490, 70–83, 2018.
Kawaguchi, T. and Watabe, N.: The organic matrices of the shell of the American oyster Crassostrea virginica Gmelin, Journal of Experimental Marine Biology and Ecology, 170(1), 11–28, doi:10.1016/0022-0981(93)90126-9, 1993.
Kim, S.-T. and O'Neil, J. R.: Equilibrium and nonequilibrium oxygen isotope effects in synthetic carbonates, Geochimica et Cosmochimica Acta, 61(16), 3461–3475, 1997.
Klein, R. T., Lohmann, K. C. and Thayer, C. W.: Bivalve skeletons record sea-surface temperature and δ18O via Mg/Ca and 18O/16O ratios, Geology, 24(5), 415–418, 1996a.
Klein, R. T., Lohmann, K. C. and Thayer, C. W.: SrCa and 13C12C ratios in skeletal calcite of Mytilus trossulus: Covariation with metabolic rate, salinity, and carbon isotopic composition of seawater, Geochimica et Cosmochimica Acta, 60(21), 4207–4221, doi:10.1016/S0016-7037(96)00232-3, 1996b.
Kominz, M. A., Browning, J. V., Miller, K. G., Sugarman, P. J., Mizintseva, S. and Scotese, C. R.: Late Cretaceous to Miocene sea-level estimates from the New Jersey and Delaware coastal plain coreholes: an error analysis, Basin Research, 20(2), 211–226, 2008.
Krantz, D. E., Williams, D. F. and Jones, D. S.: Ecological and paleoenvironmental information using stable isotope profiles from living and fossil molluscs, Palaeogeography, Palaeoclimatology, Palaeoecology, 58(3), 249–266, doi:10.1016/0031-0182(87)90064-2, 1987.
Kuznetsov, A. B., Semikhatov, M. A. and Gorokhov, I. M.: The Sr isotope composition of the world ocean, marginal and inland seas: Implications for the Sr isotope stratigraphy, Stratigr. Geol. Correl., 20(6), 501–515, doi:10.1134/S0869593812060044, 2012.
Lartaud, F., Emmanuel, L., De Rafélis, M., Ropert, M., Labourdette, N., Richardson, C. A. and Renard, M.: A latitudinal gradient of seasonal temperature variation recorded in oyster shells from the coastal waters of France and The Netherlands, Facies, 56(1), 13, 2010.
Lear, C. H., Elderfield, H. and Wilson, P. A.: A Cenozoic seawater Sr/Ca record from benthic foraminiferal calcite and its application in determining global weathering fluxes, Earth and Planetary Science Letters, 208(1), 69–84, doi:10.1016/S0012-821X(02)01156-1, 2003.
Li, Y., Qin, J. G., Abbott, C. A., Li, X. and Benkendorff, K.: Synergistic impacts of heat shock and spawning on the physiology and immune health of Crassostrea gigas: an explanation for summer mortality in Pacific oysters, American Journal of Physiology-Regulatory, Integrative and Comparative Physiology, 293(6), R2353–R2362, 2007.
Locarnini, R. A., Mishonov, A. V., Antonov, J. I., Boyer, T. P., Garcia, H. E., Baranova, O. K., Zweng, M. M., Paver, C. R., Reagan, J. R., Johnson, D. R., Hamilton, M. and Seidov, D.: World ocean atlas 2013. Volume 1, Temperature, U.S. Department of Commerce, National Oceanic and Atmospheric Administration, National Environmental Satellite, Data and Information Service, doi:10.7289/v55x26vd, 2013.
Lorrain, A., Paulet, Y.-M., Chauvaud, L., Dunbar, R., Mucciarone, D. and Fontugne, M.: δ 13 C variation in scallop shells: increasing metabolic carbon contribution with body size?, Geochimica et Cosmochimica Acta, 68(17), 3509–3519, 2004.
Lorrain, A., Gillikin, D. P., Paulet, Y.-M., Chauvaud, L., Le Mercier, A., Navez, J. and André, L.: Strong kinetic effects on Sr/Ca ratios in the calcitic bivalve Pecten maximus, Geology, 33(12), 965–968, 2005.
Lowenstam, H. A. and Epstein, S.: Paleotemperatures of the post-Aptian Cretaceous as determined by the oxygen isotope method, The Journal of Geology, 62(3), 207–248, 1954.
MacDonald, B. A. and Thompson, R. J.: Influence of temperature and food availability on the ecological energetics of the giant scallop Placopecten magellanicus. I. Growth rates of shell and somatic tissue., Marine ecology progress series. Oldendorf, 25(3), 279–294, 1985.
McArthur, J. M., Howarth, R. J. and Bailey, T. R.: Strontium Isotope Stratigraphy: LOWESS Version 3: Best Fit to the Marine Sr-Isotope Curve for 0–509 Ma and Accompanying Look-up Table for Deriving Numerical Age, The Journal of Geology, 109(2), 155–170, doi:10.1086/319243, 2001.
McArthur, J. M., Steuber, T., Page, K. N. and Landman, N. H.: Sr-isotope stratigraphy: assigning time in the Campanian, Pliensbachian, Toarcian, and Valanginian, The Journal of Geology, 124(5), 569–586, 2016.
McConnaughey, T. A.: Sub-equilibrium oxygen-18 and carbon-13 levels in biological carbonates: carbonate and kinetic models, Coral Reefs, 22(4), 316–327, 2003.
McConnaughey, T. A. and Gillikin, D. P.: Carbon isotopes in mollusk shell carbonates, Geo-Marine Letters, 28(5–6), 287–299, doi:10.1007/s00367-008-0116-4, 2008.
McConnaughey, T. A., Burdett, J., Whelan, J. F. and Paull, C. K.: Carbon isotopes in biological carbonates: respiration and photosynthesis, Geochimica et Cosmochimica Acta, 61(3), 611–622, 1997.
Meyers, S. R. and Malinverno, A.: Proterozoic Milankovitch cycles and the history of the solar system, PNAS, 201717689, doi:10.1073/pnas.1717689115, 2018.
Miller, K. G., Wright, J. D. and Browning, J. V.: Visions of ice sheets in a greenhouse world, Marine Geology, 217(3), 215–231, doi:10.1016/j.margeo.2005.02.007, 2005.
Montgomery, P., Hailwood, E. A., Gale, A. S. and Burnett, J. A.: The magnetostratigraphy of Coniacian-Late Campanian chalk sequences in southern England, Earth and Planetary Science Letters, 156(3), 209–224, doi:10.1016/S0012-821X(98)00008-9, 1998.
Mook, W. G.: Paleotemperatures and chlorinities from stable carbon and oxygen isotopes in shell carbonate, Palaeogeography, Palaeoclimatology, Palaeoecology, 9(4), 245–263, doi:10.1016/0031-0182(71)90002-2, 1971.
Mouchi, V., De Rafélis, M., Lartaud, F., Fialin, M. and Verrecchia, E.: Chemical labelling of oyster shells used for time-calibrated high-resolution Mg/Ca ratios: a tool for estimation of past seasonal temperature variations, Palaeogeography, Palaeoclimatology, Palaeoecology, 373, 66–74, 2013.
NOAA Earth System Research Laboratory: NOAA Optimum Interpolation (IO) Sea Surface Temperature (SST) http://www.esrl.noaa.gov/psd/data/gridded/data.noaa.oisst.v2.html (accessed 01/21/19).
O'Brien, C. L., Robinson, S. A., Pancost, R. D., Sinninghe Damsté, J. S., Schouten, S., Lunt, D. J., Alsenz, H., Bornemann, A., Bottini, C., Brassell, S. C., Farnsworth, A., Forster, A., Huber, B. T., Inglis, G. N., Jenkyns, H. C., Linnert, C., Littler, K., Markwick, P., McAnena, A., Mutterlose, J., Naafs, B. D. A., Püttmann, W., Sluijs, A., van Helmond, N. A. G. M., Vellekoop, J.,

Wagner, T. and Wrobel, N. E.: Cretaceous sea-surface temperature evolution: Constraints from TEX 86 and planktonic foraminiferal oxygen isotopes, Earth-Science Reviews, 172, 224–247, doi:10.1016/j.earscirev.2017.07.012, 2017.
Ogg, J. G., Ogg, G. and Gradstein, F. M.: A concise geologic time scale: 2016, Elsevier., 2016.
Palmer, R. E. and Carriker, M. R.: Effects of cultural conditions on morphology of the shell of the oyster Crassostrea virginica, in Proceedings of the National Shellfisheries Association, vol. 69, pp. 58–72., 1979.
Pearson, P. N., Ditchfield, P. W., Singano, J., Harcourt-Brown, K. G., Nicholas, C. J., Olsson, R. K., Shackleton, N. J. and Hall, M. A.: Warm tropical sea surface temperatures in the Late Cretaceous and Eocene epochs, Nature, 413(6855), 481, 2001.
Perdiou, A., Thibault, N., Anderskouv, K., Van Buchem, F., Buijs, G. J. A. and Bjerrum, C. J.: Orbital calibration of the late Campanian carbon isotope event in the North Sea, Journal of the Geological Society, 173(3), 504–517, 2016.
Prandle, D. and Lane, A.: The annual temperature cycle in shelf seas, Continental Shelf Research, 15(6), 681–704, doi:10.1016/0278-4343(94)E0029-L, 1995.
Rausch, S., Böhm, F., Bach, W., Klügel, A. and Eisenhauer, A.: Calcium carbonate veins in ocean crust record a threefold increase of seawater Mg/Ca in the past 30 million years, Earth and Planetary Science Letters, 362, 215–224, 2013.
Rayner, N. A., Parker, D. E., Horton, E. B., Folland, C. K., Alexander, L. V., Rowell, D. P., Kent, E. C. and Kaplan, A.: Global analyses of sea surface temperature, sea ice, and night marine air temperature since the late nineteenth century, Journal of Geophysical Research: Atmospheres, 108(D14), doi:10.1029/2002JD002670, 2003.
Reid, R. E. H.: The Chalk Sea, The Irish Naturalists' Journal, 17(11), 357–375, 1973.
Richardson, C. A., Peharda, M., Kennedy, H., Kennedy, P. and Onofri, V.: Age, growth rate and season of recruitment of Pinna nobilis (L) in the Croatian Adriatic determined from Mg: Ca and Sr: Ca shell profiles, Journal of Experimental Marine Biology and Ecology, 299(1), 1–16, 2004.
Roy, K., Jablonski, D. and Martien, K. K.: Invariant size–frequency distributions along a latitudinal gradient in marine bivalves, PNAS, 97(24), 13150–13155, doi:10.1073/pnas.97.24.13150, 2000.
Rucker, J. B. and Valentine, J. W.: Salinity Response of Trace Element Concentration in Crassostrea virginica, Nature, 190(4781), 1099–1100, doi:10.1038/1901099a0, 1961.
Sano, Y., Kobayashi, S., Shirai, K., Takahata, N., Matsumoto, K., Watanabe, T., Sowa, K. and Iwai, K.: Past daily light cycle recorded in the strontium/calcium ratios of giant clam shells, Nat Commun, 3, 761, doi:10.1038/ncomms1763, 2012.
Schöne, B. R. and Gillikin, D. P.: Unraveling environmental histories from skeletal diaries — Advances in sclerochronology, Palaeogeography, Palaeoclimatology, Palaeoecology, 373, 1–5, doi:10.1016/j.palaeo.2012.11.026, 2013.
SCHÖNE, B. R., Houk, S. D., FREYRE CASTRO, A. D., Fiebig, J., Oschmann, W., KRÖNCKE, I., Dreyer, W. and Gosselck, F.: Daily growth rates in shells of Arctica islandica: assessing sub-seasonal environmental controls on a long-lived bivalve mollusk, Palaios, 20(1), 78–92, 2005.
Schöne, B. R., Zhang, Z., Jacob, D., Gillikin, D. P., Tütken, T., Garbe-Schönberg, D., McConnaughey, T. and Soldati, A.: Effect of organic matrices on the determination of the trace element chemistry (Mg, Sr, Mg/Ca, Sr/Ca) of aragonitic bivalve shells (Arctica islandica)—Comparison of ICP-OES and LA-ICP-MS data, Geochemical Journal, 44(1), 23–37, 2010.
Schöne, B. R., Zhang, Z., Radermacher, P., Thébault, J., Jacob, D. E., Nunn, E. V. and Maurer, A.-F.: Sr/Ca and Mg/Ca ratios of ontogenetically old, long-lived bivalve shells (Arctica islandica) and their function as paleotemperature proxies, Palaeogeography, Palaeoclimatology, Palaeoecology, 302(1), 52–64, 2011.
Schöne, B. R., Radermacher, P., Zhang, Z. and Jacob, D. E.: Crystal fabrics and element impurities (Sr/Ca, Mg/Ca, and Ba/Ca) in shells of Arctica islandica—Implications for paleoclimate reconstructions, Palaeogeography, Palaeoclimatology, Palaeoecology, 373, 50–59, 2013.
Scotese, C.: A NEW GLOBAL TEMPERATURE CURVE FOR THE PHANEROZOIC., 2016.
Shackleton, N. J.: Paleogene stable isotope events, Palaeogeography, Palaeoclimatology, Palaeoecology, 57(1), 91–102, 1986.
Snoeck, C., Lee-Thorp, J., Schulting, R., Jong, J., Debouge, W. and Mattielli, N.: Calcined bone provides a reliable substrate for strontium isotope ratios as shown by an enrichment experiment, Rapid communications in mass spectrometry, 29(1), 107–114, 2015.
Sørensen, A. M., Surlyk, F. and Jagt, J. W. M.: Adaptive morphologies and guild structure in a high-diversity bivalve fauna from an early Campanian rocky shore, Ivö Klack (Sweden), Cretaceous Research, 33(1), 21–41, doi:10.1016/j.cretres.2011.07.004, 2012.
Sørensen, A. M., Ullmann, C. V., Thibault, N. and Korte, C.: Geochemical signatures of the early Campanian belemnite Belemnellocamax mammillatus from the Kristianstad Basin in Scania, Sweden, Palaeogeography, palaeoclimatology, palaeoecology, 433, 191–200, 2015.
Stanley, S. M. and Hardie, L. A.: Secular oscillations in the carbonate mineralogy of reef-building and sediment-producing organisms driven by tectonically forced shifts in seawater chemistry, Palaeogeography, Palaeoclimatology, Palaeoecology, 144(1), 3–19, 1998.
Stenzel, H. B.: Aragonite and calcite as constituents of adult oyster shells, Science, 142(3589), 232–233, 1963.
Steuber, T.: Isotopic and chemical intra-shell variations in low-Mg calcite of rudist bivalves (Mollusca-Hippuritacea): disequilibrium fractionations and late Cretaceous seasonality, International Journal of Earth Sciences, 88(3), 551–570, 1999.
Steuber, T., Rauch, M., Masse, J.-P., Graaf, J. and Malkoč, M.: Low-latitude seasonality of Cretaceous temperatures in warm and cold episodes, Nature, 437(7063), 1341–1344, 2005.
Strahl, J., Philipp, E., Brey, T., Broeg, K. and Abele, D.: Physiological aging in the Icelandic population of the ocean quahog Arctica islandica, Aquatic Biology, 1(1), 77–83, 2007.
Surge, D. and Lohmann, K. C.: Evaluating Mg/Ca ratios as a temperature proxy in the estuarine oyster, Crassostrea virginica, Journal of Geophysical Research: Biogeosciences, 113(G2) [online] Available from: http://onlinelibrary.wiley.com/doi/10.1029/2007JG000623/full (Accessed 28 November 2016), 2008.
Surge, D., Lohmann, K. C. and Dettman, D. L.: Controls on isotopic chemistry of the American oyster, Crassostrea virginica: implications for growth patterns, Palaeogeography, Palaeoclimatology, Palaeoecology, 172(3), 283–296, 2001.
Surge, D. M., Lohmann, K. C. and Goodfriend, G. A.: Reconstructing estuarine conditions: oyster shells as recorders of environmental change, Southwest Florida, Estuarine, Coastal and Shelf Science, 57(5), 737–756, doi:10.1016/S0272-7714(02)00370-0, 2003.
Surlyk, F. and Christensen, W. K.: Epifaunal zonation on an Upper Cretaceous rocky coast, Geology, 2(11), 529–534, 1974.

Surlyk, F. and Sørensen, A. M.: An early Campanian rocky shore at Ivö Klack, southern Sweden, Cretaceous Research, 31(6), 567–576, 2010.
Tagliavento, M., John, C. M. and Stemmerik, L.: Tropical temperature in the Maastrichtian Danish Basin: Data from coccolith Δ47 and δ18O, Geology, 47(11), 1074–1078, 2019.
Thibault, N., Husson, D., Harlou, R., Gardin, S., Galbrun, B., Huret, E. and Minoletti, F.: Astronomical calibration of upper Campanian–Maastrichtian carbon isotope events and calcareous plankton biostratigraphy in the Indian Ocean (ODP Hole 762C): Implication for the age of the Campanian–Maastrichtian boundary, Palaeogeography, Palaeoclimatology, Palaeoecology, 337–338, 52–71, doi:10.1016/j.palaeo.2012.03.027, 2012.
Thibault, N., Harlou, R., Schovsbo, N. H., Stemmerik, L. and Surlyk, F.: Late Cretaceous (late Campanian–Maastrichtian) sea-surface temperature record of the Boreal Chalk Sea, Climate of the Past, 12(2), 429–438, 2016.
Uchikawa, J. and Zeebe, R. E.: The effect of carbonic anhydrase on the kinetics and equilibrium of the oxygen isotope exchange in the CO2–H2O system: Implications for δ18O vital effects in biogenic carbonates, Geochimica et Cosmochimica Acta, 95, 15–34, 2012.
Ullmann, C. V. and Korte, C.: Diagenetic alteration in low-Mg calcite from macrofossils: a review, Geological Quarterly, 59(1), 3–20, 2015.
Ullmann, C. V., Wiechert, U. and Korte, C.: Oxygen isotope fluctuations in a modern North Sea oyster (Crassostrea gigas) compared with annual variations in seawater temperature: Implications for palaeoclimate studies, Chemical Geology, 277(1), 160–166, 2010.
Ullmann, C. V., Böhm, F., Rickaby, R. E., Wiechert, U. and Korte, C.: The Giant Pacific Oyster (Crassostrea gigas) as a modern analog for fossil ostreoids: isotopic (Ca, O, C) and elemental (Mg/Ca, Sr/Ca, Mn/Ca) proxies, Geochemistry, Geophysics, Geosystems, 14(10), 4109–4120, 2013.
Upchurch Jr, G. R., Kiehl, J., Shields, C., Scherer, J. and Scotese, C.: Latitudinal temperature gradients and high-latitude temperatures during the latest Cretaceous: Congruence of geologic data and climate models, Geology, 43(8), 683–686, 2015.
Vansteenberge, S., de Winter, N. J., Sinnesael, M., Xueqin, Z., Verheyden, S. and Claeys, P.: Benchtop µXRF as a tool for speleothem trace elemental analysis: Validation, limitations and application on an Eemian to early Weichselian (125–97 ka) stalagmite from Belgium, Palaeogeography, Palaeoclimatology, Palaeoecology, 538, 109460, doi:10.1016/j.palaeo.2019.109460, 2020.
Veizer, J.: Chemical diagenesis of carbonates: theory and application of trace element technique, [online] Available from: http://archives.datapages.com/data/sepm_sp/SC10/Chemical_Diagenesis.htm, 1983.
Veizer, J. and Prokoph, A.: Temperatures and oxygen isotopic composition of Phanerozoic oceans, Earth-Science Reviews, 146, 92–104, 2015.
Voigt, S. and Schönfeld, J.: Cyclostratigraphy of the reference section for the Cretaceous white chalk of northern Germany, Lägerdorf–Kronsmoor: A late Campanian–early Maastrichtian orbital time scale, Palaeogeography, Palaeoclimatology, Palaeoecology, 287(1), 67–80, doi:10.1016/j.palaeo.2010.01.017, 2010.
Voigt, S., Friedrich, O., Norris, R. D. and Schönfeld, J.: Campanian–Maastrichtian carbon isotope stratigraphy: shelf-ocean correlation between the European shelf sea and the tropical Pacific Ocean, Newsletters on Stratigraphy, 44(1), 57–72, 2010.
Von Bertalanffy, L.: Quantitative laws in metabolism and growth, The quarterly review of biology, 32(3), 217–231, 1957.
Wagreich, M., Hohenegger, J. and Neuhuber, S.: Nannofossil biostratigraphy, strontium and carbon isotope stratigraphy, cyclostratigraphy and an astronomically calibrated duration of the Late Campanian Radotruncana calcarata Zone, Cretaceous Research, 38, 80–96, 2012.
Waniek, J. J.: The role of physical forcing in initiation of spring blooms in the northeast Atlantic, Journal of Marine Systems, 39(1–2), 57–82, 2003.
Warter, V., Erez, J. and Müller, W.: Environmental and physiological controls on daily trace element incorporation in Tridacna crocea from combined laboratory culturing and ultra-high resolution LA-ICP-MS analysis, Palaeogeography, Palaeoclimatology, Palaeoecology, 496, 32–47, doi:10.1016/j.palaeo.2017.12.038, 2018.
Watanabe, T., Suzuki, A., Kawahata, H., Kan, H. and Ogawa, S.: A 60-year isotopic record from a mid-Holocene fossil giant clam (Tridacna gigas) in the Ryukyu Islands: physiological and paleoclimatic implications, Palaeogeography, Palaeoclimatology, Palaeoecology, 212(3–4), 343–354, 2004.
Weiner, S. and Dove, P. M.: An overview of biomineralization processes and the problem of the vital effect, Reviews in mineralogy and geochemistry, 54(1), 1–29, 2003.
Weis, D., Kieffer, B., Maerschalk, C., Barling, J., Jong, J. de, Williams, G. A., Hanano, D., Pretorius, W., Mattielli, N., Scoates, J. S., Goolaerts, A., Friedman, R. M. and Mahoney, J. B.: High-precision isotopic characterization of USGS reference materials by TIMS and MC-ICP-MS, Geochemistry, Geophysics, Geosystems, 7(8), Q08006, doi:10.1029/2006GC001283, 2006.
Wendler, I.: A critical evaluation of carbon isotope stratigraphy and biostratigraphic implications for Late Cretaceous global correlation, Earth-Science Reviews, 126, 116–146, doi:10.1016/j.earscirev.2013.08.003, 2013.
de Winter, N. J. and Claeys, P.: Micro X-ray fluorescence (µXRF) line scanning on Cretaceous rudist bivalves: A new method for reproducible trace element profiles in bivalve calcite, edited by M. R. Petrizzo, Sedimentology, 64(1), 231–251, doi:10.1111/sed.12299, 2016.
de Winter, N. J., Sinnesael, M., Makarona, C., Vansteenberge, S. and Claeys, P.: Trace element analyses of carbonates using portable and micro-X-ray fluorescence: performance and optimization of measurement parameters and strategies, Journal of Analytical Atomic Spectrometry, 32(6), 1211–1223, 2017b.
de Winter, N. J., Goderis, S., Dehairs, F., Jagt, J. W., Fraaije, R. H., Van Malderen, S. J., Vanhaecke, F. and Claeys, P.: Tropical seasonality in the late Campanian (late Cretaceous): Comparison between multiproxy records from three bivalve taxa from Oman, Palaeogeography, Palaeoclimatology, Palaeoecology, 485, 740–760, 2017a.
de Winter, N. J., Vellekoop, J., Vorsselmans, R., Golreihan, A., Soete, J., Petersen, S. V., Meyer, K. W., Casadio, S., Speijer, R. P. and Claeys, P.: An assessment of latest Cretaceous Pycnodonte vesicularis (Lamarck, 1806) shells as records for palaeoseasonality: a multi-proxy investigation, Climate of the Past, 14(6), 725–749, 2018.
de Winter, N. J., Goderis, S., Malderen, S. J. M. V., Sinnesael, M., Vansteenberge, S., Snoeck, C., Belza, J., Vanhaecke, F. and Claeys, P.: Subdaily-Scale Chemical Variability in a Torreites Sanchezi Rudist Shell: Implications for Rudist Paleobiology and

the Cretaceous Day-Night Cycle, Paleoceanography and Paleoclimatology, 35(2), e2019PA003723, doi:10.1029/2019PA003723, 2020a.
de Winter, N. J., Vellekoop, J., Clark, A. J., Stassen, P., Speijer, R. P. and Claeys, P.: The giant marine gastropod Campanile giganteum (Lamarck, 1804) as a high-resolution archive of seasonality in the Eocene greenhouse world, Geochemistry, Geophysics, Geosystems, n/a(n/a), e2019GC008794, doi:10.1029/2019GC008794, 2020b.
Yang, D., Huang, Y., Guo, W., Huang, Q., Ren, Y. and Wang, C.: Late Santonian-early Campanian lake-level fluctuations in the Songliao Basin, NE China and their relationship to coeval eustatic changes, Cretaceous Research, 92, 138–149, doi:10.1016/j.cretres.2018.07.008, 2018.
Yoshimura, T., Tanimizu, M., Inoue, M., Suzuki, A., Iwasaki, N. and Kawahata, H.: Mg isotope fractionation in biogenic carbonates of deep-sea coral, benthic foraminifera, and hermatypic coral, Anal Bioanal Chem, 401(9), 2755, doi:10.1007/s00216-011-5264-0, 2011.
Zimmt, J. B., Lockwood, R., Andrus, C. F. T. and Herbert, G. S.: Sclerochronological basis for growth band counting: A reliable technique for life-span determination of Crassostrea virginica from the mid-Atlantic United States, Palaeogeography, Palaeoclimatology, Palaeoecology, 516, 54–63, 2018.
Al-Aasm, I.S., Veizer, J.: Diagenetic stabilization of aragonite and low-Mg calcite, I. Trace elements in rudists. Journal of Sedimentary Research 56, 138–152, 1986a.
Al-Aasm, I.S., Veizer, J.: Diagenetic stabilization of aragonite and low-Mg calcite, II. Stable isotopes in rudists. Journal of Sedimentary Research 56, 763–770, 1986b.
Alberti, M., Fürsich, F.T., Abdelhady, A.A., Andersen, N.: Middle to Late Jurassic equatorial seawater temperatures and latitudinal temperature gradients based on stable isotopes of brachiopods and oysters from Gebel Maghara, Egypt. Palaeogeography, Palaeoclimatology, Palaeoecology 468, 301–313. https://doi.org/10.1016/j.palaeo.2016.11.052, 2017.
Amiot, R., Lécuyer, C., Buffetaut, E., Fluteau, F., Legendre, S., Martineau, F.: Latitudinal temperature gradient during the Cretaceous Upper Campanian–Middle Maastrichtian: $\delta^{18}O$ record of continental vertebrates. Earth and Planetary Science Letters 226, 255–272. https://doi.org/10.1016/j.epsl.2004.07.015, 2004.
Arthur, M.A., Williams, D.F., Jones, D.S.: Seasonal temperature-salinity changes and thermocline development in the mid-Atlantic Bight as recorded by the isotopic composition of bivalves. Geology 11, 655–659. https://doi.org/10.1130/0091-7613(1983)11<655:STCATD>2.0.CO;2, 1983.
Bachelet, G.: Growth and recruitment of the tellinid bivalve *Macoma balthica* at the southern limit of its geographical distribution, the Gironde estuary (SW France). Marine Biology 59, 105–117, 1980.
Barlow, R.: Asymmetric errors. arXiv preprint physics/0401042, 2004.
Barlow, R.: Asymmetric systematic errors. arXiv preprint physics/0306138, 2003.
Barrera, E., Johnson, C.C.: Evolution of the Cretaceous Ocean-climate System. Geological Society of America, 1999.
Berthelin, C., Kellner, K., Mathieu, M.: Storage metabolism in the Pacific oyster (*Crassostrea gigas*) in relation to summer mortalities and reproductive cycle (West Coast of France). Comparative Biochemistry and Physiology Part B: Biochemistry and Molecular Biology 125, 359–369. https://doi.org/10.1016/S0305-0491(99)00187-X, 2000.
Brady, E.C., DeConto, R.M., Thompson, S.L.: Deep water formation and poleward ocean heat transport in the warm climate extreme of the Cretaceous (80 Ma). Geophysical Research Letters 25, 4205–4208, 1998.
Brand, U., Veizer, J.: Chemical diagenesis of a multicomponent carbonate system-2: stable isotopes. Journal of Sedimentary Research 51, 987–997, 1981.
Brand, U., Veizer, J.: Chemical diagenesis of a multicomponent carbonate system-1: Trace elements. Journal of Sedimentary Research 50, 1219–1236, 1980.
Brunskill, G.J., Zagorskis, I., Pfitzner, J.: Geochemical mass balance for lithium, boron, and strontium in the Gulf of Papua, Papua New Guinea (project TROPICS). Geochimica et Cosmochimica Acta 67, 3365–3383. https://doi.org/10.1016/S0016-7037(02)01410-2, 2003.
Bryan, S.P., Marchitto, T.M.: Mg/Ca–temperature proxy in benthic foraminifera: New calibrations from the Florida Straits and a hypothesis regarding Mg/Li. Paleoceanography 23, PA2220. https://doi.org/10.1029/2007PA001553, 2008.
Burgener, L., Hyland, E., Huntington, K.W., Kelson, J.R., Sewall, J.O.: Revisiting the equable climate problem during the Late Cretaceous greenhouse using paleosol carbonate clumped isotope temperatures from the Campanian of the Western Interior Basin, USA. Palaeogeography, Palaeoclimatology, Palaeoecology 516, 244–267. https://doi.org/10.1016/j.palaeo.2018.12.004, 2018.
Carriker, M.R., Palmer, R.E., Prezant, R.S.: Functional ultramorphology of the dissoconch valves of the oyster *Crassostrea virginica*, in: Proceedings of the National Shellfisheries Association. pp. 139–183, 1979.
Carriker, M.R., Swann, C.P., Prezant, R.S., Counts, C.L.: Chemical elements in the aragonitic and calcitic microstructural groups of shell of the oyster *Crassostrea virginica*: A proton probe study. Marine Biology 109, 287–297, 1991.
Christensen, W.K.: Paleobiogeography and migration in the Late Cretaceous belemnite family Belemnitellidae. Acta palaeontologica polonica 42, 457–495, 1997.
Christensen, W.K.: The Albian to Maastrichtian of southern Sweden and Bornholm, Denmark: a review. Cretaceous Research 5, 313–327, 1984.
Christensen, W.K.: Upper Cretaceous belemnites from the Kristianstad area in Scania. Fossils and Strata, 1975.
Clarke, L.J., Jenkyns, H.C.: New oxygen isotope evidence for long-term Cretaceous climatic change in the Southern Hemisphere. Geology 27, 699–702, 1999.
Cochran, J.K., Kallenberg, K., Landman, N.H., Harries, P.J., Weinreb, D., Turekian, K.K., Beck, A.J., Cobban, W.A.: Effect of diagenesis on the Sr, O, and C isotope composition of late Cretaceous mollusks from the Western Interior Seaway of North America. American Journal of Science 310, 69–88. https://doi.org/10.2475/02.2010.01, 2010.
Coggon, R.M., Teagle, D.A., Smith-Duque, C.E., Alt, J.C., Cooper, M.J.: Reconstructing past seawater Mg/Ca and Sr/Ca from mid-ocean ridge flank calcium carbonate veins. Science 327, 1114–1117, 2010.
Csiki-Sava, Z., Buffetaut, E., Ősi, A., Pereda-Suberbiola, X., Brusatte, S.L.: Island life in the Cretaceous - faunal composition, biogeography, evolution, and extinction of land-living vertebrates on the Late Cretaceous European archipelago. Zookeys 1–161. https://doi.org/10.3897/zookeys.469.8439, 2015.
Dalbeck, P., England, J., Cusack, M., Lee, M.R., Fallick, A.E.: Crystallography and chemistry of the calcium carbonate polymorph switch in *M. edulis* shells. European Journal of Mineralogy 18, 601–609. https://doi.org/10.1127/0935-1221/2006/0018-0601, 2006.

De Villiers, S.: Seawater strontium and Sr/Ca variability in the Atlantic and Pacific oceans. Earth and Planetary Science Letters 171, 623–634, 1999.
de Winter, N.J., Claeys, P.: Micro X-ray fluorescence (μXRF) line scanning on Cretaceous rudist bivalves: A new method for reproducible trace element profiles in bivalve calcite. Sedimentology 64, 231–251. https://doi.org/10.1111/sed.12299, 2016.
de Winter, N.J., Goderis, S., Dehairs, F., Jagt, J.W., Fraaije, R.H., Van Malderen, S.J., Vanhaecke, F., Claeys, P.: Tropical seasonality in the late Campanian (late Cretaceous): Comparison between multiproxy records from three bivalve taxa from Oman. Palaeogeography, Palaeoclimatology, Palaeoecology 485, 740–760, 2017a.
de Winter, N.J., Sinnesael, M., Makarona, C., Vansteenberge, S., Claeys, P.: Trace element analyses of carbonates using portable and micro-X-ray fluorescence: performance and optimization of measurement parameters and strategies. Journal of Analytical Atomic Spectrometry 32, 1211–1223, 2017b.
de Winter, N.J., Vellekoop, J., Vorsselmans, R., Golreihan, A., Soete, J., Petersen, S.V., Meyer, K.W., Casadio, S., Speijer, R.P., Claeys, P.: An assessment of latest Cretaceous *Pycnodonte vesicularis* (Lamarck, 1806) shells as records for palaeoseasonality: a multi-proxy investigation. Climate of the Past 14, 725–749, 2018.
de Winter, N.J., Goderis, S., Van Malderen, S.J.M., Sinnesael, M., Vansteenberge, S., Snoeck, C., Belza, J., Vanhaecke, F., Claeys, P., Daily chemical variability in a Late Cretaceous rudist shell. Science Advances, in review.
DeConto, R.M., Hay, W.W., Thompson, S.L., Bergengren, J.: Late Cretaceous climate and vegetation interactions: cold continental interior paradox. SPECIAL PAPERS-GEOLOGICAL SOCIETY OF AMERICA 391–406, 1999.
Dellinger, M., West, A.J., Paris, G., Adkins, J.F., von Strandmann, P.A.P., Ullmann, C.V., Eagle, R.A., Freitas, P., Bagard, M.-L., Ries, J.B.: The Li isotope composition of marine biogenic carbonates: Patterns and Mechanisms. Geochimica et Cosmochimica Acta 236, 315–335, 2018.
Donnadieu, Y., Pucéat, E., Moiroud, M., Guillocheau, F., Deconinck, J.-F.: A better-ventilated ocean triggered by Late Cretaceous changes in continental configuration. Nature Communications 7, 10316. https://doi.org/10.1038/ncomms10316, 2016.
Freitas, P.S., Clarke, L.J., Kennedy, H.A., Richardson, C.A.: Inter-and intra-specimen variability masks reliable temperature control on shell Mg/Ca ratios in laboratory and field cultured *Mytilus edulis* and *Pecten maximus* (bivalvia). Biogeosciences Discussions 5, 531–572, 2008.
Friedrich, O., Herrle, J.O., Hemleben, C.: Climatic changes in the late Campanian—early Maastrichtian: Micropaleontological and stable isotopic evidence from an epicontinental sea. Journal of Foraminiferal Research 35, 228–247, 2005.
Friedrich, O., Herrle, J.O., Wilson, P.A., Cooper, M.J., Erbacher, J., Hemleben, C.: Early Maastrichtian carbon cycle perturbation and cooling event: Implications from the South Atlantic Ocean. Paleoceanography 24, PA2211. https://doi.org/10.1029/2008PA001654, 2009.
Friedrich, O., Norris, R.D., Erbacher, J.: Evolution of middle to Late Cretaceous oceans—a 55 my record of Earth's temperature and carbon cycle. Geology 40, 107–110, 2012.
Füllenbach, C.S., Schöne, B.R., Mertz-Kraus, R.: Strontium/lithium ratio in aragonitic shells of *Cerastoderma edule* (Bivalvia)—A new potential temperature proxy for brackish environments. Chemical Geology 417, 341–355, 2015.
Galtsoff, P.S.: The American Oyster: US Fish and Wildlife Service. Fishery Bulletin 64, 480, 1964.
Gillikin, D.P., Lorrain, A., Bouillon, S., Willenz, P., Dehairs, F.: Stable carbon isotopic composition of *Mytilus edulis* shells: relation to metabolism, salinity, $\delta^{13}C$ DIC and phytoplankton. Organic Geochemistry 37, 1371–1382, 2006.
Gillikin, D.P., Lorrain, A., Meng, L., Dehairs, F.: A large metabolic carbon contribution to the $\delta^{13}C$ record in marine aragonitic bivalve shells. Geochimica et Cosmochimica Acta 71, 2936–2946, 2007.
Gillikin, D.P., Lorrain, A., Navez, J., Taylor, J.W., André, L., Keppens, E., Baeyens, W., Dehairs, F.: Strong biological controls on Sr/Ca ratios in aragonitic marine bivalve shells. Geochemistry, Geophysics, Geosystems 6, Q05009, 2005.
Goodwin, D.H., Flessa, K.W., Schone, B.R., Dettman, D.L.: Cross-calibration of daily growth increments, stable isotope variation, and temperature in the Gulf of California bivalve mollusk *Chione cortezi*: implications for paleoenvironmental analysis. Palaios 16, 387–398, 2001.
Grossman, E.L., Ku, T.-L.: Oxygen and carbon isotope fractionation in biogenic aragonite: temperature effects. Chemical Geology: Isotope Geoscience section 59, 59–74, 1986.
Hay, W.W., Floegel, S.: New thoughts about the Cretaceous climate and oceans. Earth-Science Reviews 115, 262–272, 2012.
Huber, B.T., Hodell, D.A., Hamilton, C.P.: Middle–Late Cretaceous climate of the southern high latitudes: stable isotopic evidence for minimal equator-to-pole thermal gradients. Geological Society of America Bulletin 107, 1164–1191, 1995.
Huber, B.T., Norris, R.D., MacLeod, K.G.: Deep-sea paleotemperature record of extreme warmth during the Cretaceous. Geology 30, 123–126, 2002.
Huck, S., Heimhofer, U., Rameil, N., Bodin, S., Immenhauser, A.: Strontium and carbon-isotope chronostratigraphy of Barremian–Aptian shoal-water carbonates: Northern Tethyan platform drowning predates OAE 1a. Earth and Planetary Science Letters 304, 547–558. https://doi.org/10.1016/j.epsl.2011.02.031, 2011.
Huh, Y., Chan, L.-H., Zhang, L., Edmond, J.M.: Lithium and its isotopes in major world rivers: implications for weathering and the oceanic budget. Geochimica et Cosmochimica Acta 62, 2039–2051. https://doi.org/10.1016/S0016-7037(98)00126-4, 1998.
Immenhauser, A., Nägler, T.F., Steuber, T., Hippler, D.: A critical assessment of mollusk $^{18}O/^{16}O$, Mg/Ca, and $^{44}Ca/^{40}Ca$ ratios as proxies for Cretaceous seawater temperature seasonality. Palaeogeography, Palaeoclimatology, Palaeoecology 215, 221–237, 2005.
IPCC: Climate Change 2013: The Physical Science Basis. Contribution of Working Group I to the Fifth Assessment Report of the Intergovernmental Panel on Climate Change, 1535 pp. Cambridge Univ. Press, Cambridge, UK, and New York, 2013.
IRI/LDEO Climate Data Library URL http://iridl.ldeo.columbia.edu (accessed 01/11/19).
Ivany, L.C.: Reconstructing paleoseasonality from accretionary skeletal carbonates—challenges and opportunities. The Paleontological Society Papers 18, 133–166, 2012.
Jablonski, D., Huang, S., Roy, K., Valentine, J.W.: Shaping the latitudinal diversity gradient: new perspectives from a synthesis of paleobiology and biogeography. The American Naturalist 189, 1–12, 2017.
Jenkyns, H.C., Forster, A., Schouten, S., Damsté, J.S.S.: High temperatures in the late Cretaceous Arctic Ocean. Nature 432, 888, 2004.
Jenkyns, H.C., Gale, A.S., Corfield, R.M.: Carbon-and oxygen-isotope stratigraphy of the English Chalk and Italian Scaglia and its palaeoclimatic significance. Geological Magazine 131, 1–34, 1994.

Jones, D.S.: Sclerochronology: reading the record of the molluscan shell: annual growth increments in the shells of bivalve molluscs record marine climatic changes and reveal surprising longevity. American Scientist 71, 384–391, 1983.
Judd, E.J., Wilkinson, B.H., Ivany, L.C.: The life and time of clams: Derivation of intra-annual growth rates from high-resolution oxygen isotope profiles. Palaeogeography, Palaeoclimatology, Palaeoecology 490, 70–83, 2018.
Kawaguchi, T., Watabe, N.: The organic matrices of the shell of the American oyster *Crassostrea virginica* Gmelin. Journal of Experimental Marine Biology and Ecology 170, 11–28. https://doi.org/10.1016/0022-0981(93)90126-9, 1993.
Kim, S.-T., O'Neil, J.R.: Equilibrium and nonequilibrium oxygen isotope effects in synthetic carbonates. Geochimica et Cosmochimica Acta 61, 3461–3475, 1997.
Klein, R.T., Lohmann, K.C., Thayer, C.W.: Bivalve skeletons record sea-surface temperature and $\delta^{18}O$ via Mg/Ca and $^{18}O/^{16}O$ ratios. Geology 24, 415–418, 1996a.
Klein, R.T., Lohmann, K.C., Thayer, C.W.: Sr/Ca and $^{13}C/^{12}C$ ratios in skeletal calcite of *Mytilus trossulus*: Covariation with metabolic rate, salinity, and carbon isotopic composition of seawater. Geochimica et Cosmochimica Acta 60, 4207–4221. https://doi.org/10.1016/S0016-7037(96)00232-3, 1996b.
Kominz, M.A., Browning, J.V., Miller, K.G., Sugarman, P.J., Mizintseva, S., Scotese, C.R.: Late Cretaceous to Miocene sea-level estimates from the New Jersey and Delaware coastal plain coreholes: an error analysis. Basin Research 20, 211–226, 2008.
Krantz, D.E., Williams, D.F., Jones, D.S.: Ecological and paleoenvironmental information using stable isotope profiles from living and fossil molluscs. Palaeogeography, Palaeoclimatology, Palaeoecology 58, 249–266. https://doi.org/10.1016/0031-0182(87)90064-2, 1987.
Kuznetsov, A.B., Semikhatov, M.A., Gorokhov, I.M.: The Sr isotope composition of the world ocean, marginal and inland seas: Implications for the Sr isotope stratigraphy. Stratigr. Geol. Correl. 20, 501–515. https://doi.org/10.1134/S0869593812060044, 2012.
Lartaud, F., Emmanuel, L., De Rafélis, M., Ropert, M., Labourdette, N., Richardson, C.A., Renard, M.: A latitudinal gradient of seasonal temperature variation recorded in oyster shells from the coastal waters of France and The Netherlands. Facies 56, 13, 2010.
Lear, C.H., Elderfield, H., Wilson, P.A.: A Cenozoic seawater Sr/Ca record from benthic foraminiferal calcite and its application in determining global weathering fluxes. Earth and Planetary Science Letters 208, 69–84. https://doi.org/10.1016/S0012-821X(02)01156-1, 2003.
Locarnini, R.A., Mishonov, A.V., Antonov, J.I., Boyer, T.P., Garcia, H.E., Baranova, O.K., Zweng, M.M., Paver, C.R., Reagan, J.R., Johnson, D.R., Hamilton, M., Seidov, D.: World ocean atlas 2013. Volume 1, Temperature. U.S. Department of Commerce, National Oceanic and Atmospheric Administration, National Environmental Satellite, Data and Information Service. https://doi.org/10.7289/v55x26vd, 2013.
Lorrain, A., Gillikin, D.P., Paulet, Y.-M., Chauvaud, L., Le Mercier, A., Navez, J., André, L.: Strong kinetic effects on Sr/Ca ratios in the calcitic bivalve *Pecten maximus*. Geology 33, 965–968, 2005.
Lorrain, A., Paulet, Y.-M., Chauvaud, L., Dunbar, R., Mucciarone, D., Fontugne, M.: $\delta^{13}C$ variation in scallop shells: increasing metabolic carbon contribution with body size? Geochimica et Cosmochimica Acta 68, 3509–3519, 2004.
Lowenstam, H.A., Epstein, S.: Paleotemperatures of the post-Aptian Cretaceous as determined by the oxygen isotope method. The Journal of Geology 62, 207–248, 1954.
MacDonald, B.A., Thompson, R.J.: Influence of temperature and food availability on the ecological energetics of the giant scallop *Placopecten magellanicus*. I. Growth rates of shell and somatic tissue. Marine ecology progress series. Oldendorf 25, 279–294, 1985.
McArthur, J.M., Howarth, R.J., Bailey, T.R.: Strontium Isotope Stratigraphy: LOWESS Version 3: Best Fit to the Marine Sr-Isotope Curve for 0–509 Ma and Accompanying Look-up Table for Deriving Numerical Age. The Journal of Geology 109, 155–170. https://doi.org/10.1086/319243, 2001.
McArthur, J.M., Steuber, T., Page, K.N., Landman, N.H.: Sr-isotope stratigraphy: assigning time in the Campanian, Pliensbachian, Toarcian, and Valanginian. The Journal of Geology 124, 569–586, 2016.
McConnaughey, T.A.: Sub-equilibrium oxygen-18 and carbon-13 levels in biological carbonates: carbonate and kinetic models. Coral Reefs 22, 316–327, 2003.
McConnaughey, T.A., Burdett, J., Whelan, J.F., Paull, C.K.: Carbon isotopes in biological carbonates: respiration and photosynthesis. Geochimica et Cosmochimica Acta 61, 611–622, 1997.
McConnaughey, T.A., Gillikin, D.P.: Carbon isotopes in mollusk shell carbonates. Geo-Marine Letters 28, 287–299. https://doi.org/10.1007/s00367-008-0116-4, 2008.
Meyers, S.R., Malinverno, A.: Proterozoic Milankovitch cycles and the history of the solar system. PNAS 201717689. https://doi.org/10.1073/pnas.1717689115, 2018.
Miller, K.G., Wright, J.D., Browning, J.V.: Visions of ice sheets in a greenhouse world. Marine Geology, Ocean Chemistry over the Phanerozoic and its links to Geological Processes 217, 215–231. https://doi.org/10.1016/j.margeo.2005.02.007, 2005.
Misra, S., Froelich, P.N.: Lithium Isotope History of Cenozoic Seawater: Changes in Silicate Weathering and Reverse Weathering. Science 335, 818–823. https://doi.org/10.1126/science.1214697, 2012.
Montgomery, P., Hailwood, E.A., Gale, A.S., Burnett, J.A.: The magnetostratigraphy of Coniacian-Late Campanian chalk sequences in southern England. Earth and Planetary Science Letters 156, 209–224. https://doi.org/10.1016/S0012-821X(98)00008-9, 1998.
Mook, W.G.: Paleotemperatures and chlorinities from stable carbon and oxygen isotopes in shell carbonate. Palaeogeography, Palaeoclimatology, Palaeoecology 9, 245–263. https://doi.org/10.1016/0031-0182(71)90002-2, 1971.
Mouchi, V., De Rafélis, M., Lartaud, F., Fialin, M., Verrecchia, E.: Chemical labelling of oyster shells used for time-calibrated high-resolution Mg/Ca ratios: a tool for estimation of past seasonal temperature variations. Palaeogeography, Palaeoclimatology, Palaeoecology 373, 66–74, 2013.
NOAA Earth System Research Laboratory: NOAA Optimum Interpolation (IO) Sea Surface Temperature (SST) http://www.esrl.noaa.gov/psd/data/gridded/data.noaa.oisst.v2.html (accessed 01/21/19).
Ogg, J.G., Ogg, G., Gradstein, F.M.: A concise geologic time scale: 2016. Elsevier, 2016.
Palmer, M.R., Edmond, J.M.: The strontium isotope budget of the modern ocean. Earth and Planetary Science Letters 92, 11–26. https://doi.org/10.1016/0012-821X(89)90017-4, 1989.
Palmer, R.E., Carriker, M.R.: Effects of cultural conditions on morphology of the shell of the oyster *Crassostrea virginica*, in: Proceedings of the National Shellfisheries Association. pp. 58–72, 1979.
Pearson, P.N., Ditchfield, P.W., Singano, J., Harcourt-Brown, K.G., Nicholas, C.J., Olsson, R.K., Shackleton, N.J., Hall, M.A.: Warm tropical sea surface temperatures in the Late Cretaceous and Eocene epochs. Nature 413, 481, 2001.

Perdiou, A., Thibault, N., Anderskouv, K., Van Buchem, F., Buijs, G.J.A., Bjerrum, C.J.: Orbital calibration of the late Campanian carbon isotope event in the North Sea. Journal of the Geological Society 173, 504–517, 2016.
Prandle, D., Lane, A.: The annual temperature cycle in shelf seas. Continental Shelf Research 15, 681–704. https://doi.org/10.1016/0278-4343(94)E0029-L, 1995.
R Core Team: R: A language and environment for statistical computing. R Foundation for Statistical Computing. Vienna, Austria, 2013.
Rausch, S., Böhm, F., Bach, W., Klügel, A., Eisenhauer, A.: Calcium carbonate veins in ocean crust record a threefold increase of seawater Mg/Ca in the past 30 million years. Earth and Planetary Science Letters 362, 215–224, 2013.
Rayner, N.A., Parker, D.E., Horton, E.B., Folland, C.K., Alexander, L.V., Rowell, D.P., Kent, E.C., Kaplan, A.: Global analyses of sea surface temperature, sea ice, and night marine air temperature since the late nineteenth century. Journal of Geophysical Research: Atmospheres 108. https://doi.org/10.1029/2002JD002670, 2003.
Reid, R.E.H.: The Chalk Sea. The Irish Naturalists' Journal 17, 357–375, 1973.
Richardson, C.A., Peharda, M., Kennedy, H., Kennedy, P., Onofri, V.: Age, growth rate and season of recruitment of *Pinna nobilis* (L) in the Croatian Adriatic determined from Mg: Ca and Sr: Ca shell profiles. Journal of Experimental Marine Biology and Ecology 299, 1–16, 2004.
Rothschild, B.J., Ault, J.S., Goulletquer, P., Heral, M.: Decline of the Chesapeake Bay oyster population: a century of habitat destruction and overfishing. Marine Ecology Progress Series 29–39, 1994.
Roy, K., Jablonski, D., Martien, K.K.: Invariant size–frequency distributions along a latitudinal gradient in marine bivalves. PNAS 97, 13150–13155. https://doi.org/10.1073/pnas.97.24.13150, 2000.
Rucker, J.B., Valentine, J.W.: Salinity Response of Trace Element Concentration in *Crassostrea virginica*. Nature 190, 1099–1100. https://doi.org/10.1038/1901099a0, 1961.
Sano, Y., Kobayashi, S., Shirai, K., Takahata, N., Matsumoto, K., Watanabe, T., Sowa, K., Iwai, K.: Past daily light cycle recorded in the strontium/calcium ratios of giant clam shells. Nat Commun 3, 761. https://doi.org/10.1038/ncomms1763, 2012.
Schöne, B.R., Gillikin, D.P.: Unraveling environmental histories from skeletal diaries — Advances in sclerochronology. Palaeogeography, Palaeoclimatology, Palaeoecology, Unraveling environmental histories from skeletal diaries - advances in sclerochronology 373, 1–5. https://doi.org/10.1016/j.palaeo.2012.11.026, 2013.
SCHÖNE, B.R., Houk, S.D., FREYRE CASTRO, A.D., Fiebig, J., Oschmann, W., KRÖNCKE, I., Dreyer, W., Gosselck, F.: Daily growth rates in shells of *Arctica islandica*: assessing sub-seasonal environmental controls on a long-lived bivalve mollusk. Palaios 20, 78–92, 2005.
Schöne, B.R., Radermacher, P., Zhang, Z., Jacob, D.E.: Crystal fabrics and element impurities (Sr/Ca, Mg/Ca, and Ba/Ca) in shells of *Arctica islandica* – Implications for paleoclimate reconstructions. Palaeogeography, Palaeoclimatology, Palaeoecology 373, 50–59, 2013.
Schöne, B.R., Zhang, Z., Jacob, D., Gillikin, D.P., Tütken, T., Garbe-Schönberg, D., McConnaughey, T., Soldati, A.: Effect of organic matrices on the determination of the trace element chemistry (Mg, Sr, Mg/Ca, Sr/Ca) of aragonitic bivalve shells (*Arctica islandica*)—Comparison of ICP-OES and LA-ICP-MS data. Geochemical Journal 44, 23–37, 2010.
Schöne, B.R., Zhang, Z., Radermacher, P., Thébault, J., Jacob, D.E., Nunn, E.V., Maurer, A.-F.: Sr/Ca and Mg/Ca ratios of ontogenetically old, long-lived bivalve shells (*Arctica islandica*) and their function as paleotemperature proxies. Palaeogeography, Palaeoclimatology, Palaeoecology 302, 52–64, 2011.
Scotese, C.: A new global temperature curve for the Phanerozoic. Presented at the GSA Annual Meeting in Denver, Colorado, USA - 2016. https://doi.org/10.1130/abs/2016AM-287167, 2016
Snoeck, C., Lee-Thorp, J., Schulting, R., Jong, J., Debouge, W., Mattielli, N.: Calcined bone provides a reliable substrate for strontium isotope ratios as shown by an enrichment experiment. Rapid communications in mass spectrometry 29, 107–114, 2015.
Sørensen, A.M., Surlyk, F., Jagt, J.W.M.: Adaptive morphologies and guild structure in a high-diversity bivalve fauna from an early Campanian rocky shore, Ivö Klack (Sweden). Cretaceous Research 33, 21–41. https://doi.org/10.1016/j.cretres.2011.07.004, 2012.
Sørensen, A.M., Ullmann, C.V., Thibault, N., Korte, C.: Geochemical signatures of the early Campanian belemnite *Belemnellocamax mammillatus* from the Kristianstad Basin in Scania, Sweden. Palaeogeography, palaeoclimatology, palaeoecology 433, 191–200, 2015.
Stanley, S.M., Hardie, L.A.: Secular oscillations in the carbonate mineralogy of reef-building and sediment-producing organisms driven by tectonically forced shifts in seawater chemistry. Palaeogeography, Palaeoclimatology, Palaeoecology 144, 3–19, 1998.
Stenzel, H.B.: Aragonite and calcite as constituents of adult oyster shells. Science 142, 232–233, 1963.
Steuber, T.: Isotopic and chemical intra-shell variations in low-Mg calcite of rudist bivalves (Mollusca-Hippuritacea): disequilibrium fractionations and late Cretaceous seasonality. International Journal of Earth Sciences 88, 551–570, 1999.
Steuber, T., Rauch, M., Masse, J.-P., Graaf, J., Malkoč, M.: Low-latitude seasonality of Cretaceous temperatures in warm and cold episodes. Nature 437, 1341–1344, 2005.
Steuber, T., Veizer, J.: Phanerozoic record of plate tectonic control of seawater chemistry and carbonate sedimentation. Geology 30, 1123–1126. https://doi.org/10.1130/0091-7613(2002)030<1123:PROPTC>2.0.CO;2, 2002.
Strahl, J., Philipp, E., Brey, T., Broeg, K., Abele, D.: Physiological aging in the Icelandic population of the ocean quahog *Arctica islandica*. Aquatic Biology 1, 77–83, 2007.
Surge, D., Lohmann, K.C.: Evaluating Mg/Ca ratios as a temperature proxy in the estuarine oyster, *Crassostrea virginica*. Journal of Geophysical Research: Biogeosciences 113, 2008.
Surge, D., Lohmann, K.C., Dettman, D.L.: Controls on isotopic chemistry of the American oyster, *Crassostrea virginica*: implications for growth patterns. Palaeogeography, Palaeoclimatology, Palaeoecology 172, 283–296, 2001.
Surge, D.M., Lohmann, K.C., Goodfriend, G.A.: Reconstructing estuarine conditions: oyster shells as recorders of environmental change, Southwest Florida. Estuarine, Coastal and Shelf Science 57, 737–756. https://doi.org/10.1016/S0272-7714(02)00370-0, 2003.
Surlyk, F., Christensen, W.K.: Epifaunal zonation on an Upper Cretaceous rocky coast. Geology 2, 529–534, 1974.
Surlyk, F., Sørensen, A.M.: An early Campanian rocky shore at Ivö Klack, southern Sweden. Cretaceous Research 31, 567–576, 2010.
Thibault, N., Harlou, R., Schovsbo, N.H., Stemmerik, L., Surlyk, F.: Late Cretaceous (late Campanian–Maastrichtian) sea-surface temperature record of the Boreal Chalk Sea. Climate of the Past 12, 429–438, 2016.

Thibault, N., Husson, D., Harlou, R., Gardin, S., Galbrun, B., Huret, E., Minoletti, F.: Astronomical calibration of upper Campanian–Maastrichtian carbon isotope events and calcareous plankton biostratigraphy in the Indian Ocean (ODP Hole 762C): Implication for the age of the Campanian-Maastrichtian boundary. Palaeogeography, Palaeoclimatology, Palaeoecology 337–338, 52–71. https://doi.org/10.1016/j.palaeo.2012.03.027, 2012.

Ullmann, C.V., Böhm, F., Rickaby, R.E., Wiechert, U., Korte, C.: The Giant Pacific Oyster (*Crassostrea gigas*) as a modern analog for fossil ostreoids: isotopic (Ca, O, C) and elemental (Mg/Ca, Sr/Ca, Mn/Ca) proxies. Geochemistry, Geophysics, Geosystems 14, 4109–4120, 2013.

Ullmann, C.V., Korte, C.: Diagenetic alteration in low-Mg calcite from macrofossils: a review. Geological Quarterly 59, 3–20, 2015.

Ullmann, C.V., Wiechert, U., Korte, C.: Oxygen isotope fluctuations in a modern North Sea oyster (*Crassostrea gigas*) compared with annual variations in seawater temperature: Implications for palaeoclimate studies. Chemical Geology 277, 160–166, 2010.

Upchurch Jr, G.R., Kiehl, J., Shields, C., Scherer, J., Scotese, C.: Latitudinal temperature gradients and high-latitude temperatures during the latest Cretaceous: Congruence of geologic data and climate models. Geology 43, 683–686, 2015.

Vansteenberge, S., de Winter, N.J., Sinnesael, M., Xueqin, Z., Verheyden, S., Claeys, P. Benchtop µXRF as a tool for speleothem trace elemental analysis: validation, limitations and application to an Eemian to early Weichselian (125-97 Ma) stalagmite from Belgium. Palaeogeography, Palaeoclimatology, Palaeoecology, in review.

Veizer, J.: Chemical diagenesis of carbonates: theory and application of trace element technique, 1983.

Voigt, S., Friedrich, O., Norris, R.D., Schönfeld, J.: Campanian–Maastrichtian carbon isotope stratigraphy: shelf-ocean correlation between the European shelf sea and the tropical Pacific Ocean. Newsletters on Stratigraphy 44, 57–72, 2010.

Voigt, S., Schönfeld, J.: Cyclostratigraphy of the reference section for the Cretaceous white chalk of northern Germany, Lägerdorf–Kronsmoor: A late Campanian–early Maastrichtian orbital time scale. Palaeogeography, Palaeoclimatology, Palaeoecology 287, 67–80. https://doi.org/10.1016/j.palaeo.2010.01.017, 2010.

Von Bertalanffy, L.: Quantitative laws in metabolism and growth. The quarterly review of biology 32, 217–231, 1957.

Wagreich, M., Hohenegger, J., Neuhuber, S.: Nannofossil biostratigraphy, strontium and carbon isotope stratigraphy, cyclostratigraphy and an astronomically calibrated duration of the Late Campanian *Radotruncana calcarata* Zone. Cretaceous Research 38, 80–96, 2012.

Warter, V., Erez, J., Müller, W.: Environmental and physiological controls on daily trace element incorporation in *Tridacna crocea* from combined laboratory culturing and ultra-high resolution LA-ICP-MS analysis. Palaeogeography, Palaeoclimatology, Palaeoecology 496, 32–47. https://doi.org/10.1016/j.palaeo.2017.12.038, 2018.

Watanabe, T., Suzuki, A., Kawahata, H., Kan, H., Ogawa, S.: A 60-year isotopic record from a mid-Holocene fossil giant clam (*Tridacna gigas*) in the Ryukyu Islands: physiological and paleoclimatic implications. Palaeogeography, Palaeoclimatology, Palaeoecology 212, 343–354, 2004.

Weiner, S., Dove, P.M.: An overview of biomineralization processes and the problem of the vital effect. Reviews in mineralogy and geochemistry 54, 1–29, 2003.

Weis, D., Kieffer, B., Maerschalk, C., Barling, J., Jong, J. de, Williams, G.A., Hanano, D., Pretorius, W., Mattielli, N., Scoates, J.S., Goolaerts, A., Friedman, R.M., Mahoney, J.B.: High-precision isotopic characterization of USGS reference materials by TIMS and MC-ICP-MS. Geochemistry, Geophysics, Geosystems 7, Q08006. https://doi.org/10.1029/2006GC001283, 2006.

Wendler, I.: A critical evaluation of carbon isotope stratigraphy and biostratigraphic implications for Late Cretaceous global correlation. Earth-Science Reviews 126, 116–146. https://doi.org/10.1016/j.earscirev.2013.08.003, 2013.

Yang, D., Huang, Y., Guo, W., Huang, Q., Ren, Y., Wang, C.: Late Santonian-early Campanian lake-level fluctuations in the Songliao Basin, NE China and their relationship to coeval eustatic changes. Cretaceous Research 92, 138–149. https://doi.org/10.1016/j.cretres.2018.07.008, 2018.

Yoshimura, T., Tanimizu, M., Inoue, M., Suzuki, A., Iwasaki, N., Kawahata, H.: Mg isotope fractionation in biogenic carbonates of deep-sea coral, benthic foraminifera, and hermatypic coral. Anal Bioanal Chem 401, 2755. https://doi.org/10.1007/s00216-011-5264-0, 2011.

Zimmt, J.B., Lockwood, R., Andrus, C.F.T., Herbert, G.S.: Sclerochronological basis for growth band counting: A reliable technique for life-span determination of *Crassostrea virginica* from the mid-Atlantic United States. Palaeogeography, Palaeoclimatology, Palaeoecology 516, 54–63, 2018.